Distribution Agreement

In presenting this thesis or dissertation as a partial fulfillment of the requirements for an advanced degree from Emory University, I hereby grant to Emory University and its agents the non-exclusive license to archive, make accessible, and display my thesis or dissertation in whole or in part in all forms of media, now or hereafter known, including display on the world wide web. I understand that I may select some access restrictions as part of the online submission of this thesis or dissertation. I retain all ownership rights to the copyright of the thesis or dissertation. I also retain the right to use in future works (such as articles or books) all or part of this thesis or dissertation.

Signature:

_____ _____

Jue Chen Date

DJ-1 zymogen activation: implication for Parkinson disease

By

Jue Chen
Doctor of Philosophy

Graduate Division of Biological and Biomedical Science
Molecular and System Pharmacology Graduate Program

Lih-Shen Chin, Ph.D.	Lian Li, Ph.D.
Advisor	Advisor
Victor Faundez, M.D., Ph.D.	Gary Miller, Ph.D.
Committee Member	Committee Member
Haian Fu, Ph.D.	Roy Sutliff, Ph.D.
Committee Member	Committee Member

Accepted:

Lisa A. Tedesco, Ph.D.
Dean of the Graduate School

Date

DJ-1 zymogen activation: implication for Parkinson disease

By

Jue Chen

M.B., Fudan University, 2001

M.S., Fudan University, 2004

Advisors: Lih-Shen Chin, Ph.D.

Lian Li, Ph.D.

An Abstract of

A dissertation submitted to the Faculty of the Graduate

School of Emory University in partial fulfillment

of the requirements for the degree of

Doctor of Philosophy

Graduate Division of Biomedical and Biological Sciences

Molecular and System Pharmacology Program

2011

Abstract

DJ-1 zymogen activation: implication for Parkinson disease

By Jue Chen

Loss-of-function mutations in DJ-1 have been linked to early onset familial PD but the exact cellular roles of DJ-1 remain unknown. DJ-1 shares structural homology with a bacterial and archea cysteine protease family but it has an extra α-helix (H8). The H8 of DJ-1 is predicted to prevent substrate entry and formation of a mature catalytic pocket. To understand the biological functions of DJ-1, we investigated whether DJ-1 is a cysteine protease and further studied the regulation of DJ-1 zymogen activation and the role of DJ-1 protease in anti-oxidative stress response.

Our data demonstrate that removal of H8 region enhances DJ-1 protease activity by increasing substrate affinity and improving catalytic efficiency. Further, DJ-1 functions as a cysteine protease because protease activity of DJ-1 is dependent on the Cys-His catalytic diad and is inhibited by oxidation. We also find that endogenous DJ-1 undergoes C-terminal cleavage in response to mild oxidation and protease activity contributes to DJ-1 cytoprotective function.

To further understand the mechanisms by which DJ-1 zymogen is activated, we investigated whether methionine residues regulate DJ-1 zymogen activation and cytoprotective function. Methionine residues can be reversibly oxidized, serving as the basis for redox-dependent regulation of cell signaling. Our findings demonstrate that selective methionine residues are required for zymogen activation and are critical for DJ-1 cytoprotective function. Moreover, the PD linked M26I mutation alters DJ-1 secondary structure and destabilizes DJ-1 protein.

Together the findings presented in this dissertation reveal that DJ-1 functions as a cysteine protease that requires activation in response to mild oxidation and DJ-1 zymogen activation is regulated by oxidation of selective methionine residues. Furthermore, our data suggest that the pathologic effects of PD linked M26I mutation are a combination of loss of enzymatic function and mild unfolding of DJ-1 protein.

DJ-1 zymogen activation: implication for Parkinson disease

By

Jue Chen

M.S., Fudan University, 2004

M.B., Fudan University, 2001

Advisors: Lih-Shen Chin, Ph.D.

Lian Li, Ph.D.

.

A dissertation submitted to the Faculty of the Graduate

School of Emory University in partial fulfillment

of the requirements for the degree of

Doctor of Philosophy

Graduate Division of Biological and Biomedical Sciences

Molecular and System Pharmacology Program

2011

Acknowledgments

I would like to thank my advisors, Dr. Lian Li and Dr. Lih-Shen Chin, for their mentorship. Their dedication to science has inspired me and I am grateful for their patience and guidance. During the past five years, their doors have been always open to me and to any other student or post-doc fellow in the lab. I would also like to thank the members of my committee, Dr. Victor Faundez, Dr. Haian Fu, Dr. Gary Miller and Dr. Roy Sutliff. They have encouraged me, provided me with insight and I have benefitted greatly from their support. I would like to thank the Molecular and System Pharmacology program (MSP) director Dr. Edward Morgan and Dr. John Hepler. They kindly accepted me as a visitor student when I was stranded by Hurricane Katrina. I am grateful to the MSP graduate student program and to the Department of Pharmacology, for providing a scientifically-nourishing environment without sacrificing friendly human interactions.

I am grateful to the former and current members of Li lab, James Olzmann, Elizabeth Webber, James Lee, Brandi Whatley, Lisa Giles, Sammy Lee, Jeanne McKeon, Dana Fallaize, Cheryl Ho, Cris Lee, Di Sha, Jennifer Kennedy, Patrick Renald, Haishan Yin, Liang Yan and Hong Tang. They have helped me with trouble-shooting, taught me techniques, lent me reagents, and critiqued my writings and oral presentations till I wanted to cry. I would like to thank my friends for understanding my hard work towards earning this degree and for being there when I needed them.

I am extremely grateful to my family for their unconditional love and support. My parents, Xichang Chen and Wennu Ma, cultivated my passion for science and encouraged me to study abroad. They tolerated me being away and seeing them once every a few years. I cannot thank them enough. I would like to thank my sister, Yuan Chen, who provided me with laughter and perspective. Finally, I would like to thank my husband Xiangbin Zeng. His love and understanding has kept me strong and without that I would not be here.

TABLE OF CONTENTS

CHAPTER I. INTRODUCTION AND BACKGROUND

LIST OF FIGURES

CHAPTER I. INTRODUCTION AND BACKGROUND

CHAPTER II. PARKINSON DISEASE PROTEIN DJ-1 CONVERTS FROM A ZYMOGEN TO A PROTEASE BY CARBOXYL-TERMINAL CLEAVAGE

CHAPTER III. MET-17 AND MET-26 ARE CRITICALLY INVOLVED IN DJ-1 ZYMOGEN ACTIVATION AND CYTOPROTECTIVE FUNCTION

LIST OF TABLES

CHAPTER I. INTRODUCTION AND BACKGROUND

CHAPTER II. PARKINSON DISEASE PROTEIN DJ-1 CONVERTS FROM A ZYMOGEN TO A PROTEASE BY CARBOXYL-TERMINAL CLEAVAGE

CHAPTER III. MET-17 AND MET-26 ARE CRITICALLY INVOLVED IN DJ-1 ZYMOGEN ACTIVATION AND CYTOPROTECTIVE FUNCTION

CHAPTER IV. DISCUSSION AND FUTURE DIRECTIONS

CHAPTER I

INTRODUCTION AND BACKGROUND

Opening Remarks

Parkinson's disease (PD) is a progressive neurodegenerative disorder with selective lesions in dopaminergic neurons in the substantia nigra pars compacta (SNpc) (186). Despite recent progress in understanding the pathogenesis of PD, the precise mechanisms are unclear. PD is believed to be caused by a combination of physiological changes accompanied with ageing, environmental factors and genetic susceptibilities (76). Although environmental factors causing sporadic PD remain to be identified, several chemicals with the ability to induce oxidative stress or mitochondrial dysfunction have been shown to induce parkinsonism in animal models. Experimental evidence from studying familial forms of PD also implicate oxidative stress in PD development (76).

DJ-1 is encoded by a PD gene and loss-of-function mutations have been identified in patients with familial autosomal-recessive forms of PD (74). DJ-1 has been shown to protect cells against oxidative stress-induced cell death in various models but the exact molecular mechanisms are unknown. DJ-1 is a redox-sensitive protein that mediates antioxidant responses and its function is predicted to be regulated by the intracellular redox state (74). Indeed, oxidation of DJ-1 has been shown in cell culture models and in human brain samples. DJ-1 shares structural homology with a bacterial and archean intracellular protease family, but it has an extra α-helix at the C-terminus that is predicted to inhibit DJ-1 protease activity (74). The experiments described in the following chapters investigate the redox-dependent regulation of DJ-1 protease activity, the functional significance of DJ-1 as a protease, and the impact of methionine oxidation on DJ-1 structure and function.

Parkinson's Disease

1. Clinical presentations of PD

Parkinsonism refers to the syndrome rather than a single disease and is defined as any combination of six specific, independent motor features: resting tremor, bradykinesia, rigidity, loss of postural reflexes, flexed posture, and freezing. Tremor must be present and accompanied by at least one other symptom to qualify for the diagnosis of Parkinsonism (93). Parkinson disease (PD), or primary parkinsonism, is one of the four classes of parkinsonism and refers to parkinsonism arising from unknown causes. The other three classes of parkinsonism are secondary parkinsonism, which is caused by known insults to the brain (drugs, toxins, brain tumor, vascular diseases, or encephalitis); parkinsonism-plus syndromes, which are associated with other motoric neurological features (progressive supranuclear palsy, multiple system atrophy, diffuse Lewy body disease, parkinson–dementia, ALS complex of Guam, and progressive pallidal atrophy); and heredodegenerative disorders which affects multiple brain regions (Alzheimer's disease, Wilson disease, Huntington disease, frontotemporal dementia on chromosome 17, and X-linked dystonia-parkinsonism) (93). In addition to the core basal ganglia symptoms, PD patients also present with non-motor symptoms such as loss of smell sensation, weak muscle tone, soft speech, digestive problems, mood swing, and sleep disorder. However, these symptoms are easily overlooked and attributed to the natural course of aging (7) . Moreover, the relevance of these symptoms to the progression of PD remains to be investigated. Dementia occurs in about 10-15% of PD cases, usually in the more advanced stages (7). The mean duration of PD is variable, but has been reported to be about 15 years from diagnosis to death (193).

2. Epidemiology of PD

The prevalence of PD in industrialized countries is 1% of the population over 60 years and 5% in people over 85 years (186). Developed countries appear to have higher incidence of PD, perhaps due to the ageing of the population. No apparent difference in incidence of PD has been reported among various ethnic populations, suggesting no higher risks correlated to any particular ethnic group. Besides ageing, both genetic and environmental factors are believed to contribute to the progression of PD. The majority of PD cases are idiopathic and believed to be caused by unidentified environmental risk factors. This is supported by the findings that PD incidence was not different between monozygotic and dizygotic twins (337) and several pesticides can induce parkinsonism in animal models. Since PD may take decades to develop and early symptoms are normally unnoticed or misinterpreted, identifying environmental causes remains challenging. Nevertheless, several environmental, occupational, and life-style factors have been linked to PD. Pesticide exposure has been associated with higher incidences of PD (16,89,99,283), but most epidemiological studies are case-control studies that cannot provide strong evidence of a causal-relationship between pesticide exposure and PD (89,99,283). There are a few prospective studies that investigated whether pesticide exposure increases risks of PD (16,18,277). One study did not report significant association between pesticide exposure and PD (277), while the other found that pesticide exposure increases PD risk in men but not in women (18). A third study, using a larger cohort group with 140,000 subjects, reported that exposure to pesticides is associated with 70% higher incidence of PD, suggesting that pesticide exposure is a risk factor (16).

The same study reported that farmers not exposed to pesticides are not at higher risk of PD, indicating a direct role of pesticide exposure in PD pathogenesis (16). A large variety of pesticides persist in the environment and because people do not usually know or remember the one(s) to which they have been exposed, it is difficult to estimate the contribution of a single pesticide to the development of PD (132). Despite the existence of several well-characterized animal models of pesticide - induced parkinsonism, the exact contribution of pesticide exposure to human PD incidence remains unclear (132).

Besides environmental factors such as pesticide exposure, some lifestyle factors have also been reported to influence PD development. Caffeine consumption and smoking are reported to inversely correlate to PD, suggesting that antagonizing adenosine A (2A) receptors by caffeine or activation of nicotinic receptors by nicotine in cigarette smoke may counteract the degeneration of dopaminergic neurons (131,281,290,291). However, it might be due to intrinsic novelty-seeking personality traits associated with the role of dopamine in reward pathways, rather than possible neuroprotective effects of nicotine or caffeine (91). Further studies are needed to understand whether smoking or caffeine intake can really prevent PD. Gender differences in the risk of developing PD have also been reported (193,344). Researchers noticed males have a slightly higher incidence of PD after age 65, while no differences are observed between men and women prior to age 65. This is likely due to differences in steroid hormone levels or exposure to potential environmental neurotoxicants (7).

3. Pathology of PD

Despite the complex nature of PD, two pathological features of PD are observed in most idiopathic PD patients: loss of dopaminergic (DA) neurons in the substantia nigra and presence of Lewy bodies (LBs) or lewy neurites (LNs) in the surviving neurons (128). DA neurons in the nigrostriatal pathway are more susceptible to cell death than other neurons or DA neurons in other brain regions, possibly due to the detrimental effect of dopamine metabolism. DA neurons in the nigostriatal pathway contain neuromelanin, giving rise to the distinct dark pigment. In PD brain samples, the substantia nigra regions look pale compared to normal human brain samples. Other pigmented nuclei (locus cerulues, dorsal motor nucleus of the vagus) could also be affected. The degeneration of DA neurons is followed by replacement with glia cells in that region (128). LBs and LNs are cytoplasmic inclusion bodies enriched in proteins and components of the ubiquitin machinery. They are eosinophilic spherical inclusions surrounded by a halo and usually immunostained positive for α-synuclein. LBs are not restricted to PD, they are also seen in other neurodegenerative disorders such as Lewy body dementia, suggesting that the pathological pathways contributing to the formation of LBs are shared by various neurodegenerative disorders (128). In addition to DA neurons in SN, other neuronal regions and neurons of other transmitter systems also contain LBs and LN. The susceptible neurons appear to be projection neurons that have a disproportionately long axon in relation to the size of the cell soma, especially those with axons poorly myelinated (35,36). The sparsely myelinated neurons require more energy to transmit impulses and are subjected to higher levels of oxidative stress. The surrounding of oligodendroglial cells may also protect neurons from pathological sprouting. Since other brain regions and neurotransmitter systems are also affected in PD, a staging system has

been developed based on α-synucleon pathology to delineate the sequential involvement of different type of neurons (35,36).

The pathogenic relevance of LBs to PD is still under debate. Since LBs contain misfolded proteins and exist in patients with neurodegenerative disorders, they were initially thought to be toxic. However, recent findings suggest that formation of LBs may be a cellular self-defense mechanism by which misfolded proteins are isolated from the rest of cells and are prevented from attacking important cellular components. The fact that LB is more enriched in neurodegenerative patients suggests it is a cellular stress response in an attempt to clear out misfolded proteins (128).

4. Treatment of PD

PD is generally progressive, and currently there is no effective treatment to halt or slow down the progression of the disease. Current therapies can only relieve the symptoms to some degree. Because dopamine level in the basal ganglia of the brain is reduced in PD, the mainstream therapies aim to restore DAergic signaling by either providing the precursor for DA synthesis, using DA agonists to activate DA receptors, or inhibiting the metabolism of DA by inhibiting monoamine oxidase B (9).

Dopamine can not cross the brain-blood-barrier (BBB), so it can not be given peripherally and is not of great clinical value. L-levodopa (L-dopa) is the immediate precursor of dopamine synthesis and can cross BBB. L-dopa is converted to dopamine by dopa decarboxylase in both periphery and brain. To increase the bioavailability of L-dopa in the brain, it is usually given in combination with a peripheral dopa decarboxylase inhibitor (carbidopa). L-dopa can be metabolized to 3-O-methyldopa (3-OMD) via

catechol-O-methyltransferase (COMT) and this will reduce the level of dopamine reaching the brain. To prevent peripheral L-dopa from being metabolized to 3-OMD, selective COMT inhibitors (tolcapone and entacapone) are sometimes used in adjunct with L-dopa. L-dopa is most effective for relieving bradykinesia, rigidity and gait stability in the first few years of treatment. Patients could become less responsive to L-dopa treatment over time, possibly due to gradual loss of dopaminergic neurons or desensitization of dopamine receptors. Long-term usage of L-dopa may lead to an on-off side effect. During the off period, the patients present with akinesia (inability to initiate movement) and during the on period, they have improved mobility but present with dyskinesia (diminished voluntary movement and presence of involuntary movement). Co-administration of COMT inhibitors have been shown to reduce the dosage of L-dopa and the fluctuations of response to L-dopa, therefore prolonging the effectiveness of L-dopa therapy (9).

Dopamine receptor agonists directly activate dopamineric signaling without requiring enzymatic conversion or producing toxic metabolites. They can selectively activate a subset of dopamine receptors, thus limiting side effects. Dopamine agonists do not generally lead to on-off effects or dyskinesia, and are commonly used when patients do not respond L-dopa or can no longer tolerate the side effects of L-dopa. However, desensitization of receptors will develop over prolonged usage and L-dopa will be used in combination to increase efficacy. Side effects caused by dopamine agonists include peripheral edema, hypotension, cardiac arrhythmias, gastrointestinal problems, and psychiatric problems due to the overactivation of DAergic signaling in periphery as well as in other brain regions (9).

Monoamine oxidase B (MAO-B) selectively metabolizes dopamine and is targeted in PD treatment. Inhibition of MAO-B by Selegiline can increase the half-life of dopamine and prolong the effect of L-dopa. The therapeutic effect of MAO-B inhibitor alone is minor and it is usually used in adjunct with L-dopa treatment to reduce the wearing-off or on-off side effects of L-dopa. MAO-B inhibitors are contraindicated in patients also taking nonselective MAO inhibitors to avoid hypertensive crisis. It should also be used with cautions for patients taking tricyclic antidepressants or serotonin reuptake inhibitors due to potential acute toxic interactions with serotonin signaling (9).

Other complementary therapies are used to restore the balance of the cholinergic and DAergic influences on the basal ganglia by reducing muscarinic cholinergic signaling on GABAergic cells in the corpus striatum. Amantadine has mild anti-parkinsonian effects, although mechanisms of action are unknown. It may act as an antagonist of adenosine A2 receptor. The efficacy and side-effects of these drugs need to be better characterized before they can become a first-line treatment option for PD. For patients that do not respond to pharmacological intervention, surgical options are also available. Deep brain stimulation of subthalamic nucleus or globus pallidus by an implanted electrode has improved clinical symptoms of advanced PD patients (9). Novel therapeutic options using gene therapy have also been developed and some of them have gone through clinical trials. Fetal mesencephalic dopamine cell implantation is proposed to provide long-term dopamine release (275,278), but the benefits of which are inconclusive based on two studies (103,258). Human embryonic stem cells can also differentiate into dopamine neurons and may be another promising source of dopaminergic neurons (183). However, the safety and efficacy of these novel therapies

need to be carefully studied. Glial cells-derived neurotrophic factor has neuroprotective function and can be used to promote endogenous repair. Targeted delivery of either neurotrophic growth factor or viruses to produce neurotrophic factors has yielded mixed results. One study reported improved dopamine uptake after a three-month infusion of neurotrophic factor with therapeutic benefits lasting for 2 years (112). However, two other studies reported no protection (185,249) and one study showed postoperative complications in some patients (185). Further studies are needed to investigate the efficacy and ensure the safety of these treatments.

5. Toxicological models of PD

1-methyl-4-phenyl-1,2,3,6-tetrahydropyridine (MPTP)

MPTP-induced parkinsonism was first described in human subjects (187). Young drug users who intravenously injected drugs containing MPTP as an impurity developed severe parkinsonian symptoms, including tremor, rigidity, slow movement, and postural instability (187). These symptoms were alleviated by administration of L-dopa, which resembles the response of PD patients. Further study of MPTP using mice (244,298) and primate (102,312,349) models, revealed that MPTP preferentially causes degeneration of putamental versus caudate dopaminergic nerve terminals and greater loss of neurons in SNpc than in ventral tegmental area (VTA), reminiscent of PD. One pathological feature of PD missing from the MPTP model is the formation of intraneuronal inclusions. The canonical LB inclusion has not been reported in MPTP-intoxicated human patients, neither has it been demonstrated in MPTP mice or primate models (76). This is likely due

to the acute administration of MPTP in both human and animal models, which may not be long enough to allow the formation of LB-like inclusions.

The mechanism of neurotoxicity of MPTP has been studied extensively. The pro-toxin MPTP is lipophlic and can cross the BBB. It will then be metabolized to an unstable intermediate 2,3-dihydro-1-methyl-4-phenylpyridinium ($MPDP^+$) primarily by MAO-B in glia cells. $MPDP^+$ undergoes oxidation through unknown mechanism to form the active toxic molecule 1-methyl-4-phenylpyridinium (MPP^+). The polar lipophobic MPP^+ relies on transporters on plasma membrane to enter cells. MPP^+ has high affinity for dopamine transporter (DAT) that are present in dopaminergic neurons, and to a lesser degree for norepinephrine and serotonin transporters. Once inside neurons, MPP^+ will either bind to cytosolic proteins, be packed into vesicular monoamine transporter-2 (VMAT2), or enter mitochondria with the help of mitochondrial membrane potential gradient (76,339). MPP^+ inhibits complex I of the mitochondrial electron transport chain and thus stimulates the production of superoxide radicals and subsequently other reactive oxygen species (ROS) or reactive nitrogen species (RNS). Further inhibition of complex I by MPP^+ (over 70% for the somatic mitochondria and 25% for the synaptic mitochondria) impairs oxidative phosphorylation and energy production (76,339). Oxidative stress and impaired energy production occur hours after MPP^+ administration while neuronal death happens several days later. The time lapse suggests that cell signaling pathways downstream of oxidative stress and disrupted energy production have been altered to cause cell death within a few days. Various cellular pathways have been demonstrated to account for MPP^+ - mediated neuronal death, including activation of p53 and p53-regulated Bax expression as well as apoptosis signaling kinase 1 (ASK1) pathway. The

neuronal death is predominantly apoptotic, as activation of caspases has been shown and inhibitors of caspases 2, 3, and 9 prevent neuronal death induced by MPP^+ (76,339).

Rotenone

Rotenone is a member of the rotenoids family, which exists in several genera of tropical plants. It has been widely used as an insecticide and fish poison. Rotenone binds to the ubiquinone binding site of Complex I (NADH dehydrogenase) and inhibits electron transport in mitochondria. It is highly lipophilic and can pass the BBB easily (47). Chronic administration of rotenone to rats results in selective degeneration of nigrostriatl dopaminergic neurons accompanied by α-synuclein positive LB-like inclusions and motor symptoms including abnormal postures and slow movement (28). It is the first animal model to reproduce the pathologic hall mark of PD, α-synuclein positive inclusions. However, even in chronic low dose intoxication other neurons or neuronal terminals including striatal serotoninergic fibers, striatal DARPP-32-positive projection neurons, striatal cholinergic interneurones, cholinergic neurons in the pedunculopontine tegmental nucleus and noradrenergic neurones in the locus ceruleus are similarly affected in addition to striatal dopaminergic fibres and nigral dopaminergic neurones that are affected in PD patients (143). Furthermore, acute administration of rotenone causes non-neuronal toxicity and has little effect on dopaminergic neurons, challenging how rotenone, a potent complex I inhibitor that can get access to almost all organs, could preferentially affect dopaminergic neurons (188). Of course, differences in dosage regime and routes may explain the variations in the phenotypes of rotenone model. A standard and optimized model has been proposed and shown to reproduce pathological, neurochemical and behavioral features of human PD (47). However, the successful use of the rotenone

model has been restricted to rats, limiting the application of this model in combination with other genetic PD mice models (76).

6-hydroxydopamine (6-OHDA)

6-OHDA can be formed from dopamine by autooxidation or as a metabolite (175,340), which makes it more physiologically relevant. It cannot cross the BBB, so it has to be injected into the substantia nigra or striatum of the animals to target the nigrostriatal dopaminergic pathway. 6-OHDA binds to DAT and noradrenergic transporters, thus selectively affects monoaminergic neurons. It generates ROS/RNS and attacks nucleophilic components of macromolecules in the cytosol. When injected at the neuronal terminals (striatum), 6-OHDA causes a retrograde degeneration of nigrostriatal neurons, lasting for 1-3 weeks. When injected at the neurons (substantia nigra), degeneration of neurons happens within 24h. In neither case, no LB-like inclusions have been found in the 6-OHDA model (76,339).

Paraquat

Paraquat is one of the most widely used herbicides that is structurally similar to MPP^+. But despite the similar structure paraquat does not inhibit complex I of mitochondrial electron transport chain (284). Instead, it drives a vicious cycle of producing ROS (primarily superoxide radicals) by redox cycling with cellular diaphorases (79). Paraquat does not pass the BBB freely and probably depends on the neutral amino acid transport system for transport into striatal neuronal cells, possibly in a Na^+ -dependent manner (305). Systemic administration of paraquat results in degeneration of dopaminergic neurons and presence of α-synuclein positive inclusions (216). Damages to other types

of neurons remain to be examined. Paraquat, like rotenone, has been successfully used in the *Drosophila* model to study PD. *Drosophila* treated with paraquat show preferential loss of DA neurons and several PD gene knock out *Drosophila* lines exhibit vulnerability to paraquat treatment (34).

6. Genes associated with familial forms of PD

Familial forms of PD exhibit similar clinical, neurochemical, and pathological markers as sporadic forms of PD, suggesting that genetic and sporadic PD may share similar pathological pathways. To this end, elucidation of genetic and molecular pathways in the heritable forms of PD may provide a better understanding of the pathogenesis of idiopathic PD.

***PARK1/4* (SNCA or α-synuclein)**

SNCA or α-synuclein is a 144 amino-acid protein with unknown function. Two missense mutations (A53T and A30P) in α-synuclein and a triplicate of wild type α-synuclein result in autosomal dominant PD (180,279,311). The clinical symptoms and pathological features of brains from patient autopsy revealed similarity between α-synuclein affected PD patients and sporadic PD patients. The exact physiological functions of α-synuclein are not well understood but it is enriched in presynapitc nerve terminals, suggesting a possible role in modulating synaptic vesicle function (221). Biochemically, α-synuclein alone adopts an unfolded structure but in the presence of lipid membranes the N-terminus of α-synuclein changes the conformation to form a stable α-helix (77). The stabilization of α-synuclein structure upon binding to lipid membranes suggests a role of α-synuclein in cellular membrane dynamics. This is supported by findings that α-synuclein binds to

vesicular trafficking machinery and regulates synaptic function (154). Additionally, α-synuclein knock down in hippocampal culture reduces the synaptic vesicle pool although this result has not been successfully repeated in α-synuclein null mice (243). Both wild-type and disease-linked mutant α-synuclein form amyloid fibrils and nonfibrillary oligomers, termed "protofibrils", but the pathogenic mutants have a higher propensity to form protofibrils (70). The protofibrils may be the toxic species by permeabilizing membranes and therefore α-synuclein is believed to cause PD through a gain-of-toxic function mechanism (351).

***PARK2* (Parkin)**

Parkin is encoded by a gene within *PARK2* loci and is a 456 amino acid protein containing a N-terminal ubiquitin-like domain and two really interesting new gene (RING) finger domains, indicative of E3 ubiquitin ligase function (133,372). Several putative substrates of parkin have been identified, but it remains to be investigated whether these are true substrates and how these substrates are relevant to PD pathogenesis (160). Parkin has been reported to mediate ubiquitin proteasome degradation of misfolded proteins, thereby participating in the clearance of misfolded proteins (181). It has also been shown to poly-ubiquitinate misfolded proteins via formation of poly- ubiquitin chain through the internal lysine 63 residue (K63 linkage) on ubiquitin and facilitate the degradation of the substrates via the aggresome autophagy pathway (264). Recently, involvement of Parkin in mitochondrial maintenance and autophagic degradation of dysfunctional mitochondria has been demonstrated (82, 92, 273, 280).

Mutations in *Parkin* account for 50% of early-onset PD and over 95 mutations have been reported. Patients with *Parkin* mutations typically have good response to L-dopa treatment and show slow-progression (181). The absence of LB in patients carrying *Parkin* mutations as well as in Parkin-null mice suggest that Parkin protein plays a role in the formation of LB and failure to form LB may contribute to PD development . *Parkin* knockout mice show no apparent signs of nitrostriatal DA neuron degeneration or motor deficits as seen in human patients, but do exhibit decreased dopamine release and uptake, suggesting pre-synaptic changes in dopamine neurotransmission(268).

***PARK3* (Unknown)**

PARK3 locus was mapped to a region on the chromosome 2p and was implicated in autosomal dominant PD, but candidate genes within this region remain to be identified (355).

***PARK5* (UCH-L1)**

Ubiquitin carboxy-terminal hydrolase L1 (UCH-L1) is a 222 amino acid protein that is abundant in the brain and exclusively localized in neurons (362). It is predicted to play a role in maintaining neuronal function based on its localization. This is supported by findings that *UCH-L1* null mice exhibit gracile exonal dystrophy (*gad*) (293). UCH-L1 was first identified as a member of the ubiquitin carboxyl-terminal hydrolase family that hydrolyze ubiquitin from small adducts, unfolded polypeptides, or tandemly conjugated ubiquitin monomers (358). However, the activity of UCH-L1 detected in these assays is lower than any known deubiquitination protease and the endogenous substrate(s) of UCH-L1 remain unknown. In agreement with this finding, structural analysis suggests

that UCH-L1 exists in an inactive conformation and may require activation upon certain physiological stimuli (75). Additionally, UCH-L1 has been demonstrated to possess Ub ligase activity *in vitro*. Its Ub ligase activity is dependent on dimer-formation and therefore UCH-L1 may function as a deubiquitination protease in the monomeric form and as a ubiquitin E3 ligase in the dimeric form (206). A third function assigned to UCH-L1 is stabilizing mono-Ub *in vivo*, independent of its enzymatic activity (266). Association of UCH-L1 with mono-Ub has been shown to prevent mono-Ub from being degraded, and thereby increasing the free Ub pool (266). Several post-translational modifications on UCH-L1 have been reported and may affect its function. Mono-ubiquitination on UCH-L1 at Lys-157, nearby the catalytic active cysteine, seems to disrupt its binding to mono-Ub (230). Furthermore, the mono-ubiquitinated UCH-L1 has been shown to be hydrolyzed by itself in an intramolecular manner (230), however, the exact molecular mechanisms regulating this hydrolyzation are still unknown. UCH-L1 can also be oxidized at methionine or cysteine residues as well as carbonylated (58). However, whether oxidations of UCH-L1 serve as signaling roles or inactivating UCH-L1 enzymatic activity remains to be investigated. Beta-N-acetylglucosamine (*O*-GlcNAc) modification on UCH-L1 has also been found in the synaptosome fraction of rat brain (68). The physiological implication of this modification is unclear but it may alter the conformation of UCH-L1 due to changes in steric or electrostatic forces. Since O-glycosidic linkage can also compete with phosphorylation modification for serine or threonine residues, it is also likely that *O*-GlcNAc modification on UCH-L1 may regulate its phosphorylation status.

A missense mutation leading to an I93M substitution in *UCH-L1* has been reported in the autosomal dominant form of late-onset PD patients. However, there are carriers of the same mutation who were not affected at the time of the investigation and genetic linkage analysis of UCH-L1 to familiar form of PD has not provided strong evidence, therefore the association of UCH-L1 mutation with human PD has been questioned (194). Although the deubiquitination activity of I93M mutant is only 55% of that of the WT UCH-L1, the loss-of-function theory has not been well accepted (253). This is because in human patients, the I93M mutation is autosomal dominant. Additionally, the homozygous *gad* mice with no deubiquitination activity of UCH-L1 or the heterozygous *gad* mice with about 50% of deubiquitination activity of UCH-L1 show no dopaminergic cell loss (293). It has been proposed that the I93M mutation may induce PD through a gain-of-toxic-function mechanism. This is supported by the finding that the secondary structure of I93M mutant has decreased α-helix structure and overexpression of I93M mutant results in increased number of UCH-L1 positive aggregates compared to WT UCH-L1 (253). In support of the gain-of-toxic function hypothesis, transgenic mice expressing UCH-L1 I93M mutant show several pathological changes including reduced tyrosine hydroxylase positive dopaminergic neurons in the substantia nigra and presence of UCH-L1 and Ub positive aggregates in dopaminergic neurons in the substantia nigra (300). In addition to I93M mutation, a polymorphism in UCH-L1 has also been reported to affect PD susceptibility (218). The single amino acid substitution (S18Y) has been demonstrated to protect against PD, but further analysis suggests that the inverse relationship is restricted to certain populations(299). S18Y mutant is reported to have reduced ligase activity compared to WT, which could stablize α-synuclein through

mediating K63 linked polyubiquitination. Therefore, S18Y leads to reduced level of α-synuclein and less potential to have misfolded α-synuclein (205). Another study shows that S18Y adopts a more globular secondary structure compared to WT, providing some structural basis for the reduced E3 ligase of S18Y mutant (248). However, more studies are required to understand the mechanisms of the dimer-based E3 ligase of UCH-L1 and the influence of the polymorphism S18Y on UCH-L1 E3 ligase activity.

***PARK6* (PINK1)**

Pten induced kinase 1 (PINK1) is encoded by a gene located to *PARK6* loci. It is a mitochondrially targeted serine/threonine kinase. PINK1 has been shown to protect cells against oxidative stress induced apoptosis partly through phosphorylating a mitochondrial chaperone TRAP1 and the protection was abrogated by PD linked mutations (282). PINK1 knockout mice have reduced complex I activity in brain, suggesting that PINK1 is important for oxidative phosphorylation and energy production(105). In support of this, fibroblasts from PD patients carrying PINK1 mutation showed decreased respiratory activity and ATP production as well as increased ROS generation (121). PINK1 has been shown to exist in a large protein complex with mitochondrial complexes I-IV, which could explain the requirement of PINK1 for oxidative phosphorylation (80). In addition to affecting the respiratory chain, PINK1 has also been demonstrated to regulate calcium efflux from mitochondria. Recently, it has been proposed that PINK1 regulates the dynamics of mitochondria, a process crucial in maintaining mitochondrial homeostasis (81). Knockout of *PINK1* in *Drosophila* resulted in enlarged mitochondria which could be rescued by overexpressing of a fission-promoting gene dynamin-related protein 1 (Drp-1) or knockout of a fusion-promoting gene dynamic-like GTPase Opa-1, implying

that PINK1 is involved in promoting mitochondrial fission (34,82). It is unclear whether PINK1 directly acts on mitochondrial fission/fusion machinery, indirectly regulates mitochondrial dynamics through the interaction with Parkin or regulating mitochondrial membrane potential (80).

***PARK7* (DJ-1)**: refer to page 35-51.

***PARK8* (LRRK2)**

Leucine-rich repeat kinase 2 (LRRK2) was identified as a novel gene localized in the *PARK8* locus. *LRRK2* encodes a 2527 amino acid protein with a leucine-rich repeat at the N terminus and a kinase domain near the C terminus. Other domains implicated in protein-protein interactions were also found in LRRK2, including GTPase, WD40 repeats, and ankyrin repeats. It has been speculated that LRRK2 plays a role in the formation of a high molecular weight cellular signaling complex since it contains many protein-protein interaction domains(73). Mutations of *LRRK2* were found in several families with late-onset PD. More than 75 substitutions in the LRRK2 coding sequence have been identified but only several are described as pathogenic. The biological functions of LRRK2 and the pathogenic mechanisms of PD-linked mutations are unknown, but wild-type LRRK2 has been shown to auto-phosphorylate *in vitro* and pathogenic mutation G2019S of LRRK2 enhance its kinase activity. Enhanced kinase activity of LRRK2 has been reported to cause protein aggregation, reduction in neuritic length and branching, increased phosphor-tau immunopositive inclusions, and apoptosis (73). However, whether other mutants of LRRK2 also enhance its kinase activity and whether pathogenic mutations of LRRK2 alter the phosphorylation of endogenous substrates remain unclear. While the

kinase activity of LRRK2 may be crucial for its pathophysiological functions, other domains of LRRK2 involved in protein-protein interaction may also play a role in PD pathogenesis because mutations in various domains of LRRK2 (Roc, COR, MAPK, and WD40) lead to the same phenotype (73). Understanding how these mutations lead to a dominant-negative effect or gain-of-toxic effect would be crucial to elucidate the mechanisms underlying LRRK2-associated PD. Transgenic, knock out, and knockin of LRRK2 mice models have been generated, but the phenotypes remain to be elucidated.

***PARK9* (ATP13A2)**

Loss-of-function mutations in a neuronal P-type ATPase gene, *ATP13A2*, were identified in an autosomal recessive form of early onset parkinsonism with pyramidal degeneration and dementia (Kufor-Rakeb syndrome, KRS) (285). ATP13A2 is a 1180 amino acid long protein with ten transmembrane domains, reported to express strongly in brain using Northern blot analysis (285). The two frame-shift mutations that remove three or six C-terminal transmembrane domains and one in-frame deletion mutation that removes 37 amino acids of exon 13 have been identified in those KRS patients. Over-expressed wild type ATP13A2 localizes to lysosomes while the truncated mutants are retained in the endoplasmic reticulum and degraded by proteasomes (285). Several point mutations were identified later, including a homozygous missense mutation of G504R in a patient with juvenile onset parkinsonism and two heterozygous mutations (T12M, G533R) in two carriers with atypical symptoms at the age of onset between 21-40y (84). Another heterozygous mutation (A746T) was identified in three patients with idiopathic PD at an age of onset before 50y. The A746T mutation was located between the highly conserved phosphorylation region and the fifth transmembrane domain (203). The yeast ortholog of

ATP13A2 rescues DA neuron cell death induced by over-expression of α-synuclein and knock down of yeast ortholog of *ATP13A2* exacerbates misfolding of α-synuclein, suggesting a functional connection between ATP13A2 and α-synuclein (113). As α-synuclein is known to be degraded by both the proteasome and autophagy, ATP13A2 may play a role in the removal of misfolded α-synuclein via lysosomal pathways since ATP13A2 is localized to lysosome (113).

***PARK10* (Unknown)**

PARK10 locus was implicated in late onset PD (140,217). The susceptibility gene associated with PD has not been identified, although several candidate genes have been proposed, including *ubiquitin specific peptidase 24 (USP24)* (134), *human immunodeficiency virus type I enhancer binding protein 3 (HIVEP3)* (200), and *RING-finger protein 11 (RNF11)* (12) .

***PARK11* (Unknown)**

Linkage study suggests an association of *PARK11* locus at chromosome 2q36-37 with PD (271). However, *PARK11* gene remains to be defined, although a candidate gene encoding a protein involved in tyrosine kinase receptor signaling, named GRB10 interacting GYF protein 2 (GIGYF2), has been proposed (33).

***PARK12* (Unknown)**

A locus on the X-chromosome was reported as *PARK12 locus* (*Xq21-q25*) (270) and the same locus has been implicated in PD by two other groups (140,296). However, *PARK12* gene has not been identified yet.

***PARK13* (HtrA2/Omi)**

HtrA2/Omi is a nuclear encoded mitochondrial serine protease that contains a domain related to *Drosophila* death-promoting proteins Reaper at the N-terminus (137). HtrA2 is cleaved upon apoptosis stimuli and is released from mitochondria to the cytosol where the Reaper domain binds to the inhibitor of apoptosis proteins (IAPs). Binding of HtrA2 to IAPs allows for the release of IAPs from apoptosis-inducing proteins and therefore promotes apoptosis (137,325). However, HtrA2 seems to have anti-apoptotic activity by preventing mitochondrial damage induced by certain stresses. *HtrA* knockout mice show significant loss of neurons in the striatum and present with a parkinsonian like phenotype that leads to death at around 30 days (224). Additionally, a missense mutation of S276C at the protease domain of HtrA2 was found in a spontaneous, recessively-inherited mutation mouse line *mnd2* (motor neuron degeneration2). These mice exhibited altered gait, cessation of normal weight gain, ataxia, akinesia, and death at 40 days (155). Striatal neurons are most susceptible in *mnd2* mice, but other neuronal systems including brain stem and spinal cord are also affected at later stages (155). S276C mutation does not seem to affect binding of HtrA2 with IAPs or maturation of the protease but HtrA S276 mutant protein immunoprecipitated from the *mnd2* mouse tissues display reduced serine protease activity, using casein as the substrate (155). A heterozygous mutation (G399S) found in four PD patients results in defects in the activation of protease activity and mitochondrial dysfunction accompanied with altered mitochondrial morphology (323), suggesting that the protease activity or activation of HtrA2 is critical for its neuroprotection.

***PARK14* (iPLA2-VIA)**

PLA2G6 gene localized to the *PARK14* locus encodes a calcium-independent group VI phospholipase A2 (PLA2G6), a class of enzyme that catalyzes the release of fatty acids from phospholipids. PLA2G6 is active as a tetramer, with proposed roles in phospholipid remodeling, arachidonic acid release, leukotriene and prostaglandin synthesis and Fas-mediated apoptosis (20). Several transcript variants encoding multiple isoforms have been described, but the full-length nature of only two have shown to be enzymatically active (189).

Mutations in the *PLA2G6* gene were identified in patients with infantile neuroaxonal dystrophy (INAD), neurodegeneration with brain iron accumulation (NBIA) and related Karack syndromes (239). The calcium-independent PLA2 enzymes are critical in maintaining cell membrane homeostasis. Levels of phosphatidylcholine, abundant in mammalian cell membranes and important in maintaining membrane integrity, are regulated by the opposing actions of CTP: cytidy-lylphosphocholine transferase and iPLA2-VIA (17). Defects in iPLA2-VIA could lead to a relative abundance of membrane phosphate-dycholine and secondary structural abnormalities, which may underlie the axonal pathology observed in INAD and NBIA. This study suggests that phospholipase A2 dysfunction is associated with imbalance of brain iron homeostasis, which is underlying several neurodegenerative diseases including PD (17). Mutations in *PLA2G6* were found in 80% of the patients with INAD and 20% of the patients with NBIA in a genetic screen. Furthermore, all mutation carrying patients display cerebellar atrophy and half of them show brain iron accumulation, suggesting defects in phospholipid metabolism may be associated with brain iron metabolism (120).

***PARK15* (F-Box protein07)**

F-box protein 7 (Fbx07) is encoded by the *FBX07* gene localizing in the *PARK15* locus. FBX07 is a member of the F-box protein family that shares an approximately 40-amino-acid motif, the F-box. The F-box protein (FBP) is one of the four subunits of the ubiquitin protein ligase complex SCFs (SKP1-cullin-F-box) that mediates ubiquitination. FBPs serve as molecular scaffolds in the formation of protein complexes and have been implicated in cellular processes such as cell cycle, genome stability, development, synapse formation, and circadian rhythms (141). Alternatively spliced transcript variants of *FBX07* gene have been identified with the full-length but the nature of these variants has not been determined. The function of Fbx07 is unknown but it has been reported to interact with several proteins, such as the inhibitor of apoptosis protein 1 (49), the proteasome inhibitor protein (170), and the heptatoma upregulated protein (148), suggesting that it may play a role in apoptosis, proteasome degradation and mitosis.

A homozygous missense mutation in *FBX07* gene was identified in an Iranian family with "pallid-pyramidal disease" presenting both parkinsonism and pyramidal tract signs (308). Three additional mutations on *FBX07* gene was later reported in two Caucasian families. In one family, two affected siblings have a homozygous truncating mutation in exon 9 (c.C1492T>p.Arg498Stop) (101). Compound heterozygous mutations, a splice mutation (IVS7 + 1G/T), and a single base substitution in exon 1A (c.C65T > p. Thr22Met), have been identified in two affected siblings from another family (101). The affected patients present with early-onset parkinsonism and pyramidal tract defects. The disease progression is relatively slow as all the patients survive decades after the onset. In some patients, the parkinsonism is responsive to L-dopa treatment (101).

***PARK16* (Unknown)**

PARK16 locus was identified in a genome-wide association study in a Japanese population and was confirmed by single nucleotide polymorphism (SNPs) study in a pooled analysis of one Chinese and two Japanese populations. The PD associated gene(s) localized within PARK16 locus are yet to be identified (334).

7. Molecular mechanisms of PD

PD is a complex disorder with contributions from ageing, and environmental and genetic factors (376). Several shared pathways have been implicated in PD pathogenesis based on experimental evidence from both genetic and toxicological models of PD. Oxidative stress, mitochondrial dysfunction, protein misfolding, and impaired protein quality control system have emerged as key mechanisms underlying the pathogenesis of both sporadic and familial PD. All these pathways are not mutually exclusive but actually have great cross talk between each other. Impairment of one pathway has been shown to cause dysfunction of the other pathways. Different insults may initiate dysfunction in one or several particular pathways, but will affect other pathways and eventually cause the whole cellular system to collapse.

Oxidative stress

It has been recognized for decades that oxidative stress is associated with neurodegenerative disorders, including PD, but whether oxidative stress contributes to the pathogenesis of PD is still debatable (129). The first line of evidence supporting the involvement of oxidative stress in PD is that markers of oxidative modifications on macromolecules are more enriched in brain samples from postmortem PD patients. Most of the markers detected are irreversible oxidative modifications on lipids, proteins, and

DNA, because these markers are stable and readily measurable (129). The brain is enriched in polyunsaturated fatty acids, which are susceptible to oxidative modification. Markers for lipid oxidations, such as 4-hydroxy-2-nonenal and malondialdehyde, are increased in the substantia nigra of PD patients (83,368). Irreversible modifications of proteins, such as carbonyl modifications, are also significantly increased in the substantia nigra of postmortem PD brains (5,100). A Marker of RNS modification on proteins, nitrotyrosine, is also elevated in MPTP mouse model of PD (276,295). Likewise, oxidative modifications of DNA, measured by the conversion of deoxyguanosine to 8-hydroxydeoxyguanosine (8-OHdG), is also markedly increased in substantia nigra of postmortem PD brain samples (6,250). The second line of evidence is that in samples of postmortem PD patients, there is a decrease in activity of antioxidant enzymes, such as glutathione peroxidase and catalase (8,171). One exception is superoxide dismutase isoform 2 (SOD2). Increased activity of SOD2 has been reported in samples from PD patients (225,292). Since SOD2 is known to be induced by ROS in mitochondria, the increased activity of SOD2 suggests elevated level of superoxide ROS in mitochondria of PD patients. In addition to the enzymatic system, small antioxidant molecules have also been examined in PD brains. Level of glutathione has been shown to be lower in PD brain samples (310). Ubiquinone, another small antioxidant molecule has also been shown to be lower in PD patients (309). In summary, there is an accumulation of oxidatively modified lipids, proteins, and DNA in PD patients and decreased level of most antioxidant enzyme or nonenzymatic antioxidants in PD patients, suggesting that oxidative stress is involved in PD. Although the causative role of oxidative stress in PD remains to be defined, establishment of several aforementioned toxicological models of

PD (MPTP, rotenone, paraquat, and 6-OHDA) has provided strong evidence that oxidative stress contributes to the initiation and/or progression of PD.

Mitochondrial dysfunction

Substantial evidence from genetic and toxicological studies suggests that mitochondrial dysfunction is critical to PD pathogenesis. Several proteins implicated in familial forms of PD, including PINK1, DJ-1, Parkin, and HtrA2/Omi, directly or indirectly regulate mitochondrial function (refer to page 16 – 20 for details). Neurotoxins rotenone and MPP^+ that induce parkinsonism in animal models also specifically inhibit complex I of mitochondrial electron transport chain and cause mitochondrial dysfunction (refer to page 10-12 for details). The discovery that MPTP, an inhibitor of complex I, causes Parkinsonism in human beings strongly support the hypothesis that mitochondrial dysfunction plays a causal role in PD (187). The toxic effects of MPTP have been repeated in non-human primates and mice, supporting the important role of complex I inhibition in PD pathogenesis. Further evidence comes from other toxicological models using rotenone, another potent inhibitor of complex I. Rats administrated with rotenone develop parkinsonism including presence of α-synuclein positive inclusions. Whether the effects of rotenone are mediated through inhibition of complex I has been tested using a model in which rotenone-insensitive complex I subunit NDI1 was over-expressed unilaterally via viral transduction. Overexpression of NDI1 protects against rotenone induced dopaminergic degeneration, suggesting that rotenone acts through inhibiting complex I (220). Contradictory to this finding, complex I activity seems to be dispensible for rotenone-induced toxicity in mice. Knock out mice lacking NADH ubiquinone oxireductase iron sulfur protein 4 (Ndufs4) gene, which is required for the assembly of

complex I, does not affect the susceptibility of dopamine neurons to rotenone induced cell death (61). But the Ndufs4 knockout mice have normal ATP level and oxygen consumption, implying the complex I might be dispensable for aerobic metabolism. However, complex I activity decreases gradually over decades in the pathogenesis of PD, which is different from the sudden complete depletion of complex I in this animal model.

Mitochondrial complex I defect has been reported in sporadic PD patients. The SNpc seems to be affected the most, but complex I activity in other brain regions or other tissues is also lower in PD patients compared to normal individuals (124,274,294). The cause of the reduction in complex I activity is unknown but several components of complex I have been shown to be more oxidized in PD brain samples. The irreversible oxidation of these components may cause complex I dysfunction and disassembly, thereby leading to mitochondrial dysfunction and ROS generation (162). Although there is a systemic decrease in complex I activity in sporadic PD patients, DA neurons in the SNpc appear to be more prone to the impairment of complex I and mitochondrial function. The vulnerability of DA neurons in SNpc is likely due to higher ROS levels generated by dopamine metabolism and auto-oxidation, a higher level of iron that catalyzes the Fenton reaction, and a lower level of antioxidants, such as glutathionine, in these neurons (56).

In addition to reduced complex I activity, mutations in mitochondrial DNA (MtDNA) or nuclear-encoded mitochondrial proteins have also been found to cause parkinsonism, in addition to other diseases (210,326). MtDNA is more prone to mutations because MtDNA has less efficient DNA repair machinery, no protective histone, and is close to ROS generating sources (204,226). However, mitochondria have

high copies of DNA which provides protection via redundancy. The mutated MtDNAs co-exist with wild type mtDNA in a mitochondrion and can be divided into daughter mitochondria during expansion of mitochondria or during mitosis. Only when mutant MtDNA exceeds the threshold will lead to mitochondrial dysfunction. Symptoms usually occur first in post-mitotic cells with high energy demands including neurons, skeletal and cardiac muscle cells, which explains the higher susceptibility of neurons to MtDNA mutations. Proteins regulating mitochondrial fusion and fission are also likely to determine the susceptibility of cells to mitochondrial genomic instability (204,226).

An age dependent increase in somatic MtDNA deletions associated with a respiratory chain defect has been reported in dopaminergic neurons from the SN (176). The mutations within each neuron are clonal and the percentage of mutations correlate to the degree of cytochrome c oxidase deficiency, suggesting mtDNA deletions may be directly responsible for impaired mitochondrial respiration (176). Mutations in maternally inherited MtDNA were also identified in one family with PD, suggesting mitochondrial dysfunction is associated with PD development (326). MtDNA polymerase γ (POLG), an enzyme required for MtDNA synthesis, is encoded in the nucleus. Mutations in POLG cause multisystem disorders including Parkinsonism(210). The involvement of mitochondria in PD is further supported by the finding that a conditional knockout of mitochondrial transcription factor (TFAM), a protein necessary for mitochondrial replication and transcription, in midbrain DA neurons results in reduced MtDNA, respiratory chain defects, and neuronal cell death, accompanied by progressive motor symptoms that are responsive to L-dopa treatment (88). These findings suggest that mitochondrial dysfunction can lead to PD. However, DA neurons in SNpc may not be the

most susceptible, since skeletal and cardiac muscle, peripheral nervous system, and retina are equally affected by most MtDNA mutations.

Protein misfolding and impaired protein quality control

One third of the newly synthesized proteins are estimated to be folded improperly and require several protein quality control systems to keep guardian. As a counterbalance, complex protein quality control systems have evolved in cells to repair or remove faulty proteins. The first line of defense is the chaperone system, which consists of several families of highly conserved proteins that facilitate the folding or assembly, as well as targeting, transporting, and degradation of the client protein (242). Almost all heat shock proteins (HSPs) function as molecular chaperones and are classified into six families based on their molecular mass: HSP100, HSP90, HSP70, HSP60, HSP40, and small HSPs (242). Chaperones have been implicated in the pathogenesis of various neurodegenerative disorders including PD (241,242). Several HSPs are found to co-localize with α-synuclein in LBs (228), suggesting the involvement of HSPs in formation of LBs. It has been demonstrated that over-expression of HSPs can protect against neuronal cell death induced by misfolded proteins such as α-synuclein (267,288,383).

Unfolded or misfolded proteins can be tagged with ubiquitin and targeted to the proteasome for degradation. The proteasome consists of a 20S proteolytic core containing a barrel-shaped protease complex and two 19S regulatory caps on each side of the 20S core (71). Substrates are usually polyubiquitinated through K48 linkages and are recognized by the 19S proteasome. A major E3 ligase that polyubiquitinates and mediates misfolded proteins for proteasome degradation is CHIP. CHIP binds to chaperone

HSP70/HSC70 and uses chaperone(s) for substrate recognition (182). Protein degradation through UPS system is an ATP-dependent process, as misfolded proteins need to be unfolded by chaperones before they can enter the 20S protealytic core. This intrinsic feature of the proteasome limits the substrates of the proteasome to misfolded proteins that can be unfolded via chaperones since the barrel of the proteasome is too narrow to allow still misfolded/aggregated proteins to pass through. Therefore, not only can energy deficiency diminish the capacity of UPS but also result in accumulation of misfolded proteins, which could jam the proteasome and inhibit its activity (71). A decrease in proteasome activity is seen in elderly people and reduction of proteasomal function in patients with AD or PD has also been reported (71).

The autophagy-lysosome system is another quality control system that degrades cytosolic proteins. In addition to regulating the turn-over of long-lived cytosolic proteins under basal condition, macroautophagy also degrades misfolded and aggregated proteins possibly via recognizing K63 polyubiquitinated substrates through two major proteins p62 and neighbor of BRCA1 gene (NBR1) (182).

DJ-1

1. DJ-1 is oncogenic

DJ-1 was first identified in 1997 as an oncogene that could transform cells in cooperation with H-Ras (246). Since then the association of DJ-1 with cancer has been validated by several reports showing that DJ-1 level is elevated in breast cancer(190), lung cancer(212), and uveal malignant melanoma (272). Additionally, DJ-1 has been demonstrated to negatively regulate a tumor suppressor phosphatase and tensin homolog

(PTEN) (164) and positively regulate phosphatidylinositol 3-kinases/protein kinase B (PI3K/Akt) signaling (350,367), which could account for its oncogenicity. Moreover, DJ-1 was found to suppress the apoptosis signal regulating kinase (ASK1) pathway and therefore inhibit apoptosis (237,352).

2. Loss of function mutations of DJ-1 linked to PD

The association of DJ-1 with PD became apparent when it was discovered as the *PARK7* gene and mutations in DJ-1 caused autosomal recessive early onset PD (32). The first mutation reported was a large deletion including promoter regions and coding sequences, essentially resulted in no DJ-1 protein. Afterwards, several point mutations have been described, including homozygous mutations of L166P (32), M26I (2) , E64D (139), and E163K (15), as well as some heterozygous mutations (Table I-2). Only L10, A104, P158, and L166 are conserved among all species from *C.elegans* to *Homo sapiens*, other residues mutated in PD patients are not well conserved (Fig.I-1A). All the point mutations found in familial form of PD are also illustrated in 3-dimensional DJ-1 structure (Fig.I-1B). Although PD caused by DJ-1 mutations is rare [15], the study of the pathological consequences of DJ-1 deficiency has provided insights into the molecular mechanisms of oxidative stress-related neurodegeneration.

Δexon 1-5: The *DJ-1* gene contains 8 exons distributed over 24 kb and encodes a ubiquitously expressed and highly conserved protein. The first two exons are noncoding and alternatively spliced in the *DJ-1* mRNA (32). One major transcript of about 1 kb contains a 570-bp ORF that encodes a 189-aa protein and is expressed in almost all tissues including the brain regions affected in PD. The 14kb deletion found in a Dutch

family spans from 4 kb of sequence upstream of DJ-1 gene ORF start site till the start site of the exon 6, resulting in no DJ-1 protein production (32).

L166P: A homozygous point mutation (T3C transition at position 497 from the ORF start in cDNA), resulting in the substitution of a highly conserved leucine at position 166 of the DJ-1 protein by a proline was identified in an Italian family and absent from the general Italian population. This change showed complete cosegregation with the disease allele in the Italian family (32). The Leu-166 is at the center of helix 7 and proline is regarded as helix-breaker. The L166P mutation was predicted to destabilize helix 7. It was demonstrated by several investigators using different approaches that L166P mutation unfolds DJ-1 protein and results in destablization of DJ-1 protein (116,238,262). As a result of the destabilization, DJ-1 L166P expresses at very low level and has significantly less cytoprotective function compared to DJ-1 WT (116,238,262).

M26I: Homozygous missense mutation resulting in substitution of Met-26 with Ile in exon 2 was found in an Ashkenazi Jewish patient with an age-onset of 39y (2). This methionine is highly conserved among vertebrates. It is located at the middle of helix 1 but is not believed to involve in dimer formation (145,149). Controversial results have been reported regarding the secondary structure, oligomeric state, protein stability, and intracellular localization of DJ-1 M26I mutant. DJ-1 M26I mutant has been demonstrated to have reduced secondary structure and is less stable thermodynamically using circular dichroism (151) but it was shown to have no change in secondary structure and thermal stability by another investigator (184). As far as the oligomeric state, M26I mutant has been reported to still form heterodimer using coimmunoprecipitation (29,331) or

sedimentation equilibrium ultracentrifugation (184), but it has also been shown to equilibrate between unfolded monomer and higher molecular weight oligomer using size-exclusion chromatography and sedimentation-equilibrium ultracentrifugation (151). Protein level of DJ-1 M26I has been reported to be reduced (29,151,198,331) or unchanged (184,238,371), compared to DJ-1 WT. The colocalization of DJ-1 M26I with mitochondria was reported to be unchanged under basal condition (371) or increased upon treatment with paraquat (29), using both biochemical and immunostaining methods. The major discrepancy between Hulleman et al and Lakshminarasimhan et al's data is likely due to the different oxidation status of DJ-1 protein. The recombinant DJ-1 protein used by Hulleman et al is believed to be more oxidized, containing a mixture of C106-sulfinic and sulfonic acids. M26I mutation may preferentially destabilize more oxidized forms of DJ-1 used by Hulleman et al (151,184), although this requires further verification.

E64D: Homozygous mutation of E64D (c.192G>C substitution) was identified in a Turkish patient with early onset PD. The patient showed significant reduction of dopamine uptake transport (DAT) binding in striatum and loss of presynaptic dopaminergic afferents (139). The pathogenic nature of E64D mutation is undetermined. E64D is not thought to be critical for stabilizing the structure of DJ-1 because it is not conserved among vertebrates (rat DJ-1 has a glutamine residue at position 64) (22) and is located far from the dimer interface, at the C-terminal end of α-helix 2 (145,149,192) . DJ-1 E64D mutant has been crystallized and showed no apparent difference compared to DJ-1 WT (139). Although E64D displays no global structural changes based on X-ray

crystal structure (139), it appears to have a more stiff secondary structure than WT and may form more stable dimers (151). Additionally, DJ-1 E64D may have different binding profiles as E64D mutant cannot be recognized by a monoclonal antibody raised against DJ-1 WT (116). However, the same investigator also reported reduced steady state levels of DJ-1 E64D protein compared to DJ-1 WT protein (116). The cause of the discrepancy between the reduced steady state level and increased secondary and thermal stability remains unknown.

L10P: Homozygous mutation of L10P in DJ-1 was identified in a consanguineous Chinese family with disease onset of 19 years of age, the earliest age reported for any PD case linked to DJ-1 mutation (122). L10P mutant has reduced stability compared to wild-type DJ-1 and inhibition of proteasome function could increase the protein level of L10P, implying that L10P mutation may destabilize DJ-1 protein and is partly degraded through proteasome system (286). Moreover, L10P mutant has reduced solubility and inhibits proteasome function possibly caused by accumulation of insoluble L10P, implying that the structural changes resulted from L10P mutation are severe enough to cause protein misfolding and aggregation when proteasome degradation system is impaired (286). However, the effects of L10P on folding and stability are not as dramatic as L166P since L10P mutant could still form heterodimer with DJ-1 WT protein and the half-life of L10P is longer than that of L166P (286).

P158DEL: Homozygous mutation resulting in deletion of highly conserved P158 on DJ-1 was identified in a Dutch family (211). Similar to L10P, P158DEL was characterized as an “intermediate” mutant, with structural disturbances not as severe as L166P but enough

to disrupt homodimerization and reduce protein solubility and stability (286). The pathological nature of this mutation remains to be investigated.

A107P: Homozygous mutation of A107P was identified in an Iranian PD patient with early onset PD (107). Ala-107 is conserved among all species and is right next to the predicted catalytic cysteine Cys-106 (107). Replacement of Ala with Pro at residue 107 is expected to alter the catalytic activity of DJ-1 but experimental evidence is lacking to support this hypothesis.

A104T: Heterozygous substitution of A104T was found in one sporadic PD patient (125). The residue Ala-104 is well conserved and is located close to the reactive cysteine, Cys-106. The small size of alanine at that position allows for tight packing in the central parallel of β-sheet 5. The A104T mutant shows a slightly reduced secondary structure and has a melting temperature 8^{o}C lower than DJ-1 WT, suggesting that this mutation may cause mild structural disturbances (213). The crystal structure of DJ-1A104T mutant shows displacement of Lys-72 and Lys-112 as a result of steric repulsion by the bulkier side chain of Thr-104, suggesting that A104T mutation causes local perturbations without major changes in global structure of DJ-1 protein (184). The mild effect of A104T on DJ-1 structure alone may not account for the pathological consequences of this heterozygous mutation. Further studies are needed to understand whether A104T mutation alters DJ-1 function or whether A104T mutation in conjunction with other mutations is responsible for the disease.

D149A: A heterozygous mutation in exon 7 was found in an Afro-Caribbean patient resulting in substitution of a charged polar Asp to a non-polar Ala (2). No second

mutation was found, suggesting a second hit, environmental insults or other genetic mutations, may contribute to the initiation and progression of the disease (2). The pathogenic mechanism of this mutation is unknown although it has been reported recently that Asp-149 is a caspase-6 cleavage site. By mutating Asp-149 to Ala-149, DJ-1 D149A mutant is resistant to the cleavage by caspase6 and thereby abolishes anti-apoptotic function of DJ-1 (109). However, it is not well-established how cleavage of DJ-1 WT by caspase6 contributes to its anti-apoptotic activity. Additionally, stability of the cleaved fragments of DJ-1 protein remains to be examined. Another proposed mechanism is that D149 causes slight disruption of the folding and thermal stability of DJ-1 protein, as shown that D149A mutant has less secondary structure features and lower melting temperature (213).

R98Q: Heterozygous substitution of R98Q (G/A substitution at the second codon) was found in three unrelated but pathologically proven cases of idiopathic PD and a disease affected sibling (125,136). No other mutation was identified in DJ-1 coding sequence and no large rearrangement mutation on DJ-1 was found in these subjects (125). The pathogenic relevance of this mutation is still under debate. It could be benign, as evidence suggests that the protein's stability and intracellular localization are no different from DJ-1 WT (29). However, it could also cause disease in combination with other mutations or environmental insults. Lastly, it could be a risk factor that renders vulnerability to the disease. Hedrich et al. reported that presence of R98Q mutation is 1.69% in 300 early onset PD patients and 1.52% in 99 controls (136). The occurrence of this mutation is higher than 1% and is not significantly different between patients and controls, therefore

R98Q variant should be considered as a polymorphism (136). Whether this variant poses as a risk factor to PD remains to be examined.

A179T and Exon1-5 duplication: Two novel heterozygous mutations on DJ-1 were recently identified in a screening of early-onset PD patients (average age of onset 41y). All three patients present with tremor. One patient has cognitive problems, and one has depression and sleep disorder (211). The substitution of a hydrophobic alanine by a polar hydrophilic threonine at helix 8 may interfere with the activation of DJ-1 zymogen. The pathogenic mechanisms of these two mutations remain to be characterized.

3. Phenotypes of DJ-1 knockout mice

Five lines of DJ-1 knockout (KO) mice have been generated and characterized. In one of the DJ-1 KO lines, exons 3-5 were replaced with a neomycin (Neo) selectable cassette in C57Bl/6 background (165). Cortical neurons derived from DJ-1 KO embryos show 20% increase in cell death induced by H_2O_2, compared to that of WT, and this vulnerability can be rescued by overexpression of DJ-1. Mesencephalic dopaminergic neurons (TH^+) from DJ-1 KO mice also show 30% decrease in rotenone-induced cell death. However, DJ-1 KO has no influence on the vulnerability caused by non-oxidative insults such as camptothecin, a topoisomerase I inhibitor. DJ-1 KO mice at the age of 8w and 13m display no gross motor behavior under normal conditions. However, locomotor activity was reduced by 50%, compared to DJ-WT mice, when treated with MPTP. Amphetamine-induced hyperlocomotion is reduced in DJ-1 KO mice as well, indicating that DJ-1 KO mice exhibit normal locomotor behavior when unchallenged, but have deficits upon challenges to the dopaminergic system. Loss of DJ-1 also sensitizes SNpc

neurons to MPTP-induced apoptosis, assessed by the number of viable TH^+ neurons after MPTP treatment (165).

Another line of DJ-1 knockout mice were created by homologous recombination, resulting in deletion of exon 2 (114). This line of DJ-1 KO mice was found to share similar phenotypes as dopamine D2 receptor null mice, although D2 receptor mRNA and protein levels are unaltered in DJ-1 knockout mice. The DJ-1 knockout mice have normal numbers of DA neurons in SN at 12m, but the evoked DA overflow in the striatum is reduced, primarily as a result of increased reuptake. Nigral neurons from knockout mice are less sensitive to the inhibitory effects of D2 autoreceptor stimulation as the inhibitory response of nigral neurons and the blockage of action potential by D2 receptor agonist are decreased in neurons from DJ-1 knockout mice. Corticostriatal long-term potentiation is normal in medium spiny neurons of DJ-1 knockout mice (which requires D1 receptor), but long-term depression (LTD) is absent (which requires both D1 and D2 receptor). The LTD deficit is reversed by treatment with D2 but not D1 receptor agonists. Furthermore, DJ-1 knockout mice display hypoactivity in the open field. The findings suggest an essential role for DJ-1 in DA physiology and D2 receptor-mediated functions (114).

The third line of DJ-1 knockout mice shows no major phenotypes. They have normal numbers of DA neurons in the SN, normal levels of dopamine, and normal levels of dopamine metabolites in the striatum at the age of 24-27 m. The number of the noradrenergic neurons in the locus coeruleus is also unchanged. Moreover, there is no accumulation of oxidative damage or inclusion bodies in brains from aged DJ-1 knockout mice, suggesting that loss of DJ-1 alone is insufficient to cause nigral degeneration and oxidative damage in the life span of mice (366).

The fourth line of DJ-1 mice was created by making a 9.3kb deletion, including the first 5 exons and part of the promoter. This deletion mutation resembles what was reported in patients. Behavioral analyses indicate that DJ-1 deficiency leads to age-dependent and task-dependent locomotor deficits. These deficits are detectable by 5 m of age, even though no obvious DA neuron loss can be detected in 6-month- and 11-month-old mice. However, neurochemical examination reveals significant changes in striatal DA function, consisting of increased DA reuptake rates and elevated tissue dopamine content. These data provide *in vivo* evidence that loss of DJ-1 function alters nigrostriatal DA function and produces motor deficits (53).

The fifth line of DJ-1 knockout mice was generated using an embryonic stem (ES) cell line from a library created with a gene trap targeting vector (Bay genomics, Davis, CA). An ES line with β-geo trap insertion located in the DJ-1 gene locus between exon 6 and 7 causes premature termination of DJ-1 protein transcription, resulting in a truncated transcript lacking the C-terminal portion that includes α-helix 6. The resultant truncated DJ-1 protein is likely not stable because using antibodies against the N- or C-terminus could not detect the protein (215). DJ-1 KO mice show a subtle locomotor deficit without changes in striatal DA or DA metabolites levels. However, increased DA uptake and binding were found in DJ-1 KO mice, probably due to increased level of dopamine transporter (DAT) in the pre-synaptic membrane fractions (215). MPTP exposure exacerbates striatal dopamine depletion in DJ-1 KO mice without affecting DA neuronal loss, evaluated by tyrosine hydroxylase (TH) and nissl staining. Consistent with the increased DAT level in presynpatic membrane, MPP^+ uptake by DA neurons is also

increased, potentially causing vulnerability of DJ-1 knockout mice to MPTP- induced toxicity (215).

4. Structure of DJ-1 protein

DJ-1 is a 189 amino-acid long protein that belongs to the DJ-1/ThiJ/PfpI superfamily of proteins. The function of ThiJ is currently unknown, although it might be related to the biosynthesis of thiamin. PfpI is an intraceullar protease that was first identified from the archaeon *Pyrococcsu furiosus,* and it is present in most bacteria and archaea (145,149,360). All of the proteins belonging to this superfamily have hydrolase activity and contain Cys-His or Cys-His-Asp/Glu as the catalytic group (145). The catalytic cysteine residue is structurally well conserved in the glutamine amidotransferase (GAT) superfamily and is located on the short kinked-loop connecting an α-helix and a β-strand, characterized as the "nucleophile elbow". As a result, the catalytic cysteine residue falls in an unfavorably allowed region in the Ramachandran plot. The structure of the intracellular protease PH1704 from *Pyrococcsu horikoshiihas* been solved and reveals the presence of a Cys-100/His101/Glu-74' catalytic triad. A Cys-185/His-186/Asp-214 catalytic triad was found in a structural homolog of this protease, the heat shock protein Hsp31 from *E. coli* (145,149,360).

In DJ-1 the connecting loop between α-helix5 and β-strand5 was found to form the nucleophile elbow similar to its homolog protease PH1704 (145). Cys-106 is located on the nucleophile elbow and has an unfavorable main chain conformation. His-126 is the putative catalytic residue located in close proximity to Cys-106 (145,149,360). The residues around the putative catalytic site in DJ-1 are also well conserved in DJ-1

homologues but no acidic residues are positioned near the H126 side chain. Conformational changes upon activation of DJ-1 protease may be required to form the complete catalytic triad, or the active site of DJ-1 family members may contain only Cys-His as the catalytic diad, similar to caspases. A cluster of three acidic residues (Glu15, Glu16, and Asp24') and two basic residues (Arg-48 and Arg 28') has been found near Cys-106. Arg48 and Arg28' residues are approximately 8Å away from the C106 residue in DJ-1, similar to the distance for the two Arg residues that recognize the P1 Asp residue in the substrate of caspases, suggesting that the substrate binding pockets of DJ-1 could be similar to that of caspases.

Structural comparison between DJ-1 and its archaeon homolog reveals that DJ-1 contains an additional α-helix (H8) at the C terminus, which distinguishes DJ-1 from the rest of the GAT superfamily (145,149,338). The extra α-helix H8 is thought to block the catalytic site of DJ-1 and may play regulatory roles. Additionally, His-126 has been shown to form hydrogen bond interaction with Pro-184 from the other subunit of DJ-1 monomer, which imposes an unfavorable orientation on the His-126 imidazole ring to form mature catalytic diad (145). It is also likely that helix H8 may prevent the formation of the catalytic triad with an acidic residue on the counterpart as in protease 1704. Most of the helices flank the two faces of a β- sheet, but the helix H8 projects away from the rest of the protein (192). A deletion mutant of DJ-1 missing residues 178-189 is still dimeric in solution and folded properly, suggesting that helix H8 is not critical for DJ-1 dimerization (192). But it contains several hydrophobic residues that may be part of the hydrophobic patch essential for the proposed chaperone activity of DJ-1. This

is supported by the finding that deletion of residues 178-189 on DJ-1 reduces its chaperone activity by 25% (192).

5. DJ-1 as protease zymogen

We have previously shown that wild type DJ-1 has intrinsic protease activity but its activity is weak, indicating that DJ-1 may exist as a zymogen and require activation to function as a mature protease. α-helix 8 (H8) is predicted to block DJ-1 protease activation and removal of H8 either by proteolysis or conformational change may activate DJ-1 zymogen function. Cleavage of DJ-1 has been reported by several investigators. Cleavage of recombinant DJ-1 between Gly-157 and Pro-158 has been shown under severe oxidation (265). The catalytic defective mutant DJ-1 C106S is not cleaved under the same condition, suggesting that DJ-1 may undergo oxidation-dependent cleavage (265). However, since this cleavage will remove α-helix 7, predicted to involve in dimerization based on DJ-1 structure, the stability of the cleaved DJ-1 is uncertain. Recently, caspase-6 has been shown to cleave DJ-1 at the C-terminus of Asp-149 and the C-terminal fragment of DJ-1 is proposed to be cytoprotective. However, the stability of the small segment of DJ-1 has not been demonstrated and the mechanisms by which it exert cytoprotection are largely unknown (109). Matrix metalloproteinase-14 (MMP14) has been shown to hydrolyze DJ-1 in a proteomic search to identify novel MMP14 substrates. Recombinant GST-DJ-1 could also be hydrolyzed by recombinant MMP14 (200:1 ratio) *in vitro*. The cleavage site on DJ-1 has been identified to be at the C-terminus of Gly-37 and Ala-111 using Edman sequencing (42). More recently, matrix metalloproteinase-3 (MMP3) has been reported to cleave DJ-1 in cells treated with MPP^+ and the cleavage of DJ- by MMP3 impairs its antioxidant function (57). However, since

DJ-1 is predominantly a cytosolic protein while MMPs localize to the plasma membrane or matrix, how DJ-1 is cleaved by MMPs in cells and the functional consequences of DJ-1 cleavage by MMPs remains to be investigated.

6. DJ-1 is a redox-sensitive protein and has antioxidant function

During an effort to identify hydroperoxide-responsive proteins (HPRPs), DJ-1 was found to be one of the 8 proteins that shifted its isoelectic point (p*I*) to more acidic isoforms in response to H_2O_2 treatment in human endothelial cells (235). It was later confirmed that the p*I* shift of DJ-1 was not restricted to H_2O_2 treatment but also occurred when cells were treated with herbicide paraquat, a ROS inducer (236), or endotoxin, an endogenous ROS elicitor (234). Oxidation of thiol side chain of Cys-106 to sulfinic acid has been demonstrated to account for the p*I* shift of DJ-1 (168). However, mutation of Cys-53 to Ala has been reported to abolish the p*I* shift of DJ-1 as well (145), suggesting that oxidation of Cys-53 could also be responsible for the p*I* shift. In addition to oxidations on cysteine residues, other modifications, including oxidation of other amino acids (such as methionine), and phosphorylation, that would cause acidic p*I* shift of DJ-1 can not be completely ruled out. Although the p*I* shift to more acidic form has been considered as a way to quench ROS and neutralize oxidants, the functional consequences of the PI shift of DJ-1 are still unclear. The cytoprotective activity of DJ-1 against oxidative stress cannot be explained solely by its direct scavenger of ROS, other mechanisms of activation of DJ-1 function in response to oxidation may exist to explain its roles in antioxidant defense.

Besides the above mentioned redox-dependent changes, DJ-1 has also been demonstrated to be oxidized at cysteine (168) and methionine residues (59). The reactive

cysteine, Cys-106, on DJ-1 is oxidized more easily than the other two cysteines, Cys-46 and Cys-53 (168). This is supported by other reports that Cys-106 is sensitive to radiation damage during X-ray crystal structural analysis (360). Although it is acknowledged that Cys-106 is readily oxidized, the functional implication of its oxidation is still debatable. Cys-106 is highly conserved among DJ-1 homologues, including PfpI family and ThiJ family. Regardless of the exact enzymatic function DJ-1 may have, the Cys-106 is a reactive cysteine and is critical for DJ-1 enzymatic activity. As it shares structural homology to PfpI protease family, DJ-1 has been demonstrated to possess intrinsic protease activity (261). The Cys-106 is the catalytic nucleophile for DJ-1 protease activity and it has to be at the thiol state (-SH) to carry out nucleophilic attack (52,261). Cys-106 on DJ-1 has been shown to be indispensible for DJ-1 protease activity and oxidation of DJ-1 has been shown to abolish its protease activity (52), as expected for any cysteine protease. DJ-1 has also been proposed to have chaperone activity, which is only active when Cys-106 is in cysteine sulfinic acid form (303). Therefore, oxidation on DJ-1 may activate or inactivate its enzymatic activity, depending on the extent of the oxidation and the nature of the enzymatic activity. Further investigation on the biochemical property and biological function of DJ-1 is required to understand the regulation of DJ-1 function via oxidation at the critical cysteine residue. Two methionines at the core of DJ-1 protein are oxidized to MetO in brain samples from normal individuals, indicating a signaling role (59). Studies in Chapter III are aimed to address how methionine oxidation affects DJ-1 function.

DJ-1 has displayed another potential redox-dependent change. In addition to the induced expression of DJ-1 protein by oxidative stress (168,234,235) or UV irradiation

(306,329), translocation of DJ-1 to mitochondria upon oxidative stress (44) or to nuclei when cells were irradiated by UV has also been demonstrated (306). The mechanisms of the induction and translocation of DJ-1 are still unknown but it is possible that the binding profile of DJ-1 is different when cells are under oxidative stress. The redox-dependent changes of DJ-1 binding profile, possibly resulting from conformational changes of either DJ-1 or its interactors, could then lead to rapid changes in intracellular localization of DJ-1. Conformational changes of DJ-1 itself under oxidizing conditions could be induced by posttranslational modifications such as ubiquitination, SUMOylation, oxidation or phosphorylation. On the other hand, the changes in DJ-1 binding profile could also be caused by conformational changes of DJ-1 interacting proteins, which may be subjected to redox-dependent regulation. Additionally, expression of DJ-1 protein is reportedly to be induced by oxidative stress or UV irradiation too.

7. The mechanisms underlying DJ-1 mediated antioxidant function are unknown

Despite the acknowledgment that the antioxidant function of DJ-1 contributes to its cytoprotection the precise mechanism is undetermined. DJ-1 has been shown to quench H_2O_2, which may explain part of its antioxidant function (329). Although DJ-1 has also been shown to act as an atypical peroxidase, its catalytic efficiency is 1-2 orders lower than peroxiredoxin, a known peroxidase (13). No other antioxidant enzymatic activity of DJ-1 has been reported. Notably, it was demonstrated that H_2O_2 -induced ROS burst was not altered in DJ-1 $^{-/-}$ ES cells, despite the sensitivity of DJ-1 $^{-/-}$ ES cells to H_2O_2-induced apoptosis (222). This leads to the hypothesis that the main effect of DJ-1 is not to quench ROS directly but to potentiate cellular responses to ROS. This hypothesis is supported by findings that DJ-1 regulates the activity of a variety of redox-dependent

proteins, such as Akt (367), ASK1 (117,159,352), glutamate cysteine ligase (GCL) (378), p53(38,94,95,307), nuclear factor erythoroid 2-related factor 2 (Nrf2) (66), and peroxisome proliferator-activated receptor –γ coactivator 1α (PGC-1α) (364,373,375). DJ-1 has been shown to potentiate Akt pro-survival pathway in *Drosophila* (367), possibly through inhibition of the Akt inhibitor phosphotase PTEN (167). Additionally, DJ-1 was reported to suppress ASK1-mediated apoptosis by either preventing ASK1 release from its inhibitors (352) or by sequestering ASK1-effector Daxx (159). There is also evidence that DJ-1 can upregulate glutathione synthesis by increasing the transcription and enzymatic activity of the rate-limiting enzyme of glutathione synthesis GCL in response to oxidative stress (378). Understanding how DJ-1 regulates a variety of signaling proteins to increase cellular response to oxidative stress is important and will shed light on the pathophysiological mechanisms of PD.

Proteases

Proteases, also known as proteolytic enzymes, are enzymes that catalyze the breakdown of proteins by hydrolysis of peptide bonds. Using bioinformatics analysis of the mouse and human genomes, at least 500-600 proteases (~2% of the genomes) have been identified (208). Through evolution, proteases have adapted to the wide range of conditions found in complex organisms and use different catalytic mechanisms for substrate hydrolysis. Proteases can be classified into six classes based on their mechanisms of catalysis: serine, cysteine, threonine, aspartic, metallo- and glutamic proteases (with glutamic proteases being the only subtype not found in mammals so far) (208). To maintain normal cell/tissue development and organism homeostasis, protease activity needs to be tightly controlled. Inappropriate proteolysis has been implicated in

cancer, cardiovascular disease, inflammation, neurodegeneration, and infectious disease (208).

1. Catalytic strategy of cysteine proteases

For all six classes of proteases, a nucleophile is required to attack the carbonyl group of the substrate. For a cysteine protease, a cysteine residue, activated by a histidine residue, serves as the nucleophile that attacks the peptide bond (Figure I-1, adapted from figure 9.8 in chapter 9 of Biochemistry) (26). After substrate binding (step1), the reactive cysteine thiol group attacks the carbonyl group of the substrate (step 2). The nucleophilic attack changes the geometry around the carbon atom from trigonal planar to tetrahedral, which is unstable. The charge is stabilized by interactions with NH- group from the substrate in a site termed the "oxyanion hole" and this interaction helps the formation of the acyl-enzyme intermediate (step 3). The amine component is then free to depart from the enzyme (step 4) and is replaced by a water molecule (step 5). The ester group of the acyl-enzyme is now hydrolyzed by a process that is essentially a repeat of steps 2 through 4. The water molecule attacks the carbonyl group while a proton is removed by the histidine residue, which acts as a general acid catalyst now, forming a tetrahedral intermediate (step 6). This structure breaks down to form the carboxylic acid product (step 7). Finally, the release of the carboxylic acid product (step 8) allows the enzyme to function in another round of catalysis.

2. Substrate specificity of proteases

The substrate binding pocket of a protease contains so called subsites that are numbered S_1-S_n upwards towards the N terminus of the substrate (non-primed sites), and S_1`-$S_n$`

towards the C terminus (primed sites), beginning from the sites on each side of the scissile bond (Figure I-2). Each subsite can accommodate a single side chain of a substrate residue. The substrate residues being accommodated are numbered P_1-P_n, and P_1`-$P_n$`, respectively. The structure of the substrate binding pocket of a protease therefore determines which amino acid can fit in (known as the intrinsic subsite occupancy), thereby determining substrate specificity of a protease. For example, the specificity of chymotrypsin is dependent on a hydrophobic pocket at the amino-terminal side of the scissile bond (the bond to be cleaved), into which long and uncharged side chains of phenylalanine and tryptophan can fit (25).

3. Activation of zymogens

Proteases can be regulated by various ways, including transcriptional regulation, activation of zymogens, blockage by endogenous inhibitors, targeting to specific compartments, and post-translational modifications such as glycosylation, metal binding, disulfide bridging, proteolysis, and degradation (208). However, a common way of protease activation is by cleavage of zymogens. In fact, many proteases including digest proteases (pepsin, chymotrypsin, trypsin), blood clotting proteases, caspases, are activated by limited proteolysis of zymogens (208). The activation of zymogens can be either autoproteolytic (115) or proteolyzed by other proteases (86). In some cases it requires additional factors or platforms, such as the apoptosome which mediates the activation of caspase zymogens (86). Some pro-domains have no known function, such as digestive proteases, but some pro-domains of zymogens contain recognition sites for interaction with substrates or cofactors, determining localization of proteases and how the zymogen is activated (208). For example, the pro-domain of the initiator caspase-8

contains the death effector domain (DED) that recruits caspase-8 to Fas-associated protein with death domain (FADD). The recruitment allows dimerization of caspase-8, which is monomeric in the dormant state. The dimeric caspase-8 is activated through induced fit and will cleave the pro-domain. Caspase-7 is an executioner caspase and exists as a dimer in dormant state already, but the dimeric caspase-7 has little protease activity. Instead, the dimeric caspase-7 is cleaved by initiator caspases at the consensus caspase cleavage site located at the linker domain. The N-terminal pro-domain of caspase-7 is much shorter than initiator caspases and does not appear to interact with other proteins but is still required for the activation (31).

4. Physiological and pathological roles of proteases

Protein degradation is as important for cellular viability as protein synthesis and therefore proteases have been considered as the guardians of cellular homeostasis. In addition to regulating protein turnover, proteases can also modulate protein function irreversibly by limited proteolysis. A number of key cellular functions are controlled by different proteases such as the execution of apoptotic cell death by caspases, degradation and elimination of abnormal proteins by lysosomal proteases or proteasome, and cancer metastasis facilitated by metalloproteases and cathepsins (208). Therefore, dysfunction of proteases could lead to various diseases, including cancer, neurodegenerative disorder, inflammation, and infectious diseases.

The importance of properly controlled protease activity in maintaining neuronal function and survival has been recognized. Mitochondrial proteases are important for degrading misfolded proteins and maintaining the homeostasis of mitochondria. As

mitochondrial dysfunction plays a key role in neurodegenerative diseases, the importance of mitochondrial proteases in the pathogenesis of neurodegenerative diseases has been under appreciated, especially after the discovery that mutations of a mitochondrial serine protease HtrA2 lead to neurodegenerative disorders (223). Proteasomes and lysosomes, are two major organelles responsible for proteins clearance. Proteases within these two compartments are the final players that execute the degradation of unwanted proteins and are required for carrying out proteasomal or lysosomal dependent protein degradation (247). Deficiency of these proteases have been shown to cause neurodegeneration (62,71,301).

5. Cysteine proteases are sensitive to oxidative inhibition

Cysteines proteases are dependent on the reactive cysteine for initiating catalytic reaction. To carry out the nucleophlic attack, the reactive cysteine must be in the thiol state and therefore cysteine proteases are subject to oxidative or nitrosative inhibition (207). Prolonged and excess oxidation/nitrosylation has been shown to inactivate caspase function and switch the cell death pathway from apoptosis to necrosis (130). Calcium dependent cysteine protease calpain is also known to be inhibited by oxidation (123). The threshold of oxidation to inhibit individual cysteine proteases is determined by the local environment of the catalytic pocket and the availability of antioxidants or transition metals that influence the susceptibility of the reactive cysteine to oxidation/nitrosylation. Since patients affected by neurodegenerative disease show higher levels of oxidative stress due to either environmental factors or genetic variations (83,368), the enzymatic activity of cysteine proteases is likely inhibited in those patients and may be a causal

factor of the disease progression. It has been shown that cysteine protease activity is hampered in the hippocampal region of brain samples from AD patients (219).

6. Dual function proteins with protease and chaperone activity

Molecular chaperones and proteases monitor and control the folding state of proteins and failure of this control will lead to protein misfolding and aggregation, a malfunction seen in neurodegenerative disorders (118). Chaperones can bind to hydrophobic patches of amino acids in substrate proteins that become exposed to solvent under certain conditions. Molecular chaperones may mediate the unfolding and refolding of client proteins, while proteases can cleave and degrade the client proteins (118). Proteins possess chaperone-protease dual functions have been characterized, including ATPase components of the ClpAP and ClpXP proteases, Hsp31, and DegP/HtrA family proteases. These dual function proteins can distinguish substrates beyond repair from those that can be refolded. The switch between the protease-chapeone function is tightly regulated and is well characterized in one family of dual function proteins, DegP/HtrA (65).

DegP, a member of the well conserved HtrA family of serine proteases, is a heat shock protein that combines chaperone and protease activity. DegP is a bacterial protein that is critical for unfolded protein response in the bacterial envelop, whereas the human HtrA proteins are implicated in various disorders including PD (324) . The DegP/HtrA protease family is an ATP-independent serine protease family that contains an N-terminal regulatory domain, serine protease domain, and C-terminal PDZ domain. The bacterial DegP has been reported to function as a protease at temperature > 30 ^{o}C and as a chaperone at temperature < 28 ^{o}C (324). Three different oligomeric states of DegP have

been reported: hexamer ($DegP_6$), dodecamer (DegP12), and 24-mer ($DegP_{24}$). The $DegP_6$ is formed by staggered association of two trimeric rings with a central core of protease domain and PDZ domains at the periphery (324). Access to the protease domain is restricted by the PDZ domains, which is believed to control the substrate entry as well as oligomeric structure. Substrate binding will trigger further oligomerization of DegP via interaction between PDZ domains. $DegP_{24}$ has a larger pore which allows substrates to enter (324). It is thought that $DegP_6$ is the rest stage and transformation into larger oligomers allows the formation of the active catalytic pocket and activation of protease function. The conformational changes seem to dependent both on substrates binding and temperature (179,324).

Redox regulation of protein functions

1. Generation of ROS and the antioxidant systems

Reactive oxygen species (ROS) are generated as part of the normal aerobic cellular existence and as a result of environmental insults. ROS can be produced by different ways, such as irradiation (X-rays, γ-rays, ultraviolet A), metal-catalyzed oxidation systems, inflammatory processes, electron-transport processes, lipid peroxidation, glycation/glycoxidation, oxidase-catalyzed reactions, environmental pollutants (98). Through these different ways, a variety of free radicals (superoxide, hydropeoxyl radical, alkyl radical, peroxyl radical, thiyl radical, sulfinyl radical, thioperoxyl radical, disulfide radical anion, etc) and non-radical oxygen derivatives are produced. To keep the level of ROS in check, a complex antioxidant system exists in cells to reduce the level of ROS, and repair and replace the damaged bio-molecules. Antioxidant enzymes that can reduce the level of ROS, include 1) superoxide dismutases (SODs), that catalyze the breakdown

of the superoxide anion into oxygen and hydrogen peroxide, 2) peroxiredoxins, that catalyze the reduction of hydrogen peroxide, organic hydroperoxides, and peroxynitrite, 3) catalases, that catalyze the conversion of hydrogen peroxide to water and oxygen using either an iron or manganese cofactor, 4) and thioredoxin and glutathione system, that function as protein disulfide reductases (98). In addition to the enzymatic systems, small antioxidants, such as ascorbic acid, glutathione, tocopherols, and uric acid, also exist in cells to neutralize ROS without enzymatic reactions (98). A delicate balance of intracellular redox status is normally maintained by several processes, 1) the generation rate of ROS, 2) the reduction rate of ROS via antioxidant enzymes or non-enzymatic reactions, 3) the degradation of oxidatively modified products via proteases or other degradation systems. Disruption of the balance in favor of excess ROS contributes to many disease processes, including cardiovascular diseases, inflammatory diseases, neurodegenerative diseases and cancer.

2. Oxidation of the protein backbone

Oxidative modifications of lipids, DNAs and proteins are consequences of oxidative stress that may lead to cellular damage underlying various disease processes. The present work focuses on the oxidative modifications of proteins. Free amino acids and amino acid residues in proteins are highly susceptible to oxidation and can be modified on the polypeptide backbone as well as the side chains. Oxidative attack of the polypeptide backbone is initiated by the $^{\cdot}OH$ dependent abstraction of α-hydrogen atom from an amino acid residue to form carbon-centered radical. The $^{\cdot}OH$ needed for this reaction may be obtained by radiolysis of water or by metal-catalyzed cleavage of H_2O_2 (fenton

reaction) (316). The carbon-centered radical formed reacts with O_2 to form an alkyl-peroxyl radical intermediate, which can give rise to the alkyl-peroxide, which may be converted to a hydroxyl protein derivative eventually (316). These intermediates may undergo additional reactions with other amino acid residues in the same or a different protein to generate a new carbon-centered radical capable of undergoing reactions similar to those initiated by hydroxyl radical ($^{\cdot}OH$). Peptide cleavage can occur through diamide or α-amidation pathways after the generation of alkoxyl radicals. It can also occur as a result of ROS attack of glutamyl, aspartyl, and prolyl side chains (316).

3. Oxidation of amino acid side chains

All amino acid residues of proteins are susceptible to oxidation by $^{\cdot}OH$, but some amino acid side chains are known to be more susceptible to oxidation. Cysteine and methionine are two sulfur-containing amino acids that are sensitive to oxidation even under mild conditions. Both cysteine and methionine can act as a general antioxidant to sequester free radicals as well as components of signaling relay systems. In addition to sulfur-containing amino acids, aromatic amino acids such as tryptophan, phenylalanine, tyrosine and histidine are also prone to ROS attacks (316). Furthermore, Amino acid residues close to metal binding sites are sensitive to metal-catalyzed oxidation (316). A list of oxidative modifications on amino acid sides chains is provided in table I-3, adapted from the review by Berlett and Stadtman (27). Oxidation of the side-chains of lysine, arginine, proline, histidine and threonine residues has been shown to yield carbonyl derivatives, which are considered as irreversible oxidations and are commonly used as a marker for protein oxidation (316).

4. Oxidation of cysteines

Reversible oxidation on reactive cysteines is the best characterized mechanism of redox-dependent signaling. Most cysteines have a p*Ka* around 8 and are normally protonated under physiological pH, which renders them nonreactive. Cysteines with low p*Ka* exist in thiolate anions state which is stabilized by nearby positively charged or aromatic side chains via charge-charge interactions. Thiolate anions are subject to various oxidative modification, including sulfenic acid (SOH), sulfinic acid (SO_2H), sulfonic acid(SO_3H), nitrylation (SNO), glutathionylation (SSG), and disulfide bond formation (S-S) (Figure I-3) (37). Sulfenic acid is not stable and can readily form other species such as disulfide bond and sulfinic acid. Most modifications on cysteine (except for sulfonic acid) are reversible, by oxidoreductases, such as glutaredoxin or thioredoxin systems (37). These distinct reversible modifications may enable the processing of different redox signals and lead to unique protein functional changes and responses.

5. Oxidation of methionines

Methionine can be oxidized to methionine sulfoxide (MetO) and methionine sulfone ($MetO_2$) by the addition of one and two oxygen atoms, respectively (318). Met residues are oxidized to MetO by different reactive oxygen species (ROS), including hydrogen peroxide (H_2O_2), ozone (O_3), hypochlorous acid (HOCl), alkyl peroxides (ROOH), and peroxynitrite ($ONOO^-$) (Figure I-4, equation 1). The oxidized met (MetO) can be regenerated by methionine sulfoxide reductase (Msr) to Met (Figure I-4, equation2). The oxidized Msr is reduced by thioredoxin (Trx), which regenerates Msr (Figure I-4, equation3). Thioredoxin reductase (TrxR) then in turn reduces thioredoxin at the expense of NADPH (Figure I-4, equation4). Therefore, the net result of Met-based free radical scavenging is the catalytic scavenging of reactive nitrogen or oxygen species by NADPH

(320). In humans, only one MsrA has been described but three MsrB have been identified, coded by three different genes. MsrA localizes to both cytosol and mitochondria. MsrB1 is a selenium-enzyme and localizes to mitochondria, MsrB2 to cytosol, and MsrB3 to ER (256). MsrAs are stereospecific towards the S isomer on the sulfur of the sulfoxide function whereas MsrBs are specific towards the R isomer.

The side chain of MetO or $MetO_2$ with extra oxygen atom(s) is stiffer and more polar than the side chain of methionine (147). These changes induced by oxidation of methionine are expected to alter the folding and conformation of the affected protein, thus regulate protein functions, including enzymatic activity (11,302), protein-protein interactions (11), protein stability (39,50), and oligomeric state (333). Oxidation of methionine to MetO can bereversed by methionine sufoxide reductase and this serves as the foundation of methionine-mediated redox signaling similar to the cysteine-based redox regulatory system (147). Methionine oxidation to methionine sulfone ($MetO_2$) is irreversible and usually leads to loss of biological functions (147).

6. Reversible oxidation of Met can regulate protein functions

Methionine can function as a general free radical scavenger, protecting other critical residues from being oxidized and can also mediate signal transduction. The surface- or solvent- exposed methionines are believed to act as endogenous antioxidants. It was first reported that oxidation of eight methionines on α-2-macroglobulin had no influence on its enzymatic activity until continued oxidiation of six additional methionine residues and a tryptophan, suggesting that there are some methionines more susceptible to oxidation and may serve as oxidant scavengers (287). This has been supported by the finding that eight

of the 16 methionines of glutamine synthetase from *E.coli* were oxidized without affecting the catalytic function of the enzyme and all the eight oxidized methionines were found to be relatively surface exposed while the methonine residues located in the core of the protein were not oxidized (196).

In addition to functioning as a general antioxidant by scavenging free radicals, reversible oxidation of Met to MetO can mediate cell signaling in response to intracellular redox changes. Oxidation of methionine on several proteins has been shown to regulate protein function reversibly, at least *in vitro* (256). α-1 proteinase inhibitor (API) loses its ability to inhibit neutrophils elastase once its Met351 and M358 are being oxidized and MsrA has been shown to partially store the activity of API *in vitro*. HIV-2 protease becomes inactive when two methionines are oxidized and treatment of oxidized HIV-2 protease with MsrA restores half of the activity. Calmodulin (CaM) is a calcium sensitive protein that regulates a variety of protein functions via binding to those proteins in a calcium dependent manner. Oxidation of two C-terminal methionines on CaM results in nonproductive binding of CaM with its client protein plasma membrane Ca-ATPase (PMCA) due to reduced helical propensity and a global rearrangement of the tertiary structure of the C-terminal globular. This disrupted interaction can be restored by MsrA (10,23). Met oxidation on IκB has been shown to cause IκB resistant to TNFα-induced proteasome degradation and prevent the dissociation of IκB from the nuclear factor NF-κB (232). Both MsrA and MsrB are required to reverse the oxidation of degradation of IκB and restore the activation of NF-κB (232).

7. Increased methionine oxidation has been implicated in neurodegenerative disorders

Irreversible oxidation of methionine to $MetO_2$ will lead to loss of protein function and to pathological situations in most cases. Met oxidation to MetO in combination with an insufficient reduction capacity is thought to have similar consequences. Therefore, Met oxidation is regarded as one of the sources for physiological dysfunctions in several age-associated changes and degenerative diseases (320).

Oxidative stress are believed to be responsible for various age-related degenerative diseases and ageing process (315). MsrA level in various regions of brains of AD patients is significantly lower than in brains of normal people (104). This is also echoed by the increased level of MetO in AD brains and accompanied higher protein carbonyls level (104). Brain has been shown to more vulnerable to methionine oxidation. Four brain regions (cortex, brain stem, hippocampus, and hypothalamus) in mice have higher level of MetO across all three age groups, compared to other tissues including liver, heart, kidney, and muscle, (320). This is consistent with the finding that brain has lower level of Msr expression than other tissues, therefore MetO is expected to accumulate in brain (320). Furthermore, an age-dependent decrease in the activity of MsrA in rat brain and kidney was observed (317). The action of the Msr system may prevent irreversible protein damage, contribute to the cellular antioxidant resistance and extend organism's life span. A major biological role of the Msr system is suggested by the fact that the MsrA null mouse is more sensitive to oxidative stress, accumulates higher levels of carbonylated protein and has a shorter life span than WT mice (257). In addition, the hippocampal region of MsrA $^{-/-}$ mice exhibit enhanced neurodegeneration,

hypersensitivity to H_2O_2, loss of astrocytes, elevated levels of β-amyloid deposition, and tau phosphorylation compared to WT controls (257) . This suggests that a deficiency in MsrA activity fosters an oxidative stress environment that is manifested by the accumulation of faulty proteins, deposition of aggregated proteins, and premature brain cell death.

The oxidation of Met residues has been implicated in ageing and neurodegenerative disorders. Oxidation of methioninine on three different brain proteins, α-Syn in PD, β-amyloid peptide in AD, and Prion PrPc form in Creutzfeldt–Jakob disease (CJD), have been reported to inhibit fibrillation of these proteins, followed by further oxidation by other radicals and refibrillation. The formation of α-synuclein containing inclusions in the dopaminergic neurons of the substantia nigra is a pathological hall mark of PD. It is believed that soluble oligomers (protofibrils) of α-synuclein, a step prior to forming fibrils, are the toxic species. Methionine oxidation denatures proteins and converts the hydrophobic properties of Met into hydrophilic causing structural alterations (318). Oxidation of all four methionine residues in α-synuclein to MetO has been shown to inhibit fibrillation of this protein *in vitro* and enhance toxicity of α-synuclein (144,346) Prion protein, also prone to oligomerize and aggregate, has been shown to be modified by methionine oxidation. Oxidation of methionine in the cellular prion protein (PrP^c) helix-3 render it resistant to proteinase K digestion (43) and switches on α-helix destabilization required for the conversion to infectious form prion protein (PrP^{sc}) (69). Methionine oxidation on β-amyloid, the major protein component in the amyloid plaquea of AD patients, has also been shown to inhibit its fibrillation, thus enhance the toxicity (269). Methionine oxidation on another PD

relevant protein, DJ-1, has also been reported, but the functional significance remains to be elucidated (59).

Hypotheses and Organizational Overview

The finding that loss-of-function mutations in DJ-1 are linked to autosomal-recessive early onset PD has emphasized the role of oxidative stress in PD pathogenesis (32). DJ-1 has been extensively reported to potentiate cellular response to oxidative stress but the exact molecular mechanisms are still unclear (74). Structural analysis reveals that DJ-1 shares homology with a bacterial and archea protease family and the C-terminal α-helix H8 of DJ-1 may inhibit DJ-1 protease activity. The major goal of this thesis is to understand the biological function of DJ-1 and elucidate the mechanism by which DJ-1 activates antioxidant response pathways.

In chapter II, I tested the hypothesis that DJ-1 functions as a protease and that protease activity of DJ-1 is critical for its antioxidant and cytoprotective functions. My findings demonstrate that deletion of α-helix H8 enhances DJ-1 protease activity without disrupting its dimerization or secondary structure. Mutations of the putative catalytic diad of DJ-1 abolish its protease activity, suggesting that DJ-1 functions as a cysteine protease with the Cys-106 and His-126 as the catalytic diad. Similar to other cysteine proteases, DJ-1 protease activity is sensitive to oxidative inhibition. Furthermore, we provide evidence that DJ-1 zymogen undergoes C-terminal cleavage in response to mild oxidative stress and that protease activity of DJ-1 is required for its cytoprotective function against oxidative stress.

To further understand how DJ-1 zymogen is activated in response to mild oxidation, I studied the roles of methionine residues in regulating DJ-1 protease activity, zymogen activation and cytoprotective function in chapter III. Methionine residue can be reversibly oxidized to MetO and two of the four methionines (Met-17 and Met-26) on DJ-1 are oxidized to MetO in brain samples from normal individuals, suggesting that these two residues could mediate signaling transduction. Additionally, M26I mutation has been identified in PD patients but the pathogenic mechanisms are not well characterized. By mutating individual methionine to isoleucine to prevent oxidation, the functional role of reversible oxidation of individual methioines on DJ-1 was tested. My data show that DJ-1 M26I and M17I mutants prevent DJ-1 zymogen processing although only DJ-1 M26I inhibits DJ-1 protease activity. Interestingly, Met-17 and Met-26 are located in the vicinity of the α-helix H8, making them good candidates to participate in conformational changes to remove the α-helix H8 upon oxidation. Additionally, DJ-1 M26I mutant has reduced secondary structure and is less stable than DJ-1 WT, suggesting that Met-26 is structurally important. Our findings also demonstrate that the PD linked M26I mutant is partially degraded through ubiquitin proteasome system and is insoluble when proteasomal function is impaired. Finally our results suggest that M17I, M26I, and M133I mutations diminish cytoprotective function of DJ-1.

Together, my findings indicate that DJ-1 exists as a zymogen and can be activated via C-terminal proteolysis under mild oxidative stress to function as a cysteine protease. Protease activity of DJ-1 is required for its cytoprotective function, suggesting that oxidation of the reactive cysteine will abolish cytoprotection mediated by DJ-1. In addition, my data demonstrate that oxidation of Met-17 may play a role in DJ-1 zymogen

activation and activating the cytoprotective function of DJ-1. I showed that oxidation of Met-133 is also important for DJ-1 mediated cytoprotection, but the mechanisms remain to be explored. I also demonstrated that the PD-linked M26I mutation causes unfolding and destabilization of DJ-1, contributing to PD pathogenesis. These findings have enriched our understanding of the biological functions of DJ-1, the pathogenic mechanisms of DJ-1 M26I mutation, and the role of methionine oxidation in regulating protein function.

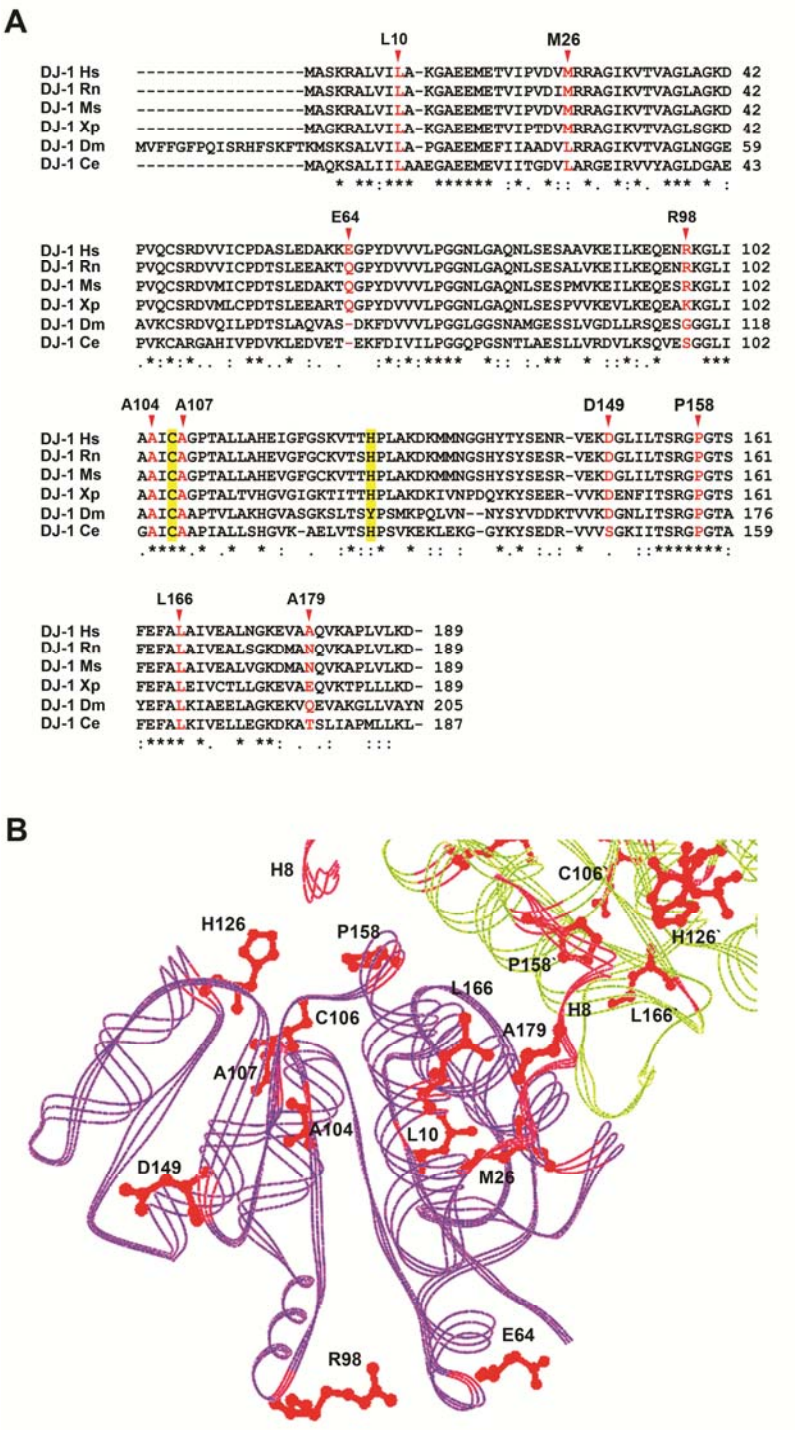

Figure I-1. Mutations on DJ-1 associated with PD. (A) Sequence alignment of DJ-1 homologues from different species with residues found to be mutated in PD patients highlighted in red and marked with arrow head. The catalytic diad residues (Cys-106 and

His-126 in *Homo sapiens*) were highlighted in yellow. Accession numbers are as follows: *Hs* DJ-1,NP_009193; *Rn* DJ-1, NP_476484.1; *Ms* DJ-1, NP_065594.2; *Xl* DJ-1, NP_001083896.1; *Dm* DJ-1, NP_651825.3; *Ce* DJ-1, AAB37889.1. *Hs, Homo sapiens; Rn, Rattus norvegicus; Ms, Mus musculus; Xl, Xenopus laevis; Dm, Drosophila melanogaster; Ce, Caenorhabditis elegans.* (B) The 3D-structure of the DJ-1 homodimer was determined by X-ray crystallography previously (PDB ID:1Q2U) (150) and illustrated using 3D Molecular Viewer software (Invitrogen). One monomer was depicted in purple and the other in green. Side-chains of residues found to be mutated in PD patients were highlighted in red. Side-chains of the catalytic diad of DJ-1 protease (Cys-106 and His-126) were also highlighted in red in both monomers and the α-helix H8 was also highlighted in red.

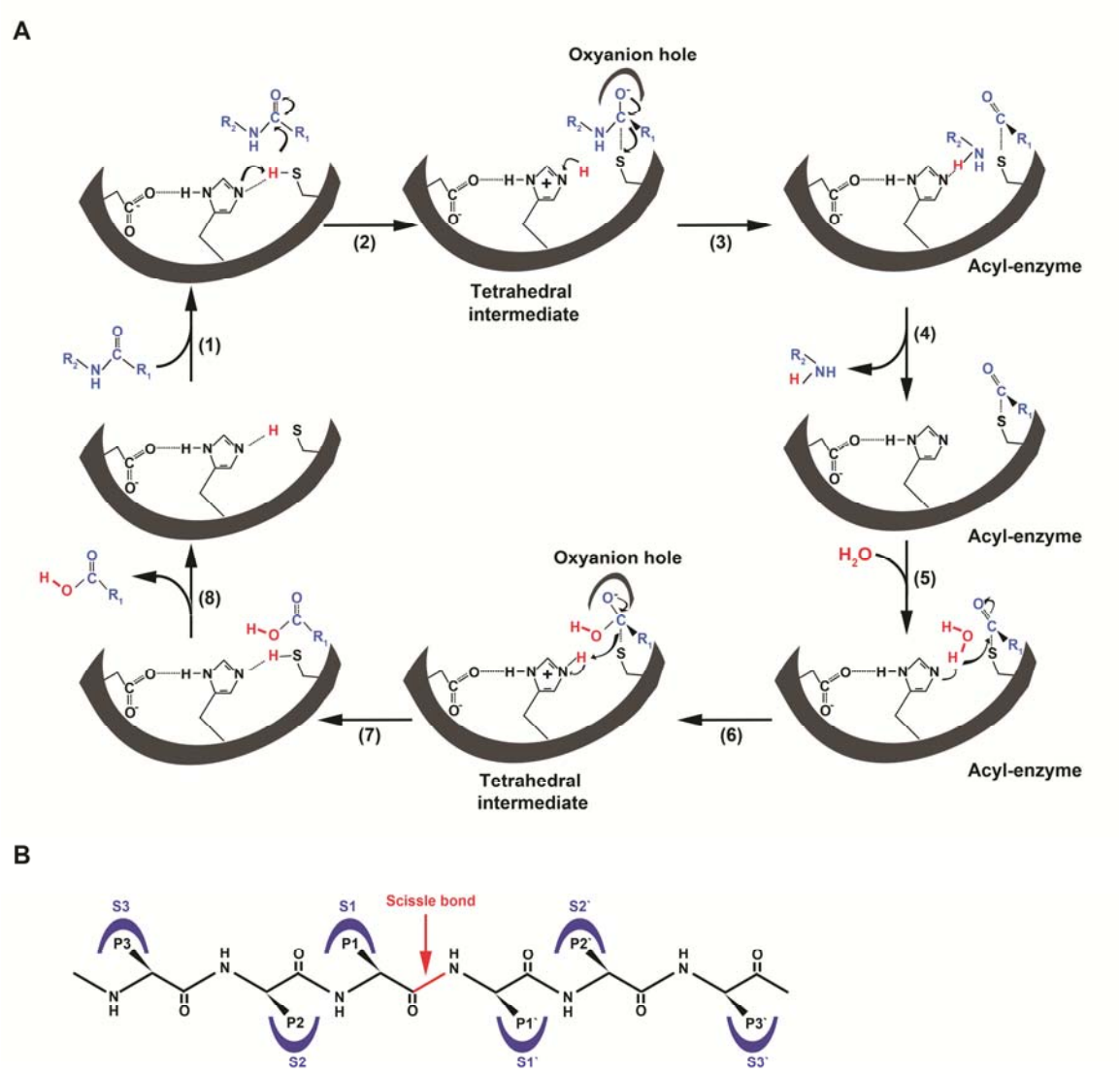

Figure I-2. Catalytic strategy of cysteine proteases and substrate specificity determinants of proteases. (A) The catalytic cysteine residue in a cysteine acts as a nucleophile to attack the peptide bond upon substrate binding (step1). The nucleophilic attack of the carbonyl group of the substrate by the cysteine thiol changes the geometry around the carbon atom from trigonal planar to unstable tetrahedral (step2). The charge is stabilized by interactions with NH- group from the protein in a site termed the "oxyanion hole", which helps the formation of the acyl-enzyme intermediate (step 3). The amine

component is then departed from the enzyme (step 4) and is replaced by a water molecule (step 5). The ester group of the acyl-enzyme is hydrolyzed by a process that is essentially a repeat of steps 2 through 4. The water molecule attacks the carbonyl group while a proton is removed by the histidine residue, which acts as a general acid catalyst, forming a tetrahedral intermediate (step 6). This structure breaks down to form the carboxylic acid product (step 7). Finally, the release of the carboxylic acid product (step 8) allows the enzyme to function in another round of catalysis. Adapted from figure 9.8 in chapter 9 of Biochemistry) (26). (B) Protease subsites determine substrate specificity. The binding pocket of the protease is composed of subsites (S), which are the side chains of amino acid that can accommodate peptide bonds (P) adjacent to the scissile bond (the bond to be hydrolyzed, highlighted in red) and position scissile bond into the active site. Subsites on the protease are numbered S_1-S_n upwards towards the N terminus of the substrate (non-primed sites), and S_1`-$S_n$` towards the C terminus (primed sites), beginning from the sites on each side of the scissile bond. The substrate residues are numbered P_1-P_n, and P_1`-$P_n$`, respectively. Adapted from figure 9.11 in chapter 9 of Biochemistry) (26)

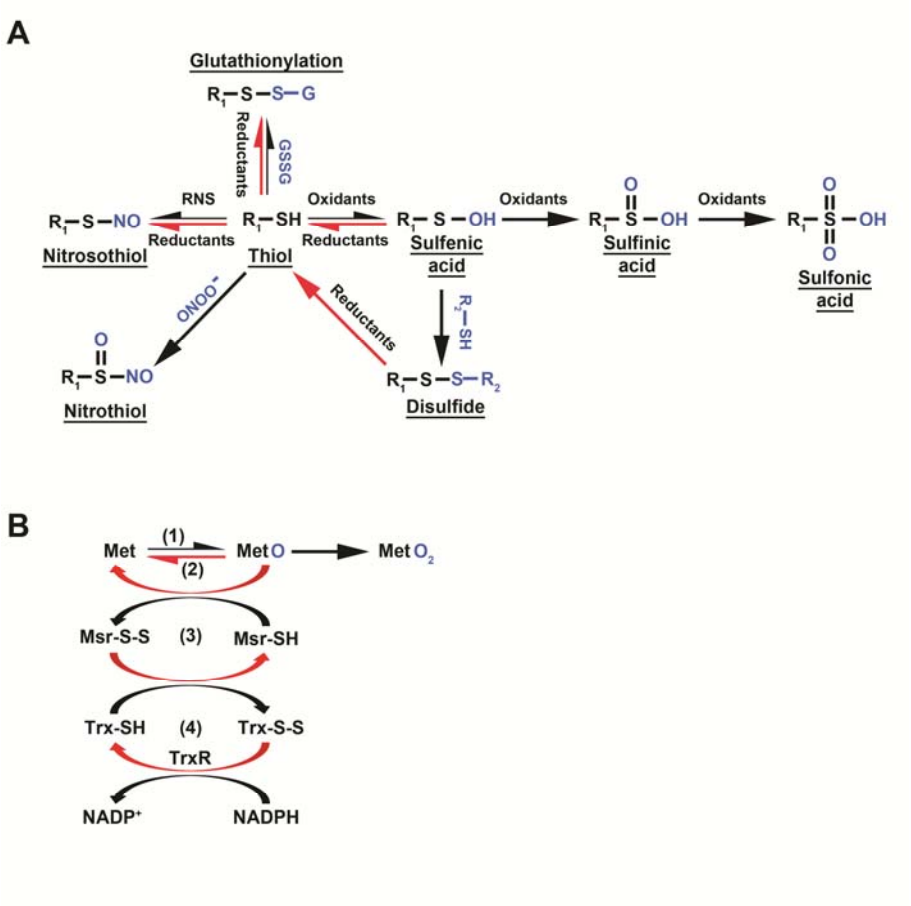

Figure I-3. Oxidative modifications on cysteines and methionines. (A) Oxidative modifications on cysteines. Oxidation of cysteine thiol groups (R_1-SH) results in sulfenic acid formation (R_1-SOH). Sulfenic acid can react to nearby thiols (R_2-SH) and form disulfide bond (R_1-S-S-R_2). Sulfenic acid will also be further oxidized to sulfinic acid (R_1-SO_2H) and sulfonic acid (R_1-SO_3H) under severe oxidation. Reaction of cysteine thiol to oxidized glutathione (GSSG) leads to formation of S-glutathionylation (R-S-SG). Cysteine thiol can also be oxidized by reactive nitrogen species (RNS) and peroxynitrite ($ONOO^-$) to form S-nitrosothiol and S-nitrothiol, respectively. Most modifications on cysteine (except for sulfonic acid) are reversible, by oxidoreductases, such as glutaredoxin or thioredoxin systems. Adapted from figure 1 in (37). (B) Methionine (Met) can be oxidized to methionine sulfoxide (MetO) and methionine sulfone ($MetO_2$)

by various reagents (equation 1). MetO can be reduced to Met by methionine sulfoxide reductase (Msr), during which Msr itself is oxidized from reducing (Msr-SH) to oxidized form (Msr-S-S) (equation2) by forming intramolecular disulfide bond between the catalytic cysteine and a resolving cysteine. The oxidized Msr (Msr-S-S) is in turn reduced by thioredoxin (Trx), at the expense of oxidation of Trx from Trx-SH to Trx-S-S (equation3). The oxidized Trx (Trx-S-S) is then reduced by thioredoxin reductase (TrxR) with NADPH as the ultimate reducing agent (equation4). Adapted from Figure 1 in (320).

Table I-1. Loci identified in familial forms of PD

Locus	Gene product	Inheritance	Lewy body pathology	Clinical symptoms
PARK1	α-synuclein	AD	Yes	Dementia
PARK2	Parkin	AR	No	Early onset
PARK3	Unknown	AD	Yes	Dementia
PARK4	α-synuclein	AD	Yes	Dementia, postural tremor
PARK5	UCH-L1	AD	No report	Not described
PARK6	PINK-1	AR	No report	Early onset, tremor
PARK7	DJ-1	AR	No report	Early onset, dystonia, psychiatric alterations
PARK8	LRRK2	AD	Yes	Late onset, tremor
PARK9	ATP13A2	AR	N/A	Kufor-Rakeb syndrome, very early onset
PARK10	Unknown	Unknown	N/A	Late onset
PARK11	Unknown	Unknown	N/A	Late onset
PARK12	Unknown	Susceptibility	No report	Late onset
PARK13	HtrA2/Omi	Susceptibility	No report	Late onset
PARK14	PLA2G6	AR?	No report	INAD, NBIA
PARK15	FBX07	AR?	No report	Pallid-pyramidal disease
PARK16	Unknown	Unknown	N/A	Late onset

Table I-2. DJ-1 mutations found in PD patients

Mutations	Onset (y)	Duration (y)	Types of mutations	References
Δexon 1-5	30-40	10-17	Homozygous	(32)
L166P	27-35	18-32	Homozygous	(32)
M26I	39	N/A	Homozygous	(2)
E64D	<40	N/A	Homozygous	(138)
L10P	19	N/A	Homozygous	(122)
P158DEL	34	N/A	Homozygous	(211)
A107P	<31	N/A	Homozygous	(107)
A104T	35	9	Heterozygous	(125)
D149A	36	N/A	Heterozygous	(2)
A179T	41	N/A	Heterozygous	(211)
Exon 1-5 Duplication	41	N/A	Heterozygous	(211)
R98Q	39-49	N/A	Polymorphism	(125,136)

Table I-3. Oxidative modifications on amino acid side chains

Amino acid	Oxidative modifications on side chains
Cysteine	Disulfide, sulfinic acid, sulfenic acid, sulfonic acid
Methionine	Methionine sulfoxide, methionine sulfone
Tryptophan	2-, 4-, 5-, 6-, and 7-Hydroxytryptophan, nitrotryptophan, kynurenine, 3-hydroxykynurinine, formylkynurinine Phenylalanine
Phenylalanie	2,3-Dihydroxyphenylalanine, 2-, 3-, and 4-hydroxyphenylalanine
Tyrosine	3,4-Dihydroxyphenylalanine, tyrosine-tyrosine cross-linkages, Tyr-*O*-Tyr, cross-linked nitrotyrosine
Histidine	2-Oxohistidine, asparagine, aspartic acid
Arginine	Glutamic semialdehyde
Lysine	*a*-Aminoadipic semialdehyde
Proline	2-Pyrrolidone, 4- and 5-hydroxyproline pyroglutamic acid, glutamic semialdehyde
Threonine	2-Amino-3-ketobutyric acid
Glutamyl	Oxalic acid, pyruvic acid

CHAPTER II

Parkinson disease protein DJ-1 converts from a zymogen to a protease by carboxyl-terminal cleavage

Abstract

Mutations in DJ-1 cause recessively transmitted early-onset Parkinson disease (PD), and oxidative damage to DJ-1 has been associated with the pathogenesis of late-onset sporadic PD. The precise biochemical function of DJ-1 remains elusive. Here we report that DJ-1 is synthesized as a latent protease zymogen with low intrinsic proteolytic activity. DJ-1 protease zymogen is activated by the removal of a 15-amino acid peptide at its C-terminus. The activated DJ-1 functions as a cysteine protease with Cys-106 and His-126 as the catalytic diad. We show that endogenous DJ-1 in dopaminergic cells undergoes C-terminal cleavage in response to mild oxidative stress, suggesting that DJ-1 protease activation occurs in a redox-dependent manner. Moreover, we find that the C-terminally cleaved form of DJ-1 with activated protease function exhibits enhanced cytoprotective action against oxidative stress-induced apoptosis. The cytoprotective action of DJ-1 is abolished by the C106A and H126A mutations. Our findings support a role for DJ-1 protease in cellular defense against oxidative stress and have important implications for understanding and treating PD.

Introduction

Parkinson disease (PD) is the most common neurodegenerative movement disorder, characterized by the loss of dopaminergic neurons in the substantia nigra pars compacta (186). Mutations in DJ-1 have been identified as the cause for an autosomal recessive, early-onset familial form of PD (2,32,125,135). Accumulating evidence indicates that DJ-1 mutations trigger neurodegeneration via a loss-of-function pathogenic mechanism (74). Our previous studies reveal that DJ-1 is widely expressed in many tissues and cell types, including dopaminergic neurons (262,264) and that oxidative damage to DJ-1 is linked to the pathogenesis of late-onset sporadic form of PD (60). Increasing evidence suggests that DJ-1 may also be involved in other age-related neurodegenerative disorders, such as Alzheimer disease, Lewy body dementia, and parkinsonism-dementia-amyotrophic lateral sclerosis complex (60,119,251,289).

DJ-1 is a 189-amino acid protein that was originally identified as an oncogene (246) and was also independently described as a regulatory subunit of a RNA-binding complex (142) and a protein involved in male infertility (172,173). Abnormal expression of DJ-1 has been associated with cancer (365,370), supporting the emerging view that there may be potential overlap in the underlying biochemical dysfunction between PD and cancer (67,163,354). DJ-1 has been implicated in multiple cellular processes, including oxidative stress response, protein quality control, anti-apoptotic signaling, transcriptional regulation, and translational control (74). Despite recent progress in the characterization of DJ-1, the precise biochemical function of DJ-1 remains unknown.

DJ-1 is an evolutionarily conserved protein that shares significant sequence homology with the PfpI family of bacterial intracellular proteases and with Hsp31, an *E. coli*

chaperone which also possesses protease activity (1,21,87,126,127,209,214). We and other groups have solved the crystal structure of human DJ-1, which shows that DJ-1 adopts a helix-strand-helix sandwich structure similar to that of bacterial protease PH1704 and Hsp31 (145,149,192,338,360). However, unlike PH1704 and Hsp31, DJ-1 does not have a Cys-His-Glu/Asp catalytic triad. Instead, DJ-1 contains the putative catalytic nucleophile Cys-106 which has the potential to form a Cys-His diad with His-126 (145,149,338). Although the lack of a catalytic triad has been used to argue against a protease function of DJ-1 (192,360), it has been proposed that DJ-1 may use the Cys-His diad to carry out its protease function (145,338). A fully functional Cys-His catalytic diad has been demonstrated in several cysteine proteases, such as caspases (322,353,359) .

Proteases perform essential functions in regulating diverse cellular processes by catalyzing the cleavage of peptide bonds (65,208,227,343,356). To avoid potentially hazardous consequences of unregulated protease activity, proteases generally reside in cells as latent precursors called zymogens and require an activation event for conversion into the catalytically active form (86,252). We have previously shown that full-length recombinant DJ-1 protein exhibits weak intrinsic proteolytic activity (262), suggesting that full-length DJ-1 is a protease zymogen. In this study, we investigated the mechanism for activating DJ-1 protease zymogen and characterized the role of DJ-1 protease in cytoprotection. Our results reveal that DJ-1 protease zymogen is activated by cleavage of a 15-amino acid peptide at its C-terminus and support a role for DJ-1 protease in cellular defense against oxidative stress-induced apoptosis.

Experimental procedures

Expression constructs and antibodies

The pCHA-DJ-1, pMyc-DJ-1, pET3E-DJ-1, and the corresponding C106A mutant forms of DJ-1 have been described previously (262). Conventional molecular biological techniques were used to generate the following additional DJ-1 constructs in the pCHA, pMyc, and pET3E vectors: DJ-1 H126A, DJ-1 WTΔC (residues 1-174) and its mutant forms DJ-1 C106AΔC and H126AΔC. All expression constructs were sequenced to confirm that the fusion was in the correct reading frame and there were no unwanted changes in the codons.

The rabbit polyclonal anti-DJ-1 antibodies, P7F and P7C, generated against purified full-length recombinant DJ-1 protein and a synthetic DJ-1 C-terminal peptide (residues 171–189), respectively, were described in our previous studies (262,264) . Other antibodies used in this study include the following: anti-HA (12CA5), anti-Myc (9E10.3, Neomarkers), anti-actin (Chemicon), anti-NeuN (Millipore), and anti-active-caspase-3 (Cell signaling). All secondary antibodies were purchased from Jackson ImmunoResearch Laboratories, Inc.

DJ-1 knockout mice and primary cell cultures

DJ-1 knockout mice were generated by Dr. Charles R. Gerfen at the National Institute of Mental Health and described previously (Manning-Boğ AB et al., 2007). A breeding colony of DJ-1 knockout mice was established from breeding pairs obtained from the National Institute for Neurological Disease and Stroke/University of California Los Angeles Repository for Parkinson disease Mouse Models using standard mouse

husbandry procedures (262,264). The genotype of the offspring was determined by PCR and the elimination of the DJ-1 protein was confirmed by Western blot analysis. Primary cortical and midbrain neuronal cultures were prepared from postnatal 0.5 day (P0.5) wild-type and DJ-1 knockout pups as described previously (4,111,191). Primary cortical and midbrain neuronal cultures were maintained in NeuroBasal Media (Gibco) supplemented with cytosine arabinoside (AraC) (Sigma) for 3–7 days. MEF cultures were prepared from embryonic day 13 mice as described (111,264), and early passage cells were used for all experiments.

Protein expression and purification

Wild-type and mutant DJ-1 proteins were expressed in *Escherichia coli* BL21 cells (CodonPlus) as untagged proteins and purified under reducing conditions as we described previously (149,262) by ammonium sulfate fractionation, Sepharose QXL ion exchange chromatography, and Sephacryl S-100 gel filtration chromatography (Amersham). Fractions containing DJ-1 were identified by SDS-PAGE and confirmed by immunoblot analysis with anti-DJ-1 antibody P7F. Protein concentration was determined by using the bicinchoninic acid (BCA) assay (Pierce).

Protease activity assays

Protease activities of DJ-1 WT and its mutants were measured by using a continuous, real-time fluorescence-based protease assay as described (156,262). Briefly, purified wild-type or mutant DJ-1 protein was incubated with BODIPY FL-labeled casein (10 μg/ml; Molecular Probes) in 50 mM Tris-HCl, pH 7.4, 200 mM NaCl, and 5 mM $CaCl_2$ at 37 °C. An increase in fluorescence upon protease-catalyzed hydrolysis of casein was

monitored continuously in a PerkinElmer Life Sciences LS55 luminescence spectrometer using an excitation wavelength of 505 nm and emission wavelength of 513 nm. Kinetic parameters (K_m and k_{cat}) were obtained as described (24) by fitting the data to the equation: $V = k_{cat} [S]_0 / (1 + K_m [E]^{-1})$. Trypsin (Athena Environmental Sciences, Inc.) was used as a positive control for the protease activity assay. The effect of redox state on DJ-1 protease activity was determined by pre-incubation of 50 μM DJ-1 WT or 50 μM DJ-1 WTΔC protein with 1 mM β-ME, 1 mM H_2O_2, or H_2O at 37 °C for 30 min before protease activity measurement.

DJ-1 cleavage analysis

For detection of endogenous DJ-1 cleavage *in vivo*, SH-SY5Y cells were treated with various concentrations of H_2O_2, rotenone, or MPP^+ for 24 h as indicated. The levels of full-length and processed forms of endogenous DJ-1 in the cell lysates were analyzed by immunoblotting with anti-DJ-1 antibodies P7C and P7F and quantified by using Scion Image software (NIH). For analysis of DJ-1 self-cleavage *in vitro*, 7.5 μg of purified recombinant DJ-1 WT, DJ-1 C106A, or DJ-1 WTΔC proteins were incubated with various concentrations of H_2O_2 as indicated at 37 ^oC for 30 min in a total reaction volume of 20 μl containing 50 mM Tris-HCl, pH 7.4, 200 mM NaCl, and 5 mM $CaCl_2$. The reaction was stopped by boiling in Laemmli sample buffer, and the proteins were resolved by SDS-PAGE followed by immunoblotting with the P7F antibody.

Cell transfection, immunoprecipitation, and immunoblot analysis

Cells were transfected with the indicated plasmids using Lipofectamine 2000 (Invitrogen) according to the manufacturer's instructions. Cell lysates were prepared from transfected

cells and immunoprecipitations were carried out as described previously (111,169,191,262,264) using anti-HA antibody followed by the recovery of immunocomplexes with protein G-Sepharose beads (Sigma). Immunocomplexes were then dissociated by boiling in the Laemmli sample buffer, resolved by SDS-PAGE, and immunoblotted with the indicated primary antibodies and horseradish peroxidase-conjugated secondary antibodies. Results were visualized using enhanced chemiluminescence (ECL).

Immunofluorescence confocal microscopy

Cells were fixed in 4% paraformaldehyde, stained with appropriate primary and secondary antibodies and processed for indirect immunofluorescence microscopy as described previously (111,169,191,262,264). Analysis and acquisition were performed using a Zeiss LSM 510 confocal laser-scanning microscope. Images were imported in TIFF format using LSM-510 software (Carl Zeiss MicroImaging, Inc.) and processed using Adobe Photoshop (Adobe Systems, Inc.) to adjust the contrast and brightness.

Cell viability and apoptosis assays

Cell viability was assessed using either the lactate dehydrogenase (LDH) release assay as described (106) or the 3-(4,5-dimethylthiazol-2-yl)-2,5-diphenyltetrazolium bromide (MTT) assay as described (Pridgeon et al., 2007; James Lee et al., 2008). For analysis of apoptosis in transfected SH-SY5Y cells, transfected cells were identified by the green fluorescence emitted from co-transfected GFP expression vector and apoptotic cell death was measured by morphological assessment of nuclei stained with 4′,6-diamidino-2-phenylindole (DAPI, Molecular Probes) as described (Pridgeon et al., 2007). The

percentage of transfected cells with nuclear fragmentation and chromatin condensation was scored for apoptosis. For analysis of apoptosis in transfected *DJ-1*$^{-/-}$ cortical neurons, cells were triple-stained with anti-NeuN as a neuronal cell marker, anti-DJ-1 antibody P7F for detection of transfected wild-type or mutant DJ-1, and DAPI for assessment of nuclear morphology. The percentage of DJ-1-transfected neurons with apoptotic nucleic was scored for apoptosis. For analysis of apoptosis in transfected *DJ-1*$^{-/-}$ midbrain neurons, transfected neurons were identified by immunostaining with anti-DJ-1 antibody P7F, and the extent of apoptotic cell death was determined by measurement of caspase-3 activation with anti-active-caspase-3 antibody and assessment of nuclear integrity with DAPI staining. The percentage of DJ-1-transfected neurons with active caspase-3 staining or with apoptotic nucleic was scored for apoptosis as described (369) .

Statistical analysis

All experiments were repeated at least three times. Data were subjected to statistical analysis by ANOVA and a *p* value of less than 0.05 was considered statistically significant.

Results

Cleavage of the C-terminal 15-amino acid peptide activates DJ-1 protease function without affecting its dimerization

We and other groups have previously reported that DJ-1 exists as a homodimer in the crystal structure (Fig. 1A) as well as in solution (145,149,192,262,338,360). The monomeric structure of DJ-1 is highly homologous to that of bacterial protease PH1704

except that DJ-1 has an additional α-helix, helix H8, at the C-terminus (Fig. 1B). This extra helix is generated because DJ-1 is 15 residues longer at the C-terminus than PH1704 and other proteases of the PfpI family (149,338). The H8-containing, 15-amino acid C-terminal tail is evolutionally conserved in DJ-1 orthologs across different species (209). In the crystal structure of DJ-1, the 15-amino acid C-terminal tail appears to block the access of substrates to the putative catalytic site containing the highly conserved, predicted catalytic nucleophile Cys-106 (Fig. 1A) (145,149,338).

The most commonly known mechanism for activation of protease zymogen is via specific proteolytic cleavage to remove an N-terminal peptide, often referred to as the pro-region (252). For some cysteine proteases, such as caspases, the activation involves the cleavage of an internal linker peptide (86,322). Based on the DJ-1 structural data (145,149,338) and sequence homology analysis (209), we hypothesized that activation of DJ-1 protease zymogen may involve the cleavage of its H8-containing C-terminal 15-amino acid peptide (Fig. 1A). To test this hypothesis, we generated DJ-1 WTΔC, a truncated form of wild-type DJ-1 lacking the C-terminal 15 amino acids (residues 175-189) (Fig. 1B and 1C). Recombinant DJ-1 proteins were expressed in *E. coli* and purified through ion-exchange and size-exclusion chromatography until the protein is pure as seen a single band on coomassie blue stain (Fig. 1D). The purified recombinant proteins were confirmed to be DJ-1 using immunoblot analysis (Fig. 1E). Co-immunoprecipitation analysis showed that HA-tagged DJ-1 WTΔC protein was able to dimerize with Myc-tagged DJ-1 WTΔC protein as well as with DJ-1 WT, the full-length form of wild-type DJ-1 protein (Fig. 2A and 2C), confirming that deletion of the C-terminal 15-residues has no effect on DJ-1 dimerization. We then assessed the protease activities of purified

recombinant DJ-1 WTΔC and DJ-1 WT proteins (Fig. 2D) by using a continuous, real-time fluorescence-based protease assay with BODIPY FL-labeled casein as the substrate (156,262). We found that DJ-1 WTΔC protein exhibited much higher protease activity than DJ-1 WT protein (Fig. 2D and 2E), indicating that removal of the C-terminal 15-amino acid peptide activates the protease function of DJ-1.

The C-terminally cleaved form of DJ-1 is an active cysteine protease with a functional Cys-His catalytic diad

Although DJ-1 does not contain a canonical Cys-His-Glu catalytic triad found in the PfpI family of cysteine proteases such as PH1704, structural comparison reveals that Cys-106 of DJ-1, like the catalytic nucleophile Cys-100 of PH1704, resides in a "nucleophile elbow" with a strained backbone conformation (145,149,338). Moreover, Cys-106 is located in close proximity to His-126 in the crystal structure (Fig. 1A) and has the potential to form a Cys-His catalytic diad with His-126 (145,338). A functional role of Cys-106 and His-126 is further suggested by the fact that both of these residues are evolutionally conserved in all DJ-1 orthologs across various species (21). However, whether Cys-106 and His-126 can form a catalytic diad is debatable (145,149,338,360) because in the crystal structure, the His-126 imidazole ring is in an unfavorable orientation for diad formation as it forms a hydrogen bond with the main-chain carbonyl group of Pro-184 in the helix H8 (Fig. 1A).

Our finding that removal of the helix H8-containing C-terminal 15-amino acid peptide activates DJ-1 protease function (Fig. 2) raises the possibility that elimination of the hydrogen bond formation between His-126 and Pro-184 by the C-terminal cleavage

may enable His-126 to form a catalytic diad with Cys-106 for carrying out the proteolytic function of activated DJ-1 protease. To test whether Cys-106 and His-126 can form a catalytic diad in the activated DJ-1, we used site-directed mutagenesis to generate DJ-1 C106AΔC and H126AΔC mutants, which replaced Cys-106 and His-126 with an Ala residue in the C-terminally cleaved form of DJ-1, respectively (Fig. 1C). Co-immunoprecipitation analysis confirmed that neither C106AΔC nor H126AΔC mutation affected DJ-1 dimerization (Fig. 2B and 2C). Protease activity assays revealed that the protease activity of DJ-1 WTΔC protein was abolished by the C106A mutation of the predicted catalytic nucleophile Cys-106 (Fig. 2D and 2E). Similarly, the protease activity of DJ-1 WTΔC protein was also abrogated by the H126A mutation of the putative Cys-His catalytic diad component His-126 (Fig. 2D and 2E). Together, these data support that the C-terminally cleaved form of DJ-1 is an active cysteine protease which uses the diad formed by Cys-106 and His-126 for catalysis.

DJ-1 cysteine protease is susceptible to inactivation by oxidation

Cysteine protease usually requires a reducing environment for achieving full activity because oxidation of the catalytic thiol group on the active site cysteine abolishes its ability to mediate nucleophilic attack for breaking the peptide bond (322). Given our result suggesting that DJ-1 functions as a cysteine protease with Cys-106 as the catalytic nucleophile (Fig. 2D and 2E), we next assessed whether DJ-1, like other cysteine proteases, can be inactivated by oxidation. Our protease assays revealed that pre-incubation of DJ-1 WTΔC protein with the oxidizing agent H_2O_2 (1 mM) for 30 min completely abrogated protease activity of DJ-1 WTΔC protein (Fig. 3A and 3B). In contrast, pre-incubation with the reducing agent β-mercaptoethanol (β-ME; 1 mM) did

not significantly alter protease activity of DJ-1 WTΔC protein (Fig. 3A and 3B). Similarly, protease activity of DJ-1 WT was also virtually abolished by pre-incubation with H_2O_2 but not by pre-incubation with β-ME (Fig. 3C and 3D). These results, together with the previous report that Cys-106 is the most sensitive cysteine residue of DJ-1 to H_2O_2-mediated oxidation(168), further support the function of DJ-1 as a cysteine protease and indicate that DJ-1 protease, in its active form or precursor form, is susceptible to inhibition by oxidation.

C-terminal cleavage activates DJ-1 protease by enhancing substrate binding as well as catalysis

To further characterize the activation of DJ-1 protease function by the C-terminal cleavage, we performed kinetic analyses of casein proteolysis catalyzed by DJ-1 WT and DJ-1 WTΔC proteins (Fig. 4). The kinetic parameters K_m and k_{cat} were determined from the double reciprocal plots (Fig. 4B and 4D) as described (24) and summarized in Table 1. As a positive control, we analyzed trypsin-mediated casein proteolysis in parallel and found that trypsin has a K_m of 6.5 μM and k_{cat} of 1.4 s^{-1}, which are similar to the values reported previously (90,96), validating our assay system. Our analyses showed that the K_m value of DJ-1 WTΔC is more than 5-fold lower than that of DJ-1 WT (Table 1), suggesting that the cleavage of the C-terminal 15-amino acid peptide enhances substrate binding. Moreover, DJ-1 WTΔC has a 4.6-fold greater k_{cat} value than DJ-1 WT (Table 1), suggesting that the C-terminal cleavage also enhances the catalysis. The combination of these two effects leads to a 26-fold greater catalytic efficiency (k_{cat}/K_m) for DJ-1 WTΔC compared to DJ-1 WT (Table 1). The increase in catalytic efficiency after zymogen activation is often referred to as zymogenicity (322,327). Our kinetic studies thus

indicate that DJ-1 protease has a zymogenicity of 26, when activated by the removal of the C-terminal 15-amino acid peptide.

Endogenous DJ-1 in dopaminergic cells undergoes C-terminal cleavage in response to mild oxidative stress

The observed activation of DJ-1 protease zymogen upon removal of its C-terminal 15 residues (Fig. 2 and 4) prompted us to investigate whether endogenous DJ-1 can undergo C-terminal proteolytic processing in human SH-SY5Y dopaminergic cells. For detection of C-terminally cleaved form of endogenous DJ-1, we took advantage of two anti-DJ-1 antibodies, P7C and P7F, which we generated and characterized previously (262,264). P7C was generated against the C-terminal 20 residues of DJ-1 (Fig. 1D), and this antibody selectively recognizes full-length DJ-1 but not C-terminally cleaved form of DJ-1, such as DJ-1 WTΔC (Fig. 5, A-C). In contrast, P7F was raised against purified full-length DJ-1 recombinant protein (Fig. 1D), and this antibody is capable of detecting both full-length and C-terminally cleaved forms of DJ-1 (Fig. 5, A-C). Using these antibodies, we found that, under normal cell culture conditions, endogenous DJ-1 existed primarily in the full-length form in cells (Fig. 5, A-C), indicating that, in common with other proteases, DJ-1 is synthesized as a latent protease zymogen. In response to oxidative stress induced by H_2O_2 (Fig. 5A), rotenone (Fig. 5B), or 1-methyl-4-phenylpyridinium (MPP^+) (Fig. 5C), endogenous DJ-1 underwent C-terminal cleavage, resulting in a processed form of DJ-1 protein (DJ-1_p) that was recognized specifically by the P7F antibody but not by the P7C antibody (Fig. 5, A-C). The endogenous DJ-1_p protein had an apparent molecular weight of ~17 kDa, which was very close to that of recombinant DJ-1 WTΔC (Fig. 5, A-C), supporting that the proteolytic processing of endogenous DJ-1

occurs at its C-terminus near residue 174. Interestingly, the level of endogenous DJ-1_p was significantly higher in cells treated with low concentrations of rotenone, MPP^+, or H_2O_2 (Fig. 5), namely at a dosage equivalent to the LD_{10} of rotenone, LD_{25} of H_2O_2 or LD_{10} of MPP^+ where there was no overt cell death (Fig. 5 compared with Supplementary Fig. 1). Together, these data suggest that endogenous DJ-1 protease zymogen in dopaminergic cells is activated in response to mild oxidative stress.

Previous studies have shown that auto-proteolysis is involved in activation of a number of protease zymogens (31,115), therefore we sought to determine whether DJ-1 is capable of auto-proteolysis in response to oxidative stress. Purified recombinant DJ-1 WT, DJ-1 C106A, or DJ-1 WTΔC proteins were incubated with various concentrations of H_2O_2 and the potential proteolysis of these proteins was assessed by immunoblot analysis with anti-DJ-1 antibody P7F. As shown Supplementary Fig. 2, no detectable self-cleavage of DJ-1 proteins was observed, arguing against the possibility that DJ-1 is activated by auto-proteolysis.

DJ-1 protease activation by C-terminal cleavage enhances its cytoprotective function

To determine the functional consequence of DJ-1 protease activation in cells, we first examined the effect of DJ-1 C-terminal cleavage on the vulnerability of SH-SY5Y cells to oxidative stress induced by PD-relevant toxicant rotenone. Consistent with previous reports (46,329,377), we found that over-expression of full-length DJ-1 WT protein in SH-SY5Y cells significantly reduced rotenone-induced apoptotic cell death, as measured by the lactate dehydrogenase (LDH) release assay (Fig. 6A and 6B) and apoptotic nuclear

morphology analysis (Fig. 7). The cytoprotective action of DJ-1 was further enhanced by the C-terminal cleavage, as transfected SH-SY5Y cells expressing DJ-1 WTΔC were significantly more resistant to rotenone-induced apoptosis than cells expressing similar level of DJ-1 WT (Fig. 6A and 6B, Fig. 7). The ability of DJ-1 WT and DJ-1 WTΔC to protect SH-SY5Y cells against rotenone-induced apoptosis were abrogated by the catalytic site mutations C106A and H126A (Fig. 6A and 6B), indicating that the protease activity of DJ-1 is required for its cytoprotective action.

To provide further evidence for the involvement of DJ-1 protease activation in cytoprotection, we assessed the role of DJ-1 C-terminal cleavage in cellular defense against oxidative stress using the mouse embryonic fibroblasts (MEFs) cultured from the DJ-1 knockout (*DJ-1*$^{-/-}$) mice (259). The *DJ-1*$^{-/-}$ MEF cells lack DJ-1 expression, as confirmed by immunoblot analysis with anti-DJ-1 antibody P7F (Fig. 6C), and thus allow experiments to directly compare the cytoprotective actions of the full-length and C-terminally cleaved forms of DJ-1 without interference from endogenous DJ-1. We found that *DJ-1*$^{-/-}$ MEFs were significantly more susceptible than *DJ-1*$^{+/+}$ MEFs to rotenone-induced cell death (Fig. 6C and 6D). The pro-apoptotic phenotype of *DJ-1*$^{-/-}$ MEFs were suppressed more effectively by expressing DJ-1 WTΔC than by expressing DJ-1 WT in these cells (Fig. 6C and 6D), indicating that the C-terminally cleaved form of DJ-1 has a stronger cytoprotective capability than the full-length DJ-1. The capability of DJ-1 WTΔC and DJ-1 WT to suppress the pro-apoptotic phenotype of *DJ-1*$^{-/-}$ MEFs was abolished by the C106A mutation of the putative catalytic nucleophile (Fig. 6C and 6D). These data, together with the observed effects of DJ-1 truncation and mutations on its

protease activity (Fig. 2), support that DJ-1 protease activation by C-terminal cleavage enhances its cytoprotective function.

Activated DJ-1 protease exerts enhanced neuroprotection against oxidative stress-induced apoptosis

To directly determine the role of DJ-1 protease activation in neuroprotection, we expressed the full-length and C-terminally cleaved form of wild type and mutant DJ-1 in primary cortical neurons cultured from *DJ-1*$^{-/-}$ mice. Immunostaining of transfected *DJ-1*$^{-/-}$ cortical neurons with anti-DJ-1 antibody P7F confirmed that DJ-1 WT and DJ-1 WTΔC and their C106A mutant forms were expressed at similar levels with an intracellular distribution pattern (Fig. 8A) similar to that of endogenous DJ-1(262,264). Apoptosis assays revealed that expression of DJ-1 WTΔC protein was significantly more effective in reducing rotenone-induced apoptosis in *DJ-1*$^{-/-}$ cortical neurons than full-length DJ-1 WT protein (Fig. 8). The ability of DJ-1 WT and DJ-1 WTΔC to rescue the pro-apoptotic phenotype of *DJ-1*$^{-/-}$ cortical neurons was abrogated by the protease-dead C106A mutation (Fig. 8), indicating that the protease activity of DJ-1 is required for its neuroprotective action. We then repeated the same experiments in primary midbrain neurons cultured from *DJ-1*$^{-/-}$ mice and found that, compared to full-length DJ-1 WT protein, the C-terminally cleaved form of DJ-1 exerted a stronger neuroprotective action in *DJ-1*$^{-/-}$ midbrain neurons in a protease-dependent manner (Fig. 9). Together, these findings provide strong evidence that DJ-1 protease activation by C-terminal cleavage enhances its neuroprotective function.

Discussion

The identification of homozygous mutations in DJ-1 as a cause for autosomal recessive PD (2,32,125,135) and the association of abnormal DJ-1 expression with cancer (365,370) highlight the importance of understanding the biochemical function of this ubiquitously expressed protein. Although DJ-1 has been implicated in several cellular processes (74), the precise biochemical function of DJ-1 remains elusive. The present study reveals that DJ-1 is synthesized as a latent protease zymogen and its C-terminal cleavage activates DJ-1 cysteine protease function. Our data indicate that DJ-1 protease plays a role in cellular defense against oxidative stress-induced apoptosis and provide new insight into the mechanism of action for DJ-1 in normal physiology and PD pathogenesis.

We and other groups have previously shown that DJ-1 exhibits conspicuous structural and sequence similarity to the PfpI family of bacterial intracellular proteases (145,149,192,338,360). However, whether DJ-1 can function as a protease remains unclear because unlike PfpI proteases, DJ-1 lacks a canonical Cys-His-Glu catalytic triad and in the crystal structure, access to its predicted catalytic nucleophile Cys-106 appears to be blocked by the extra helix (helix H8) at its C-terminus (Fig. 1B). Our biochemical analyses reveal that full-length DJ-1 protein is a cysteine protease zymogen which can be activated by cleavage of its helix H8-containing C-terminal 15-amino acid peptide (residues 175-189). We find that the activated DJ-1 protease, in common with several known cysteine proteases such as caspases (322,353,359), uses a Cys-His diad formed by its Cys-106 and His-126 for catalysis. Our kinetic analyses show that the removal of C-terminal 15-amino acid peptide results in a 5-fold decrease in the K_m and a 4.6-fold increase in the k_{cat} value, indicating that the C-terminal cleavage activates DJ-1 protease

by facilitating substrate binding as well as catalysis. These results are consistent with predictions from the crystal structure of full-length DJ-1 (145,149,192,338,360) and support a model in which the C-terminal cleavage converts DJ-1 into an active conformation by removing the helix H8 that blocks substrate entry and eliminating the interactions (e.g., the hydrogen bond between His-126 and Pro-184) that stabilize the inactive conformation of the zymogen.

Our finding that the protease activity of the C-terminally cleaved form of DJ-1 as well as the full-length DJ-1 is abolished by the C106A mutation supports the role of Cys-106 as the catalytic nucleophile of DJ-1 protease. We have shown that, DJ-1, in common with other cysteine proteases (322), requires a reducing environment for the catalytic thiol group to function and its protease activity is inhibited by oxidation. The oxidation-induced inactivation of DJ-1 protease could explain the failure to detect the protease activity of full-length DJ-1 in previous studies using non-reducing conditions during purification of DJ-1 protein and/or in the protease assays (192,303). The active site cysteine, Cys-106, was found to be oxidized during purification under non-reducing conditions (360), and similar oxidation of the active site cysteine during purification has also been reported for other cysteine proteases such as caspases (322).

Our cellular studies indicate that endogenous DJ-1, in common with other proteases, resides in cells as a latent protease zymogen and requires limited proteolysis at its C-terminus for activation. Our finding that DJ-1 zymogen is activated by C-terminal proteolytic processing in response to mild oxidative stress points to a role for DJ-1 protease in cellular defense against oxidative stress. The observation that the C-terminal cleavage of endogenous DJ-1 is reduced under strong oxidative stress conditions suggests

that the protease responsible for cleaving endogenous DJ-1 might be a cysteine protease whose activity is inhibited by oxidation. Our results argue against the possibility that DJ-1 is activated via auto-proteolysis, although we cannot exclude this possibility completely because auto-proteolysis of DJ-1 may require a cofactor(s), as in the case of caspase-9 activation by Apaf-1 apoptosome (86). Alternatively, DJ-1 zymogen may be activated by a yet unidentified protease, similar to the activation of executor caspases by the initiator caspases or the serine protease granzyme B (86,304). Future studies are needed to further elucidate the mechanism of DJ-1 protease activation.

The crystal structure of full-length DJ-1 also shows a high degree of structural similarity to that of *E. coli* chaperone protein Hsp31 (145,149,192,338,360), and full-length DJ-1 has been reported to have chaperone activity (192,303). It has been proposed that DJ-1 chaperone interacts with its client proteins via a hydrophobic patch composed of a cluster of surface-exposed hydrophobic residues primarily from helix H7 and helix H8 (192). Consistent with this idea, deletion of DJ-1 helix H8-containing C-terminal 16-amino acid peptide (residues 174-189), which is predicted to disrupt the proposed hydrophobic patch, results in a significant reduction in the chaperone activity of DJ-1 (192). The opposite effects of C-terminal truncation on DJ-1 chaperone and protease activities raise the possibility that DJ-1 is a chaperone-protease dual function enzyme that switches from a chaperone to a cysteine protease upon oxidative stress-induced C-terminal cleavage. Previously, a chaperone-protease dual function has been described for *E. coli* heat shock protein DegP, which switches from a chaperone to a serine protease at elevated temperature (65,178,313). In addition, Hsp31 has been suggested to switch from a chaperone to a cysteine protease in a temperature-dependent manner (214) .

Our data reveal that DJ-1 protease activation by C-terminal cleavage enhances its cytoprotective function against oxidative stress-induced apoptosis in both neuronal (SH-SY5Y cells, primary cortical neurons and primary midbrain neurons) and non-neuronal (mouse embryonic fibroblasts) cells. We find that the cytoprotective action of DJ-1 depends on its cysteine protease activity, as the catalytic site mutations C106A and H126A abolish the cytoprotective capability of the C-terminally cleaved DJ-1 as well as full-length DJ-1. Our findings raise the possibility that DJ-1 cysteine protease may exert cytoprotection against oxidative stress by mediating limited proteolysis of its substrate(s) or acting as a deubiquitinating or deSUMOylating enzyme (231,357) for regulating ubiquitination or SUMOylation of its substrate(s). Future studies to identify substrate(s) of DJ-1 cysteine protease should advance our understanding of DJ-1 cytoprotective action and its dysregulation in PD and other neurodegenerative diseases.

Acknowledgements

We thank Dr. Charles R. Gerfen and the National Institute of Neurological Disorders and Stroke/University of California Los Angeles Repository for Parkinson Disease Mouse Models for providing the DJ-1 knockout mice. The confocal imaging analysis was performed in Emory Neuroscience Core Facility supported in part by National Institutes of Health Grants P30 NS055077. This work was supported by National Institutes of Health Grants NS050650 and AG034126 (LSC) and ES015813 and GM082828 (LL).

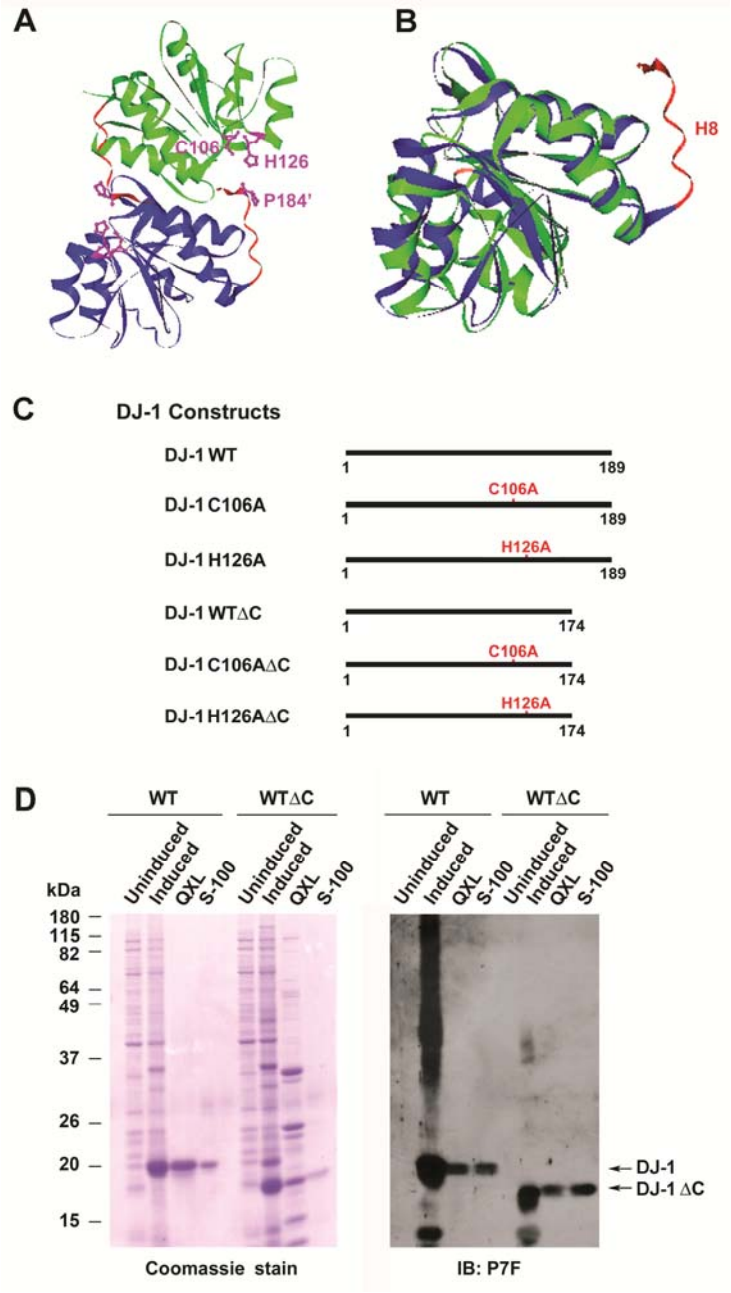

Figure II-1. Structural comparison of DJ-1 with intracellular protease PH1704 and generation of DJ-1 mutant proteins. (**A**) Ribbon diagram of the crystal structure of DJ-1 dimer. One monomer is colored in green and the other in blue. The α-helix H8 and its C-terminal region are highlighted in red. The side chains of Cys-106, His-126, and Pro-184' (' indicates from the other subunit of DJ-1 dimer) are in purple. The figure was

produced based on the published DJ-1 structure using the VectorNTI program (Invitrogen). (**B**) Superposition of DJ-1 monomer structure (blue) over that of PH1704 (green). The putative catalytic cysteines in PH1704 (Cys-100) and in DJ-1 (Cys-106) are highlighted in pink and the α-helix H8-containing C-terminal region of DJ-1 in red. (**C**) Schematic representation of wild-type and mutant DJ-1 proteins used in this study. **(D)** Purification of untagged wild-type and mutant DJ-1 proteins. Lysates from un-induced or induced *E. coli BL21* cells expressing indicated DJ-1 proteins and the fractions containing DJ-1 proteins purified by Sepharose QXL ion exchange chromatography and Sephacryl S-100 gel filtration chromatography were resolved on SDS-PAGE, followed by Coomassie blue stain (left panel) or immunoblotting with the anti-DJ-1 antibody P7F (right panel).

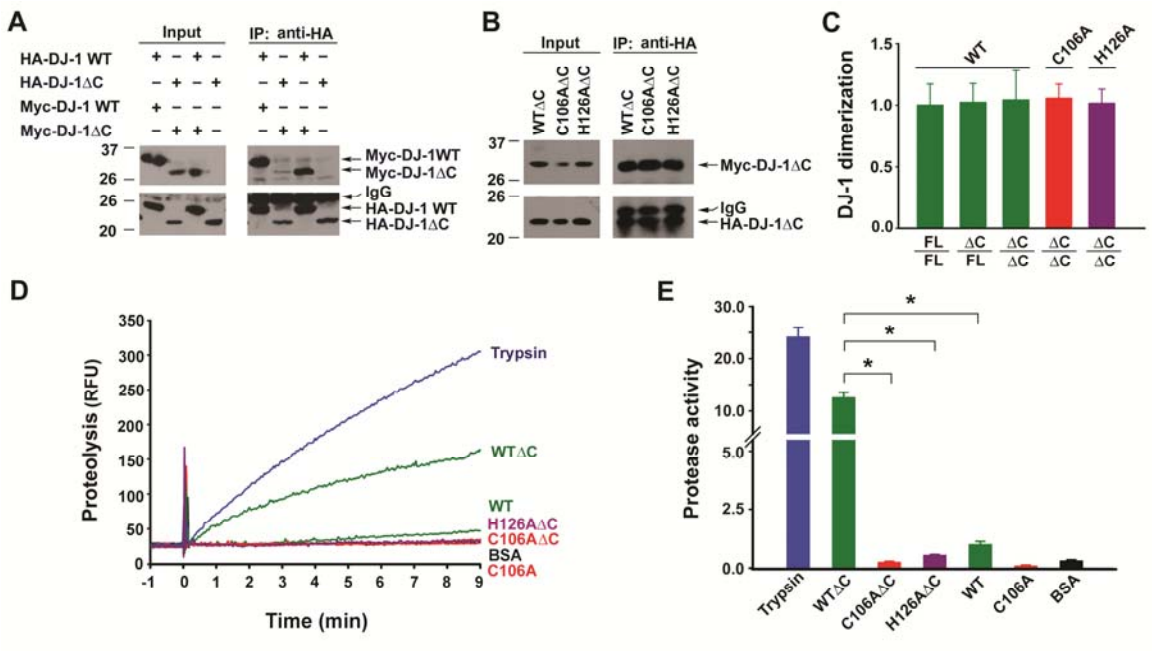

Figure II-2. Deletion of the C-terminal tail enhances DJ-1 protease activity without affecting its dimerization. (**A, B**) Lysates from HeLa cells expressing the indicated HA- and/or Myc-tagged DJ-1 proteins were immunoprecipitated with anti-HA antibody, followed by immunoblotting with anti-Myc and anti-HA antibodies. (**C**) DJ-1 dimerization was determined by quantification of the intensity of co-immunoprecipitated Myc-tagged DJ-1 band and normalized to the amount of HA-tagged DJ-1 band in the same immunoprecipitate. Data represents mean ± SEM from three independent experiments. (**D**) Protease activity of the indicated proteins was measured by a continuous, real-time fluorescence-based protease assay using BODIPY FL-casein (10 μg/ml) as the substrate. Fluorimetric recordings of 0.6 μM trypsin (blue), 50 μM DJ-1 WT or DJ-1 WTΔC (green), DJ-1 C106A or DJ-1 C106AΔC (red), DJ-1 H126AΔC (purple), and BSA (black). RFU, relative fluorescence units. (**E**) Protease activity of each protein was quantified by measuring the initial velocity of the proteolytic reaction from the fluorimetric trace shown in Fig. 2D. Protease activity on the Y-axis indicates

the measured protease activity of each protein after normalization to the protease activity of DJ-1 WT. Data represents mean ± SEM from three independent experiments. $*p < 0.05$.

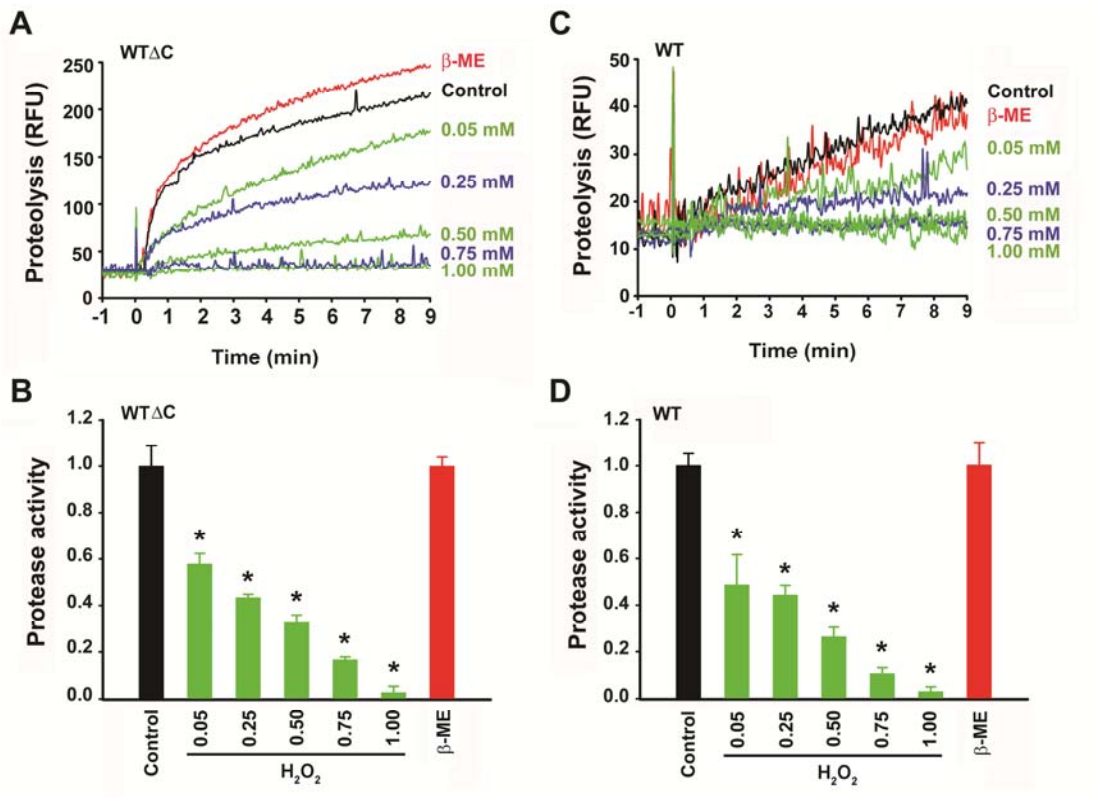

Figure II-3. Inhibition of DJ-1 cysteine protease function by oxidation. (**A**, **C**) Protease activity of 50 μM DJ-1 WTΔC (A) or 50 μM DJ-1 WT (C) was measured after pre-incubation with the indicated concentrations of H_2O_2 or 1 mM β-ME, or mock-treated (control) at 37 °C for 30 min by a real-time fluorescence-based protease assay using the fluorogenic substrate BODIPY FL-casein (10 μg/ml). RFU, relative fluorescence units. (**B, D**) Protease activity was quantified by measuring the initial velocity of the proteolytic reaction under the indicated conditions and normalized to the protease activity of mock-treated DJ-1 WTΔC (B) or DJ-1 WT (D). Data represents mean ± SEM from three independent experiments. *$p < 0.05$.

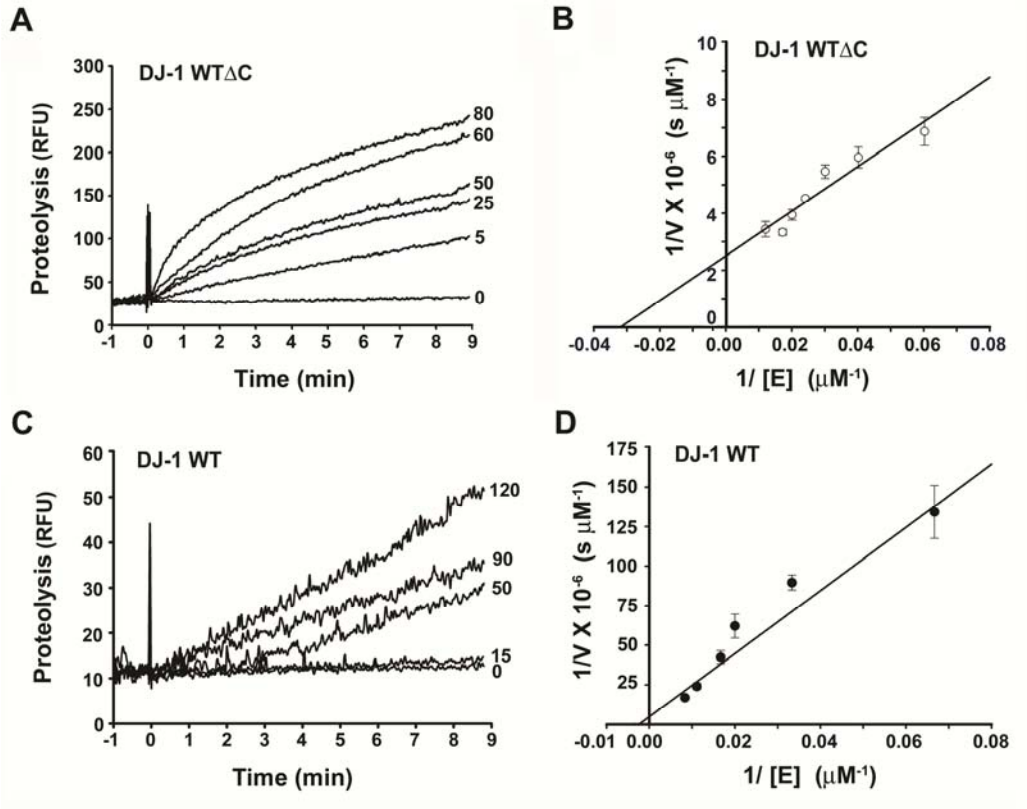

Figure II-4. Kinetic analyses of the full-length and C-terminally cleaved forms of DJ-1 protease. (**A**, **C**) Protease activities of the indicated concentrations (in μM) of DJ-1 WT (A) and DJ-1 WTΔC (C) measured in a real-time protease assay using the fluorogenic substrate BODIPY FL-casein (10 μg/ml). RFU, relative fluorescence units. (**B**, **D**) Double reciprocal plot of 1/V versus 1/[E] for DJ-1 WT (B) and DJ-1 WTΔC (D). Each data point represents mean ± SEM from three independent experiments.

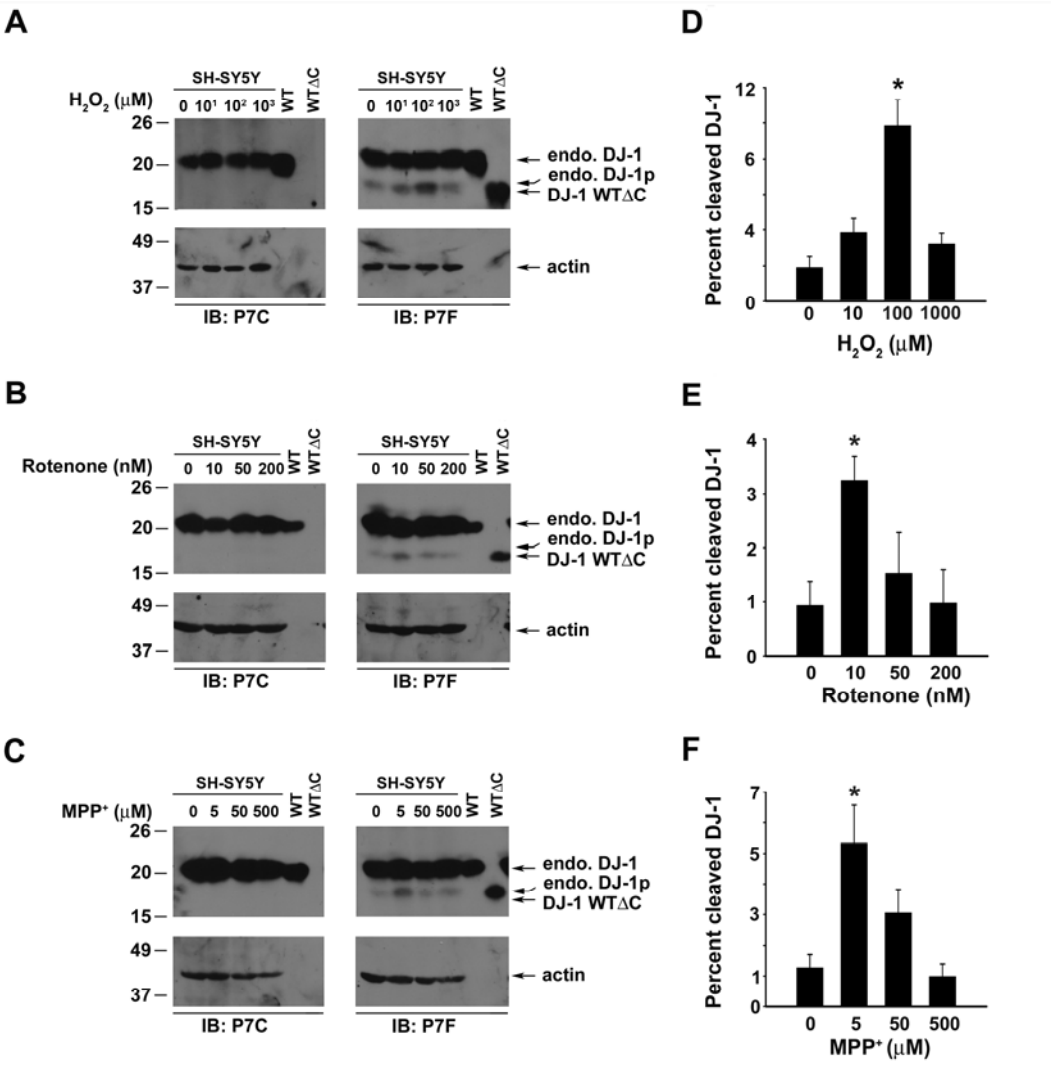

Figure II-5. Analysis of C-terminal cleavage of endogenous DJ-1 under normal and oxidative stress conditions. (**A-C**) SH-SY5Y cells were treated with indicated concentrations of H_2O_2 (A), rotenone (B), or MPP^+ (C) for 24 h, and the levels of full-length endogenous DJ-1 (endo. DJ-1) and C-terminally processed form of endogenous DJ-1 (endo. DJ-1_p) in the cell lysates were analyzed by immunoblotting with anti-DJ-1 antibody P7C or P7F as indicated. Purified recombinant full-length DJ-1 WT and DJ-1 WTΔC proteins were included as positive controls. Actin was used as a loading control. (**D-F**) The levels of the cleaved DJ-1 and full-length DJ-1 proteins were quantified by

measuring the intensity of the DJ-1_p and the full-length DJ-1 protein band, respectively. Percent cleaved DJ-1 on the Y-axis indicates the level of cleaved DJ-1 protein as a percentage of the total level of DJ-1 proteins (full-length DJ-1 plus DJ-1_p) in each cell lysate. Data represents mean ± SEM from three independent experiments. $*p < 0.05$.

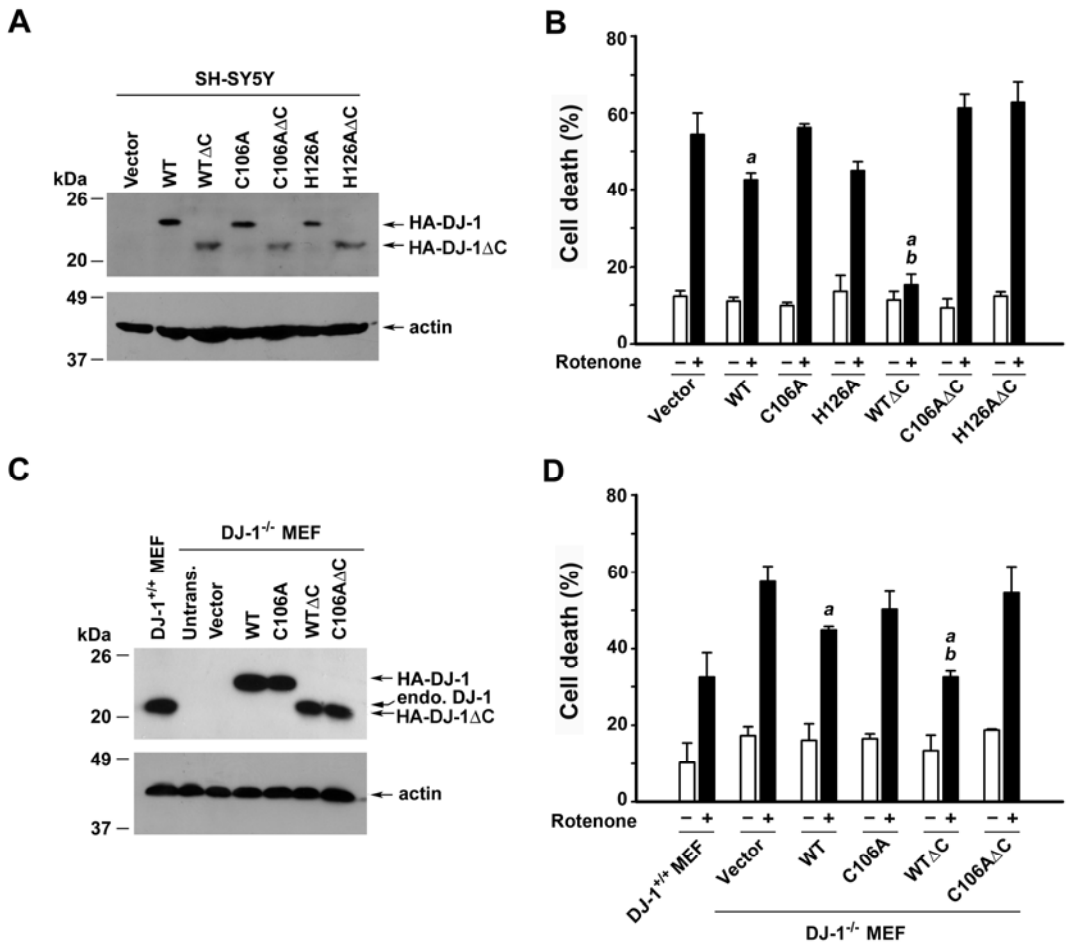

Figure II-6. C-terminal cleavage enhances DJ-1 cytoprotective action and this effect is dependent on DJ-1 protease activity. (**A**, **C**) Lysates from SH-SY5Y cells (A) or *DJ-1*$^{-/-}$ MEFs (C) transfected with the pCHA vector or indicated HA-tagged wild-type or mutant DJ-1 were analyzed by immunoblotting with anti-HA antibody (A) or anti-DJ-1 antibody P7F (C). The amount of cell lysates loaded in each lane was verified using anti-actin antibody. (**B**, **D**) SH-SY5Y cells (B) or *DJ-1*$^{-/-}$ MEFs (D) transfected with indicated plasmids were treated with 100 nM rotenone for 24 h. The extent of cell death was assessed by measuring LDH released to the culture medium and normalized to the total level of LDH release upon cell lysis. Data represent mean ± SEM from four independent experiments. [a]Significantly different from the corresponding vector-transfected control

($p < 0.05$). [b]Significantly different from the corresponding DJ-1 WT-transfected control ($p < 0.05$).

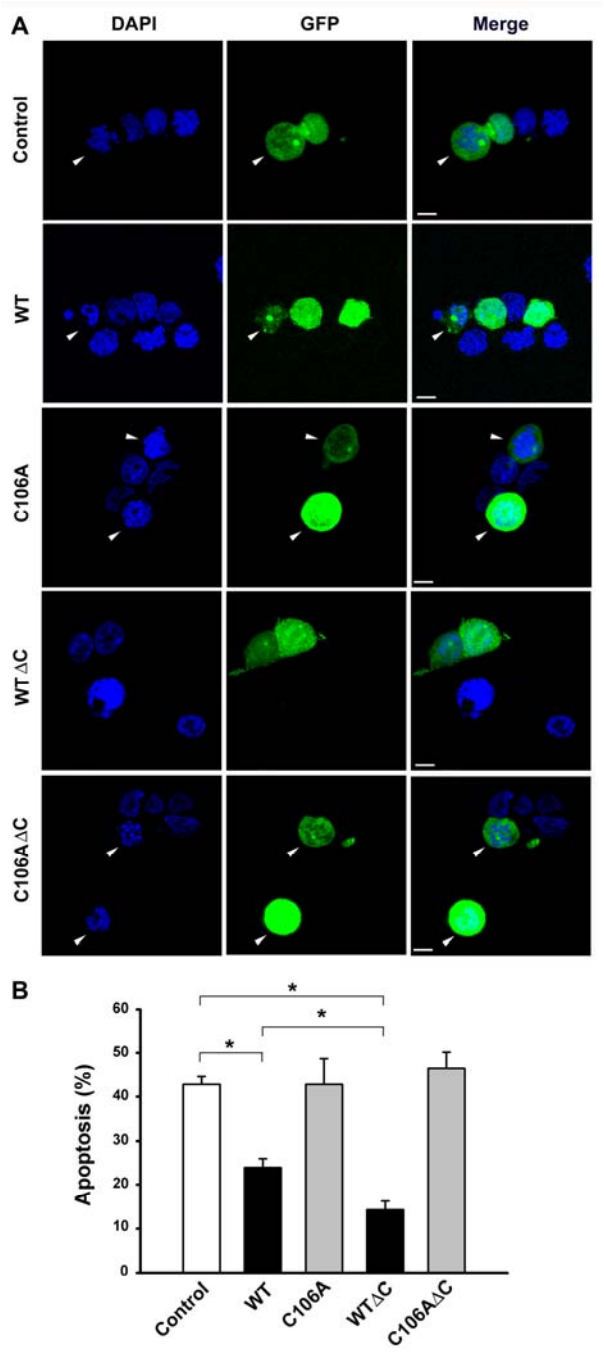

Figure II-7. The ability of DJ-1 to protect against rotenone-induced apoptosis is augmented by its C-terminal cleavage. (**A**) SH-SY5Y cells co-transfected with an expression vector encoding green fluorescent protein (GFP) and vehicle (control) or indicated DJ-1 plasmids were treated with 100 nM rotenone for 24 h. Transfected cells

were shown by GFP fluorescence (green) and nuclear integrity was assessed by DAPI staining (blue). Arrowheads indicate transfected cells with apoptotic nuclei. Scale bar, 10 μm. (**B**) Apoptosis is expressed as the percentage of transfected cells with apoptotic nuclear morphology. Data represent mean ± SEM from four independent experiments. *$p < 0.05$.

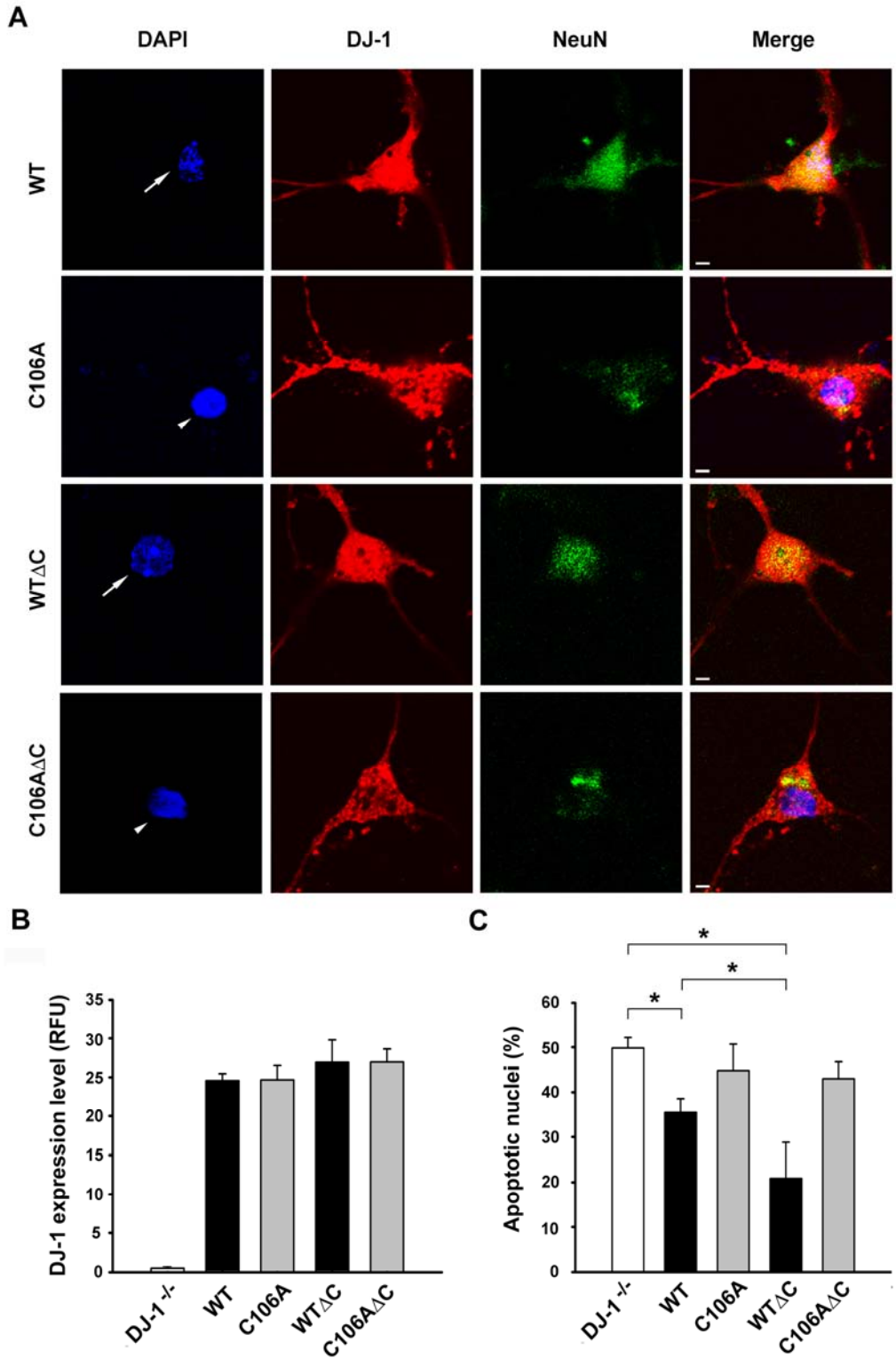

Figure II-8. DJ-1 WTΔC is more effective than DJ-1 WT in suppressing the pro-apoptotic phenotype of *DJ-1*$^{-/-}$ cortical neurons. (**A**) *DJ-1*$^{-/-}$ cortical neurons transfected

with indicated DJ-1 plasmids were treated with 5 nM rotenone for 24 h. Neurons were stained with anti-NeuN antibody (green), transfected neurons were identified by anti-DJ-1 (P7F) immunostaining (red) and nuclear integrity was assessed by DAPI staining (blue). Arrows indicate neurons with normal nuclei, whereas arrowheads indicate neurons with apoptotic nuclei. Scale bar, 10 μm. (**B**) The expression level of wild type or mutant DJ-1 protein was quantified and is presented as the fluorescence intensity of DJ-1 immunofluorescence in transfected neurons. Data represent mean ± SEM from three independent experiments. RFU, relative fluorescence units. (**C**) Apoptosis is expressed as the percentage of transfected neurons with apoptotic nuclear morphology. Data represent mean ± SEM from four independent experiments. $*p < 0.05$.

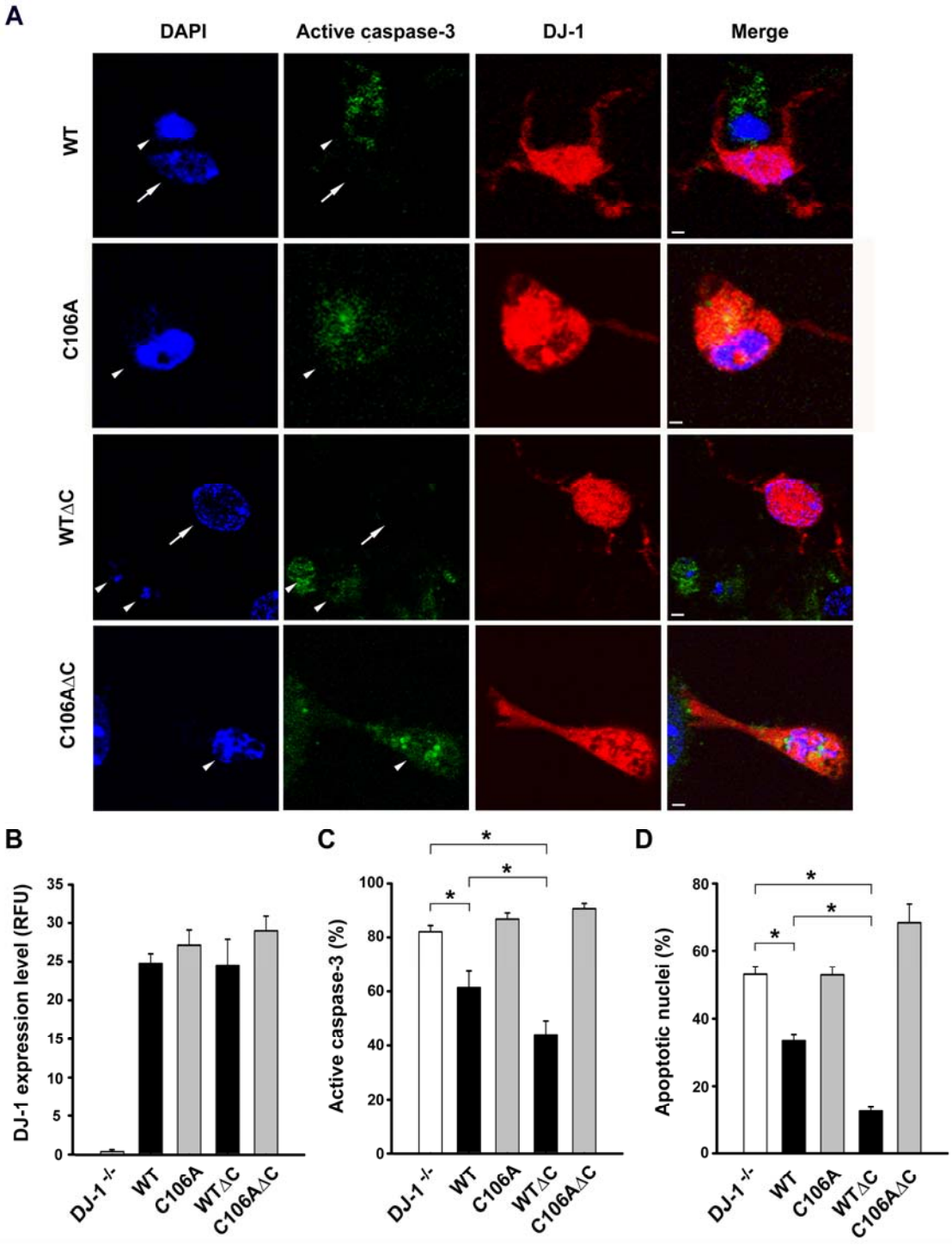

Figure II-9. C-terminal cleavage enhances the ability of DJ-1 to rescue the pro-apoptotic phenotype of *DJ-1*$^{-/-}$ midbrain neurons. (**A**) *DJ-1*$^{-/-}$ midbrain neurons transfected with indicated DJ-1 plasmids were treated with 5 nM rotenone for 24 h.

Transfected neurons were identified by anti-DJ-1 (P7F) immunostaining (red), caspase-3 activation was assessed with anti-active-caspase-3 antibody (green) and nuclear morphology visualized by DAPI staining (blue). Arrows indicate neurons with normal nuclei and no active caspase-3 staining, whereas arrowheads indicate neurons with apoptotic nuclei and active caspase-3 staining. Scale bar, 20 μm. (**B**) The expression level of wild type or mutant DJ-1 protein was quantified and is presented as the fluorescence intensity of DJ-1 immunofluorescence in transfected neurons. Data represent mean ± SEM from three independent experiments. RFU, relative fluorescence units. (**C**, **D**) The percentage of transfected neurons with active caspase-3 staining (C) or with apoptotic nuclei (D) was quantified. Data represent mean ± SEM from four independent experiments. $*p < 0.05$.

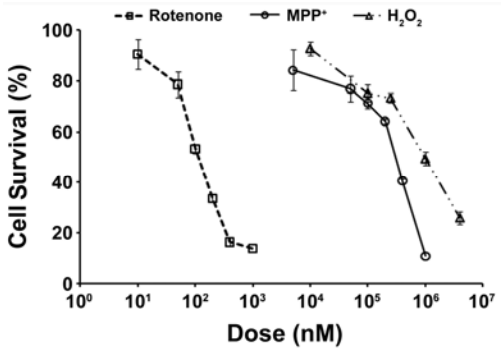

Figure II-10. Rotenone, MPP^+, and H_2O_2 induce cell death in SH-SY5Y cells in a dose-dependent manner. Cells were treated with indicated concentrations of rotenone, MPP^+, and H_2O_2 for 24 h, and the extent of cell survival was assessed by using the MTT assay. Data represent mean ± SEM from six to eight independent experiments.

Table II-1 Summary of DJ-1 kinetic parameters

	k_{cat} (s^{-1})	K_m (μM)	k_{cat}/K_m ($M^{-1}.s^{-1}$)
DJ-1 WT	0.023 ± 0.018	173.4 ± 23.7	1.3×10^2
DJ-1 WTΔC	0.105 ± 0.011	31.3 ± 3.0	3.4×10^3
Trypsin	1.436 ± 0.234	6.5 ± 0.3	2.2×10^5

CHAPTER III

MET-17 AND MET-26 ARE CRITICALLY INVOLVED IN DJ-1 ZYMOGEN ACTIVATION AND CYTOPROTECTIVE FUNCTION

ABSTRCT

PD linked protein DJ-1 exists as a zymogen that is activated by C-terminal cleavage in responseto mild oxidative stress, but the molecular mechanisms regulating DJ-1 zymogen activation remain unclear. Two methionines, M17I and M26I, on DJ-1 are oxidized in brains from normal human beings, suggesting that oxidation of these two methionine are physiologically relevant. To understand whether methionine oxidation regulates DJ-1 zymogen activation, we studied the role of individual methionine on DJ-1. Here we report that M17I and M26I mutations prevented DJ-1 zymogen activation. Furthermore, the loss of zymogen activation caused by M17I mutation is not due to changes in protein structure or stability. However, M26I mutant displays reduced secondary structure, thermal stability and protein stability, suggesting that structural disturbance may contribute to the loss of zymogen activation and protease activity induced by the PD linked mutation M26I. Moreover, we found that DJ-1 M17I, M26I, and M133I mutants loss cytoprotective function, implying that these methionines are important for DJ-1 cytoprotective function. Our findings suggest that Met-17 and Met-26 are important for DJ-1 zymogen cleavage and cytoprotection. Additionally, data presented in this study also provide novel insights into the pathogenic mechanisms of the PD linked M26I mutation.

INTRODUCTION

Parkinson disease (PD) is a progressive neurodegenerative disorder pathologically characterized by loss of dopaminergic neurons in nigrostriatal pathway. The etiology of PD is complex, with contributions from both environmental factors and genetic predisposition (72). Autosomal recessive mutations in DJ-1 cause early onset familial form of PD (32), suggesting that DJ-1 is important in maintaining normal neuronal functions and survival. In support of this hypothesis, DJ-1 has been shown to protect neuronal cells against apoptosis induced by oxidative stress (45,54,74,114,166), although the precise molecular mechanisms are unclear. We have previously shown that DJ-1 exists as a zymogen that is activated by C-terminal proteolysis in response to mild oxidative stress and protease activity of DJ-1 is required for its cytoprotective function (51). However, how DJ-1 zymogen is activated in response to oxidation remains unknown.

Methionine is a sulfur-containing amino acid that is susceptible to oxidation. Methionine can be oxidized to form methionine sulfoxide (MetO) and methionine sulfone ($MetO_2$) (319). Oxidation of methionine to MetO can be reversed by methionine sulfoxide reductases (Msr) (50), and the reversible oxidation of Met has been shown to mediate redox-dependent signaling similar to the cysteine-based redox regulatory system (147). Methionine oxidation to $MetO_2$ is irreversible and usually leads to loss of biological functions (147). DJ-1 contains four methionine residues, among them the positions 17 and 26 in human DJ-1 are occupied by hydrophobic residues from different species and are well conserved in all mammalian species (Fig.1A) (150,338). Notably,

homozygous mutation of M26I was identified in a patient with early onset PD (2), but controversial results have been reported regarding the secondary structure, oligomeric state, protein stability, and intracellular localization of DJ-1 M26I mutant (29,151,184,199,331,371). The influence of M26I mutation on DJ-1 protease activity or zymogen activation has not been studied. Interestingly, we have previously demonstrated that Met-17 and Met-26 were oxidized to MetO in control brain samples while Met-133 and Met-134 were not (59). Based on the proximity of Met-17 and Met-26 to helix H8 (Fig. 1B) and their susceptibility to oxidation, it is plausible that oxidation of Met-17 and Met-26 is physiologically important and may induce local conformational changes necessary for the activation of DJ-1 zymogen. These findings raise our interest in examining the roles of methionine, reversible oxidation of methionine in particular, in regulating DJ-1 structure and function.

To understand the role of individual methionine residue in DJ-1 zymogen activation and to further characterize the pathological mechanisms of M26I mutation, we conducted a systematic methionine mutagenesis. We found that M17I mutation abolishes zymogen cleavage without affecting secondary structure and thermal stability of DJ-1 protein. While DJ-1 M26I zymogen is also unable to be cleaved to generate mature protease, it is also slightly unfolded and unstable. Additionally, we showed that cytoprotective function of DJ-1 is abolished by M17I, M26I, and M133I mutations. Findings presented in this study reveal a potential role of methionine oxidation in activating DJ-1 zymogen and cytoprotection, and elucidate the pathogenic mechanisms of the PD linked mutation M26I.

EXPERIMENTAL PROCEDURES

Expression constructs and reagents

DJ-1 WT and mutants were cloned into mammalian expression vectors with the indicated epitope fused to the amino-terminal of DJ-1 protein as described (51). All expression constructs were sequenced to confirm that the fusion was in the correct reading frame. The rabbit polyclonal anti-DJ-1 antibodies, P7F and P7C, generated against purified full-length recombinant DJ-1 protein and a synthetic DJ-1 C-terminal peptide (residues 171–189), respectively, were described in our previous studies (262) . Other antibodies used in this study include the following: anti-HA (12CA5), anti-Myc (9E10.3, Neomarkers), anti-actin (Chemicon), and anti-MAP2 (Millipore). All secondary antibodies were purchased from Jackson ImmunoResearch Laboratories, Inc.

Protein expression and purification

Wild-type and mutant DJ-1 proteins were expressed as untagged proteins and purified from BL21 *E. coli* (CodonPlus) as described previously (260,262). Briefly, bacterial lysates were fractionated by ammonium sulfate, followed by Sepharose QXL ion exchange chromatography and Sephacryl S-100 gel filtration chromatography (Amersham). Fractions containing DJ-1 were identified by SDS–PAGE and confirmed by immunoblot analysis with anti-DJ-1 antibody P7F. Protein concentration was determined by using the bicinchoninic acid assay (Pierce).

Circular dichroism analysis of recombinant DJ-1 proteins

Circular dichroism (CD) spectra were acquired on an AVIV 62 DS spectrometer equipped with a sample temperature controller as previously described (51,262). Far-UV

CD spectra of 12.5 μM recombinant DJ-1 proteins were monitored from 200 to 250 nm with a step size of 0.5 nm and slit width of 1.5 nm, using a 0.1 cm path-length quarz cuvette at 25 °C. Each spectrum is the average of five scans. The results are expressed as the mean residue ellipticity, $[\Theta]_{MRE}$ (deg-cm^2/ dmol) = $[\Theta]_{obs}$ / 10 [p]nl, where $[\Theta]_{obs}$ is the observed ellipticity in millidegrees, [p] is the molar concentration of the protein, n is the number of residue per mole of protein, and l is the pathlength in centimeters. The percentage of α-helix was calculated using the assumption that for 100% α-helix, the $[\Theta]_{MRE}$ at 222nm is $[\Theta]_{222}$ = -36,300 (1-2.57/x), where x is the number of amino acids in the protein (262). Thermal denature measurements were performed at a wavelength of 222 nm in 2°C increments from 5°C to 95 °C with an equilibration time of 1 min and an integration time of 30 sec. Melting temperature is defined as the temperature at which 50% of the α-helical structure is denatured as described (55).

Cell transfection, immunoblot and immunoprecipitation analysis

SH-SY5Y cells were transiently transfected with the indicated plasmids using lipofectAMINE 2000 (Invitrogen) for 24h as instructed by the manufacturer. Lysates from the cells were immunoprecipitated using anti-HA antibody (12CA5). The immunocomplex was recovered by incubation with protein G-Sepharose beads (Sigma) and then dissociated by boiling in the Laemmli sample buffer, resolved by SDS-PAGE and probed with the indicated antibodies. Antibody binding was detected by using the enhanced chemiluminescence system (Amersham Biosciences).

Pulse-chase assay

Pulse-chase experiments were performed as described previously (262). Briefly, SH-SY5Y cells expressing N-terminally Myc-tagged DJ-1 WT or DJ-1 mutants were labeled by incubation for 1 hr with Met/Cys-free medium containing 100 μCi of [^{35}S] Met/Cys express protein labeling mix (MP Biologicals). After extensive washes, cells were incubated for the indicated chase time in non-radioactive media containing excess Met/Cys. At the indicated time points, cells were lysed and equal amount of proteins from each lysate was subjected to immunoprecipitation using an anti-Myc antibody. Immunoprecipitated proteins were resolved by SDS-PAGE and analyzed by a PhosphorImager (Amersham Biosciences).

Treatment of cells with proteasome inhibitor

SH-SY5Y cells expressing N-terminally Myc-tagged wild-type or mutant DJ-1 were incubated for 16 hr at 37 ˚C with the proteasome inhibitor MG132 (20μM, Sigma) or vehicle [0.1 % Me_2SO (DMSO)]. Cells were then lysed, and an equal amount of proteins from each lysate was analyzed by immunoblotting for Myc-tagged DJ-1 and actin. The relative level of wild-type or mutant DJ-1 was quantified using Scion program (NIH) and normalized against the actin level in the corresponding cell lysate from the same gel. To control for the possibility of overexposure, each immunoblot was subjected to multiple exposures. The intensities of the DJ-1 bands from at least two different exposures of the same immunoblot were quantified and the average for comparison. Experiments were repeated at least three times, and the data were subjected to statistical analysis using one-way ANOVA analysis followed by Dunnett's Post-Hoc test, compare to DJ-1 WT expressing cells.

Primary cortical neuronal cultures and virus infection

DJ-1 knockout mice were generated and described previously (262). Primary cortical neuronal cultures were prepared from postnatal 0.5 day (P0.5) wild-type and DJ-1 knockout pups and plated onto poly-L-lysine-coated glass coverslips at a density of 50,000 cells/ cm^2 as described previously (260). Primary cortical neuronal cultures were maintained in NeuroBasal Media (Gibco) supplemented with cytosine arabinoside (AraC) (Sigma) for 3–7 days. *DJ-1*$^{-/-}$ cortical neurons were infected with lenti-virus carrying either an empty vector encoding eGFP, or N-terminally HA-tagged DJ-1 proteins at a multiplicity of infection (MOI) of 5 and allow to incubate for 48 h before experiments as described (51,110,191).

Cell death and apoptosis assays

Cell viability assay in SH-SY5Y cells transiently expressing Myc-vector or indicated Myc-DJ-1 was assessed using the lactate dehydrogenase (LDH) (Roche) release assay as described (14,78). Cells were treated with 200 nM rotenone for 24 h and LDH activity in the culture media was measured.

For flow cytometry assay, SH-SY5Y cells stably overexpressing indicated DJ-1 or empty vector were treated with 200 nM rotenone for 24 h in trigas incubator with 5% O_2 and 5% CO_2 level. Cells were washed with PBS three times, followed by resuspending in PBS containing 0.1 μM of calcein acetoxymethyl (CaAM, Invitrogen) and 1 μM of ethidium homodimer-1 (EH-1, Sigma) at a density of 0.5 X 10^6 cells /ml. Cells were incubated at dark for 20 min and before analyzed using BD LSRII flow cytometer.

Samples were excited using 488 nm laser. EH-1 was detected using 550LP dichroic mirror and passed through 575/26 nm bandpass filter. CaAM was detected using 505LP dichroic mirror and passed through 530/30 nm bandpass filter. Compensations were calculated using unstained cells and single-fluorescence stained cells. 10,000 events were collected for each sample. Cell derbies were gated out using side-scatter parameter. The same quadrant gating parameters on CaAM and EH-1 scatter graph were applied to all samples for quantification of cell death. Data was analyzed using FlowJo software.

For analysis of apoptosis in primary neurons, cells infected with lentivirus for 48 h were treated with 5 nM rotenone for 24 h before fixation. Neurons were triple-stained with anti-MAP2 as a neuronal cell marker, anti-DJ-1 antibody P7F for detection of transfected wild-type or mutant DJ-1, and DAPI for assessment of nuclear morphology. The percentage of DJ-1-transfected neurons with apoptotic nucleic was scored for apoptosis as described (51).

Statistical analysis

All experiments were repeated at least three times. Data were subjected to statistical analysis by ANOVA and a p value of less than 0.05 was considered statistically significant.

RESULTS

M17I and M26I mutations abolish DJ-1 zymogen activation without affecting dimerization

DJ-1 zymogen needs to be converted to an active protease through proteolytic process at the C-terminus by unknown mechanisms in response to mild oxidative stress (51). Although the redox-dependent events that trigger the proteolysis of DJ-1 under mild oxidation remain to be identified, it is possible that the proteases cleaving DJ-1 are active under mild oxidation. It is also plausible that oxidative modification on DJ-1 induces conformational changes of DJ-1 that make it a better substrate for the C-terminal proteolysis. To investigate the latter possibility, we compared the C-terminal cleavage of DJ-1 WT and methionine mutants under mild oxidation conditions as described (51). Briefly, C-terminally truncated DJ-1 can be recognized by P7F antibody generated against the full length DJ-1 but cannot be recognized by P7C antibody generated against the C-terminal 20 amino acids of DJ-1 (51). As expected, Myc-tagged DJ-1 WT could be cleaved at the C-terminus, generating Myc-DJ-1ΔC with similar length as the active form of DJ-1 protease when cells were treated with either rotenone or H_2O_2 (Fig.2A and 2B). DJ-1 M133I and DJ-1 134I mutants had similar C-terminal cleaved species as Myc-DJ-1WTΔC and the percentage of DJ-1 M133I and M134I zymogen activation is comparable to that of DJ-1 WT (Fig.2C and 2D). This suggests that oxidation of Met-133 and Met-134 is not involved in regulating DJ-1 C-terminal proteolysis. However, DJ-1 M17I and DJ-1 M26I did not have the C-terminal cleaved species with similar molecular weight as Myc-DJ-1WTΔC in response to mild oxidative stress (Fig.2), suggesting that oxidation of these two residues might be required for the activation of DJ-1 zymogene. It is also likely

mutations of these two residues disrupt dimerization of DJ-1, resulting in unfolding of DJ-1 protein. Interestingly, DJ-1 M26I mutant had a distinctive cleaved form missing around 4kDa of the C-terminal tail under both normal and oxidizing conditions (referred to as Myc-DJ-1 M26IΔC1), implying that mutation on Met-26 may alter the folding and dimerization of DJ-1 resulting in abnormal proteolysis of DJ-1.

DJ-1 has been reported to form homo-dimer by several groups (338,361) and the dimer formation is thought to be important for the stability of DJ-1 (262). To determine whether loss of zymogen activation caused by M17I and M26I is due to disruption of DJ-1 dimerzation, we performed co-immunoprecipitation assay in a neuronal cell line SH-SY5Y co-expressing HA- and Myc-tagged DJ-1 proteins. If DJ-1 can form homodimer, Myc-tagged DJ-1 should be able to be immunoprecipitated using antibody against HA-tag. All the Met mutants, even DJ-1 M26I mutant, could form homodimer as well as heterodimer (Fig.3), similar as DJ-1 WT (data not shown for DJ-1 WT homodimer) (51,262). This finding suggests that the prevention of zymogen cleavage by M17I and M26I mutations is not due to disruption of dimerization.

M26I mutation, but not M17, M133I, or M134I, inhibits DJ-1 protease activity

We have previously shown that DJ-1 functions as a cysteine protease and protease activity of DJ-1 is required for its neuroprotection (51). To determine whether any methionine residue is critical for the protease activity of DJ-1, we assessed protease activity of the recombinant wild-type and mutant DJ-1 proteins as described (51). Same concentration of DJ-1 M17I, M133I and M134I zymogen displayed similar protease

activity as DJ-1 WT zymogen (Fig. 4A and 4B), suggesting that these three methionines are not crucial for DJ-1 protease activity. Furthermore, protease activity of DJ-1 M17IΔC, M133IΔC and M134I ΔC was not significantly different from that of DJ-1 WTΔC (Fig. 4C and 4D), indicating that these methionines are not involved in DJ-1 protease activity when DJ-1 is converted to an active protease. However, DJ-1 M26I and DJ-1 M26I ΔC lost protease activity, indicated by almost no hydrolysis of the substrates (Fig. 4). These findings suggest that although both M17I and M26I mutations abolish DJ-1 zymogen activation (Fig.2), only M26I mutation inhibits DJ-1 protease activity (Fig. 4).

Only M26I mutation affects secondary structure and thermal stability of DJ-1 protein

To examine whether methionine to isoleucine mutations will affect DJ-1 protein folding and secondary structure, we assessed secondary structure content and thermal stability of these mutants using circular dichroism spectroscopy. Consistent with previous report, the far-UV CD spectrum of wild-type DJ-1 showed characters of both α-helix and β-strands (254), indicated by the negative ellipiticity at 222 nm and 218 nm (Fig. 5A). The secondary structure content of wild-type DJ-1 in solution is approximately 35.7% α-helix, determined using method as described (262). The value agrees with the secondary structural content of DJ-1 calculated from the crystal structure using PDB annotation for secondary structure in 1P5F. In contrast, M26I mutant has lower α-helix content (29.6%) (Fig. 5D and table 1) compared to wild-type DJ-1 protein, implying that this mutation may cause local structural perturbation or global destabilization. The far-UV CD spectra

of the M17I, M133I and M134I after normalized to molar protein concentration are similar to the spectrum of the wild-type DJ-1 protein, suggesting that these three mutants preserve the secondary structure of DJ-1 protein (Fig. 5D and 5F). All these three mutants have similar percentage of α-helix as the wild-type DJ-1 (table 1), consistent with the notion that substitution methionine with isoleucine is a conservative mutation (11,147).

To further assess the structural effects of each mutant, we monitored the melting temperature (T_m) of each protein using thermal denature CD at 222 nm as a measurement of α-helix content. In agreement with previous report, the T_m of DJ-1 WT is about 70 ^oC (Fig.5B and table 1) (151,213). The T_m of DJ-1 M26I mutant is 7 ^oC lower than that of DJ-1 WT, implying that the α-helix structure of DJ-1 M26I is more unstable that DJ-1 WT (Fig. 5E and table1). All other full length mutants have similar T_m as DJ-1 WT, suggesting that these mutations do not affect the stability of the secondary structure (Fg.5E, 5G and table1).

The spectrum of the active DJ-1 protease without the C-terminal α-helix (DJ-1WTΔC) displays characters of both α-helix and β-strand as well, similar to DJ-1 WT (Fig. 5A). However, DJ-1WTΔC has lower α-helix content (33.5%) compared to DJ-1 WT (35.7%), as would expected since DJ-1WTΔC has one less α-helix than DJ-1 WT. The T_m of DJ-1WTΔC is 5 ^oC lower than DJ-1 WT (Fig. 5B and table 1), suggesting that the active form of DJ-1 protease is more dynamic in secondary structure than DJ-1 zymogen. Compared to DJ-1WTΔC, the T_m of DJ-1C106A ΔC, M17IΔC, M133IΔC, and M134IΔC is within ±2 ^oC different from that of DJ-1 WTΔC (Fig. 5B, Suppl. Fig.1 and table 1). The % of α-helix of these mutants is only ± 1% different from that of DJ-1 WTΔC (Fig. 5B, Suppl. Fig.1 and table 1). Therefore, these mutations may not affect the

secondary structure and thermal stability of the active form of DJ-1 protease. However, DJ-1M26IΔC has 22.5% less α-helix compared to DJ-1WTΔC and has a T_m of 52 ^oC, 13 ^oC lower than DJ-1WTΔC (Suppl. Fig.1 and table 1). The structural disturbance caused by M26I mutation is observed in both DJ-1 full length and DJ-1ΔC background, suggesting that Met-26 is structurally important for both DJ-1 zymogen and mature DJ-1 protease. Although M26I mutation does not disrupt dimerization (Fig.3), it seems to alter the secondary structure and thermal stability of DJ-1 protein.

M26I mutant is unstable and degraded by ubiquitin proteasome pathway

We and others have shown that DJ-1 WT protein is a long-lived protein and is not degraded through ubiquitin proteasome pathway under physiological condition (262). Since M26I mutant displayed reduced secondary structure (Fig.5 and table1), we next wanted to examine whether M26I protein is not stable as protein unfolding may lead to destabilization. We examined the half-life ($t_{1/2}$) of the DJ-1 methionine mutants using pulse-chase assay and found that the $t_{1/2}$ DJ-1 WT protein is about 34 h (Fig. 6), consistent with previous report (50). However, DJ-1 M26I has a shorter half-life (21.3 h) than DJ-1 WT (Fig.6A and 6B), suggesting that M26I mutation may cause conformational changes in DJ-1 protein resulting in faster degradation.

One of the PD linked mutant DJ-1 L166P has been shown to be degraded through proteasome system, a major route for degrading misfolded proteins or short-lived protein (262). Next we investigated whether DJ-1 M26I mutant, which has a shorter $t_{1/2}$ than DJ-1 WT, is also degraded by proteasome. We found that the level of DJ-1 WT was not increased by treatment of proteasome inhibitor MG132 (Fig. 7A and 7B), consistent with

previous report that DJ-1 WT was not degraded via proteasome system (262). However, the basal level of DJ-1 M26I mutant was much lower than that of DJ-1 WT and other mutants (Fig. 4D), in agreement with other reports (262). Furthermore, protein level of DJ-1 M26I mutant was significantly increased by the impairment of proteasomal function (Fig.7D and 7E), indicating that DJ-1 M26I mutant is partially degraded through proteasome system. Most of the proteins degraded through proteasome systems are marked by poly-ubiquitination then targeted to proteasome for degradation. To test whether DJ-1 M26I mutant is poly-ubiquitinated, we performed *in vivo* ubiquitination assay and found that DJ-1 M26I could be poly-ubiquitinated (Suppl.2A). The poly-ubiquitinated DJ-1 M26I was enhanced when proteasomal function was inhibited by MG132, suggesting that the ubiquitinated DJ-1 M26I was mostly degraded through proteasome system. These findings support that hypothesis that DJ-1 M26I is degraded through ubiquitin proteasome pathway. Additionally, we also demonstrate that M26I forms aggregate upon impairment of proteasome or macroautopahgy function (Suppl Fig. 2C), suggesting that misfolded M26I can be degraded by both proteasomal and lysosomal pathways.

Surprisingly, M17I mutant had much longer $t_{1/2}$ than DJ-1 WT (Fig.4A and 4B), indicating that oxidation of Met-17 may normally facilitate the degradation of DJ-1 protein since preventing oxidation of methionines could prolong its half-life. However, preventing oxidations on Met-133 or Met-134 did not appear to affect the $t_{1/2}$ of DJ-1 protein (Fig. 4A and 4C), implying that oxidations on these two methionine residues will not affect the stability of DJ-1 protein.

Met-17, Met-26 and Met-133 are critical for DJ-1 cytoprotective function

DJ-1 has been extensively reported to have neuroprotective function (29,199,331) and protease activity of DJ-1 is required for its neuroprotection (45,330,378). To determine how individual methionine residue regulates DJ-1 cytoprotective function, we first examined the effects of DJ-1 WT and methionine mutants on the vulnerability of SH-SY5Y cells to oxidative stress induced by rotenone. SH-SY5Y cells either transiently overexpressing (Fig. 8A and 8B) or stably overexpressing (Fig. 8C and Fig. 8D) Myc-DJ-1WT have significantly reduced cell death induced by rotenone compared to cells overexpressing Myc-vector, as measured by LDH release assay (Fig. 8B), and percentage of cells stained positive with EH-1 and negative with CaAM for dead cells using flow cytometry (Fig. 8D and Suppl. Fig.3). The cytoprotective function of DJ-1 was abolished by mutation of M17I, M26I, and M133I (Fig. 8), suggesting that either preventing oxidation of these methionine residues (M17I and M133I) or structural disturbance introduced by these mutations (M26I) could abrogate DJ-1 function.

To provide further evidence that selective methioines are critical for DJ-1 neuroprotective function, we assessed cytoprotective function of DJ-1 WT and the methionine mutants in primary cortical neurons cultured from the DJ-1 knockout (DJ-1 $^{-/-}$) mice. The DJ-1 $^{-/-}$ cortical neurons allow for direct comparison the cytoprotection of DJ-1 WT and methionine mutants without interference with endogenous DJ-1 as they lack DJ-1 expression, confirmed by immunocytochemistry analysis with anti-DJ-1 antibody (P7F) (Fig.9A). All DJ-1 proteins have similar intracellular distribution as endogenous DJ-1, and were expressed at similar level except for DJ-1 M26I mutant (Fig. 9A and 9B) (51). Expression of DJ-1 WT protein significantly reduced rotenone-induced apoptosis in DJ-1

$^{-/-}$ neurons, compared to neurons expressing empty-vector, consistent with previous reports that DJ-1 has neuroprotection. However, neurons expressing DJ-1 M17I, M26I, and M133I have significantly higher apoptosis than neurons expressing DJ-1 WT, confirming our findings in dopaminergic cell lines (Fig. 9).

DISCUSSION

We have previously demonstrated that DJ-1 exists as a zymogen and is activated by C-terminal cleavage under mild oxidation , but the mechanisms regulating DJ-1 zymogen cleavage are unknown (380). Findings presented in this study support that Met-17 and Met-26 are required for DJ-1 zymogen cleavage in response to mild oxidative stress. Additionally, our data also suggest that reduced secondary structure and destabilization of DJ-1 protein are the primary pathogenic mechanisms of DJ-1 M26I mutation.

Our results demonstrate that mutation of Met-17 and Met-26 prevents zymogen activation without affecting DJ-1 dimerization (Fig.2 and Fig.3). Notably, these two methionines are buried in the core of DJ-1 protein and are close to the helix 8 (H8, highlighted in purple in Fig. 1B) (150,338), which has been shown to inhibit DJ-1 protease function (51). But in contrary to the conventional thinking that methionines at protein surface are more easily oxidized than those located at the core of the protein (196,197,319,321), Met-17 and Met-26 are more prone to oxidation. These two methionines were found to be oxidized to MetO (a reversible oxidation) in control brain samples while Met-133 and Met-134 are not (59). Based on the proximity of Met-17 and Met-26 to helix H8 and their susceptibility to oxidation, it is plausible that oxidation of Met-17 and Met-26 is physiologically important and may induce local conformational changes necessary for the activation of DJ-1 zymogen. Furthermore, unlike DJ-1 M26I that has reduced protease activity, DJ-1 M17I has comparable protease activity as DJ-1 WT, either in the precursor form or in the active form) (Fig.4), suggesting that DJ-1 M17I specifically affects zymogen activation while DJ-1 M26I may have more general effects.

We also found that DJ-1 M17I mutant has normal secondary structure and therefore is unlikely to alter the global structure of DJ-1 protein (Fig. 5).

Our findings further suggest that the PD relevant M26I mutant adopts a less well-folded structure and is unstable, which may account for its loss-of-function. While DJ-1 M26I has been demonstrated to loosen the packing of DJ-1 by repelling the Ile-31 residue (151,184), it has also been shown to cause no significant changes in secondary structure and stability of DJ-1 protein (151). Our data suggest that DJ-1 M26I mutant has lower α-helix content and is stable than DJ-1 WT (Fig.5, Fig.6 and table 1), supporting that DJ-1 M26I is slightly unfolded. The degradation pathway and solubility of DJ-1 M26I has not been determined previously. We demonstrated here that DJ-1 M26I mutant is partially degraded through ubiquitin proteasome pathway and macroautophagy, characteristic of misfolded or unfolded proteins (Fig.7 and Suppl.2). Additionally, DJ-1 M26I mutant also forms aggregate when proteosomal and autophagic degradation is inhibited (Suppl.2), suggesting that the misfolded DJ-1 M26I is cleared by both pathways. These findings have provided novel insights into the pathological mechanisms PD caused by M26I mutation.

We found that mutations of Met-17, Met-133, and Met-134 to Ile do not affect protein folding and thermal stability (Fig.2), consistent with the notion that Met to Ile mutation is conservative (184). Our data showing that the stability of DJ-1 is unaltered by M133I and M134I mutations (Fig. 6) is in agreement with a previous report (254). However, using a more sensitive assay (pulse-chase assay) we found that M17I mutation stabilizes DJ-1 protein instead of reported no change in protein stability (352), It is

unlikely that M17I mutant alters the secondary structure of DJ-1 protein as we demonstrated that DJ-1 M17I has similar α-helix content and T_m as DJ-1 WT using CD measurement (Fig.5). However, DJ-1 protein has been shown to be unfolded under oxidizing condition (352), which may lead to faster degradation of DJ-1 protein. It is possible that Met-17 residue on DJ-1WT is oxidized to some degree at basal condition without causing global changes in protein folding but will accelerate DJ-1 degradation. Therefore, preventing the oxidation of Met-17 by mutagenesis could stabilize DJ-1.

Our data reveal that M17I, M26I and M133I mutations abolish DJ-1 cytoprotective function against oxidative stress induced apoptosis. The lack of cytoprotective function of DJ-1 M26I is possibly due to structural disturbance. Although oxidation of Met-17 may contribute to the faster degradation of DJ-1 without altering global secondary structure, the stabilization of DJ-1 protein via M17I mutation does not necessarily enhance its cytoprotective function. As we have shown that M17I mutant cannot be converted to a mature protease (Fig. 2) and the protease activity of DJ-1 is required for its cytoprotection (59). The deficiency in protease activation could explain the loss of cytoprotective function of DJ-1 M17I. Although M133I mutation does not affect DJ-1 zymogen cleavage, protease activity, secondary structure or protein stability, it still abolishes DJ-1 cytoprotective function. Since Met-133 residue is at the periphery of DJ-1 protein, this residue may involve in establishing protein-protein interaction in response to oxidative stress , which may be necessary for DJ-1 to activate down-stream effectors. In conclusion, our study suggests that selective methionine residues (Met-17 and Met-133) serve important signaling roles and are critical for DJ-1 cytoprotective function via

different mechanisms. Our findings also provide further evidence that the PD linked mutation M26I causes unfolding of DJ-1 protein and faster degradation through ubiquitin proteasome system and macroautophagy, therefore account for the lack of cytoprotective function of DJ-1 M26I.

ACKNOWLEDGEMENT

We thank Dr. Charles R. Gerfen and the National Institute of Neurological Disorders and Stroke/University of California Los Angeles Repository for Parkinson Disease Mouse Models for providing the DJ-1 knockout mice. The lenti-virus was prepared in Emory Neuroscience Core Facility supported in part by National Institutes of Health Grants P30 NS055077. This research project was supported in part by the flow cytometry core of the Emory University School of Medicine. This work was supported by National Institutes of Health Grants NS050650 and AG034126 (LSC) and ES015813 and GM082828 (LL).

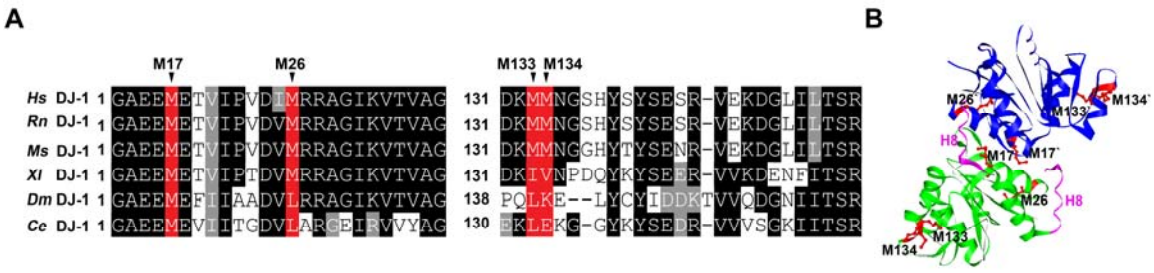

Fig.1. Alignment of DJ-1 methionine residues and depiction of methionines in DJ-1 homo-dimer structure. **(A)** Sequence alignment of DJ-1 proteins containing the four methionine reisudes (highlighted in red) in DJ-1 homologues from different species. Accession numbers are as follows: *Hs* DJ-1,NP_009193; *Rn* DJ-1, NP_476484.1; *Ms* DJ-1, NP_065594.2; *Xl* DJ-1, NP_001083896.1; *Dm* DJ-1, NP_651825.3; *Ce* DJ-1, AAB37889.1. *Hs, Homo sapiens; Rn, Rattus norvegicus; Ms, Mus musculus; Xl, Xenopus laevis; Dm, Drosophila melanogaster; Ce, Caenorhabditis elegans.* **(B)** The 3D-structure of the DJ-1 homodimer was determined by X-ray crystallography previously (PDB ID:1Q2U) (51) and illustrated using Invitrogen 3D Molecular Viewer software. One monomer was depicted in blue and the other in green. Side-chains of the four methionines were highlighted in red. α-helix H8 were highlighted in magenta.

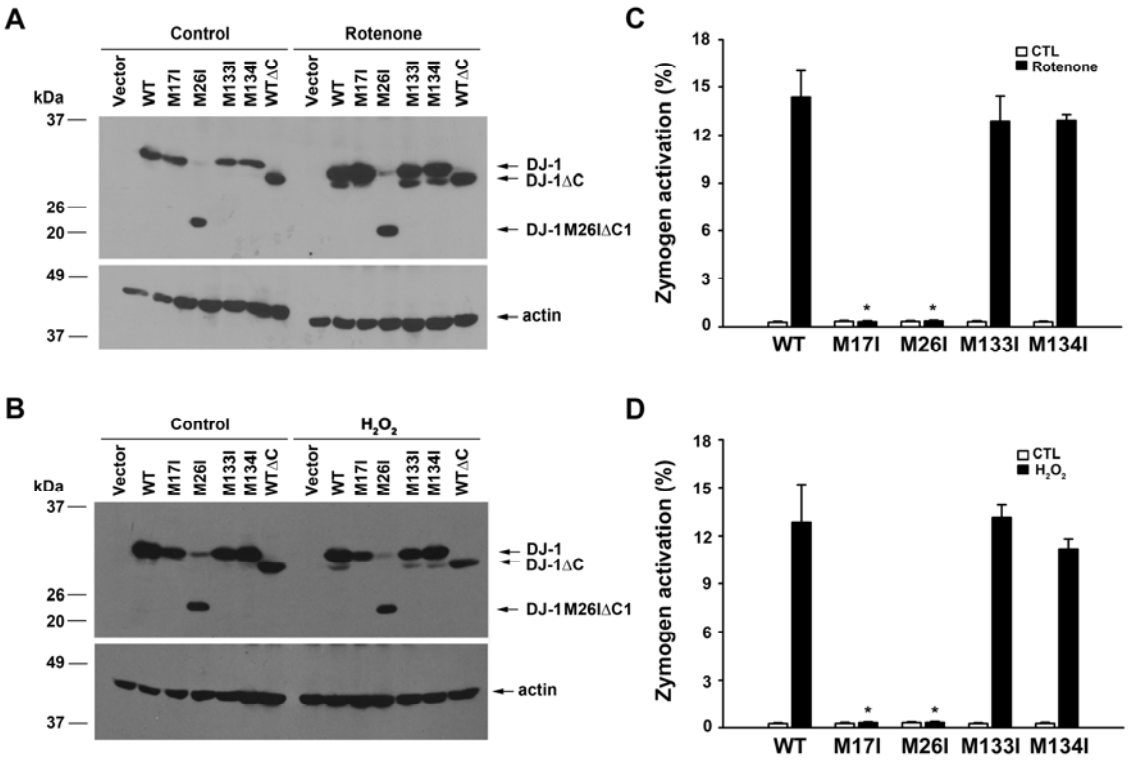

Fig.2. M17I and M26I mutations prevent activation of DJ-1 zymogen. (A and B) SH-SY5Y cells stably expressing the indicated Myc-DJ-1 proteins were treated with 10 nM rotenone (A), 100 μM H_2O_2 (B), or vehicle for 24 h, and levels of full length Myc-DJ-1 and C-terminally processed form of Myc-DJ-1 in the cell lysates were analyzed by immunoblotting with anti-Myc antibody. Lysates from cells overexpressing Myc-DJ-1WTΔC were run in parallel as a size control. (**C and D**) The levels of the Myc-DJ-1ΔC and full-length Myc-DJ-1 proteins were quantified by measuring the intensity of both bands. Zymogen activation (%) on the *Y*-axis indicates the level of Myc-DJ-1ΔC as a percentage of the total level of DJ-1 proteins (Myc-DJ-1 and Myc-DJ-1ΔC) in each cell lysate. Data represent mean ± SEM from three independent experiments. * Significantly different from DJ-1 WT expressing cells ($p < 0.05$).

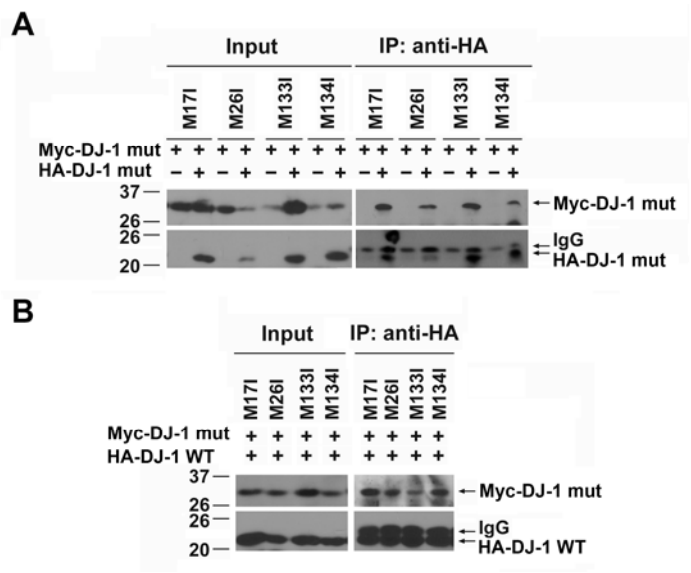

Fig.3. M17I and M26I mutations do not disrupt DJ-1 dimer formation. (A) All methionine mutants can form homo-dimer. SH-SY5Y cells expressing HA-vector or HA-tagged DJ-1 WT or indicated DJ-1 mutants and Myc-tagged DJ-1 WT or indicated DJ-1 mutants were lysed and subjected to immunoprecipitation with anti-HA antibody followed by immunoblotting with anti-HA and anti-Myc antibodies. **(B)** All methionine mutants can form hetero-dimer with DJ-1 WT. SH-SY5Y cells expressing HA-tagged DJ-1 WT and Myc-tagged DJ-1 WT or indicated DJ-1 mutants were lysed and subjected to immunoprecipitation with anti-HA antibody followed by immunoblotting with anti-HA and anti-Myc antibodies.

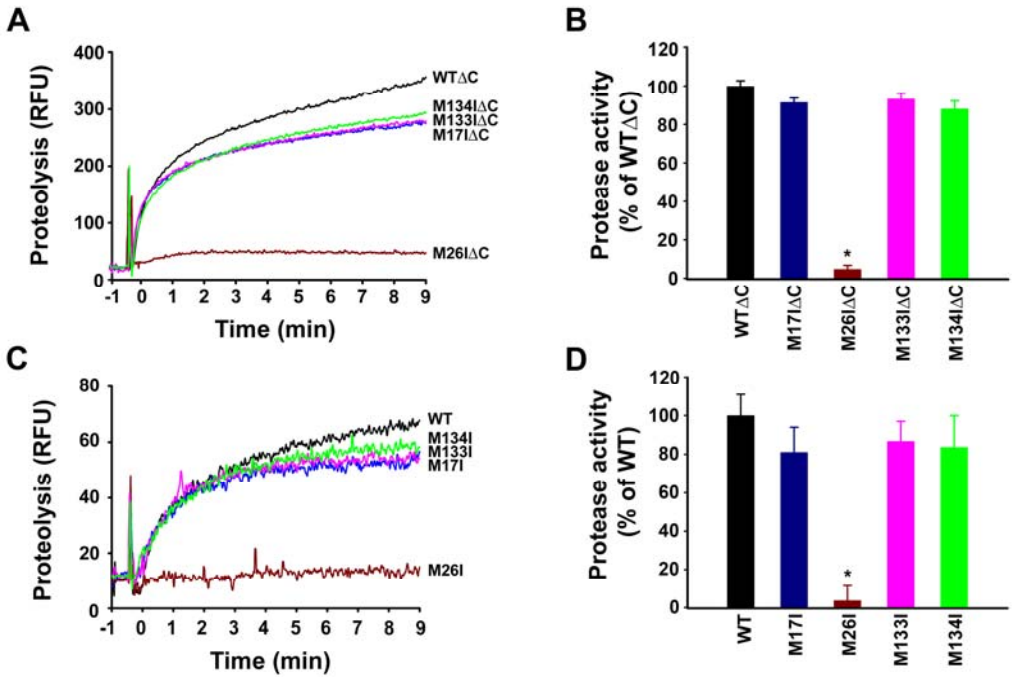

Fig.4. M26I mutation abolishes DJ-1 protease activity. (A) Protease activity of the indicated proteins was measured by a continuous, real-time fluorescence-based protease assay using BODIPY FL-casein (10 µg/ml) as the substrate. Fluorimetric recordings of 50 µm of DJ-1 WTΔC (black), DJ-1 M17IΔC (blue), DJ-1M26IΔC (dark green), DJ-1 M133IΔC (Magenta), and DJ-1 M134IΔC (lime). RFU, relative fluorescence units. **(C)** Fluorimetric recordings of 100 µm of DJ-1 WT (black), DJ-1 M17I (blue), DJ-1M26I (dark green), DJ-1 M133I (Magenta), and DJ-1 M134I (lime). RFU, relative fluorescence units. (**B and D**) Protease activity of each protein was quantified by measuring the initial velocity of the proteolytic reaction from the fluorimetric trace shown in (A) or (C). Protease activity on the *Y*-axis indicates the measured protease activity of each protein after normalization to the protease activity of DJ-1 WTΔC (B) or DJ-1 WT (D). Data represents mean ± SEM from three independent experiments. * Significantly different from DJ-1 WT ΔC (B) or DJ-1 WT (D) ($p < 0.05$).

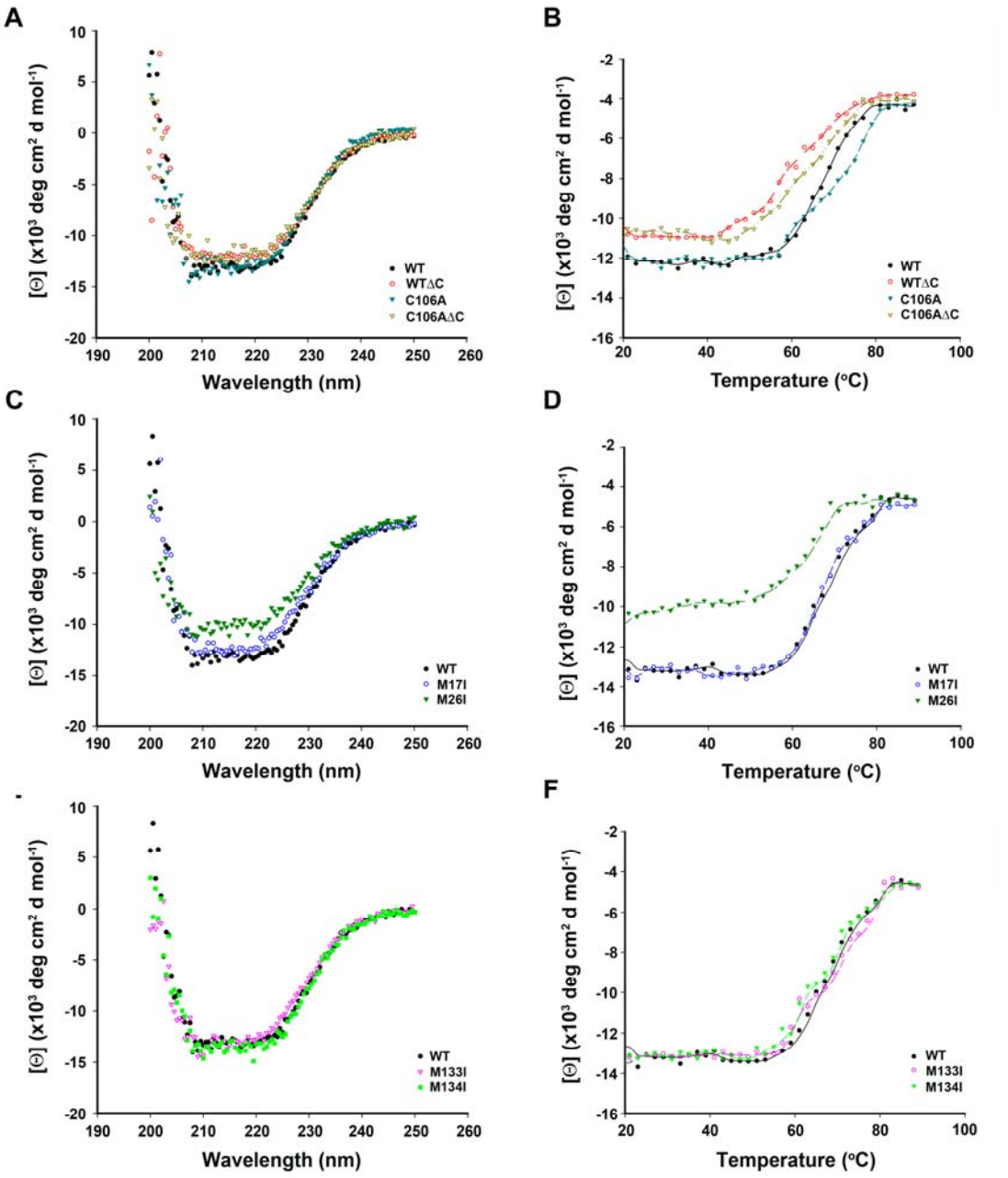

Fig.5. Far UV CD spectroscopic analysis of the secondary structure and thermal unfolding of DJ-1 WT and methionine mutants. (A, C, and E) Far UV CD spectra of DJ-1 WT and the indicated DJ-1 mutants at 25 °C. **(B, D, and F)** Thermal denaturation of DJ-1 and the indicated DJ-1 mutants. Ellipticity was recorded at 222 nm at temperatures from 20 °C to 90 °C with 2 °C step increases. deg, degrees. Curves are color-coded as

follows. In A and B: WT, black; C106A, red; WTΔC, cyan; C106AΔC, yellow. In C and D: WT, black; M17I, dark green; M26I, blue. In E and F: WT, black; M133I, magenta; M134I, lime.

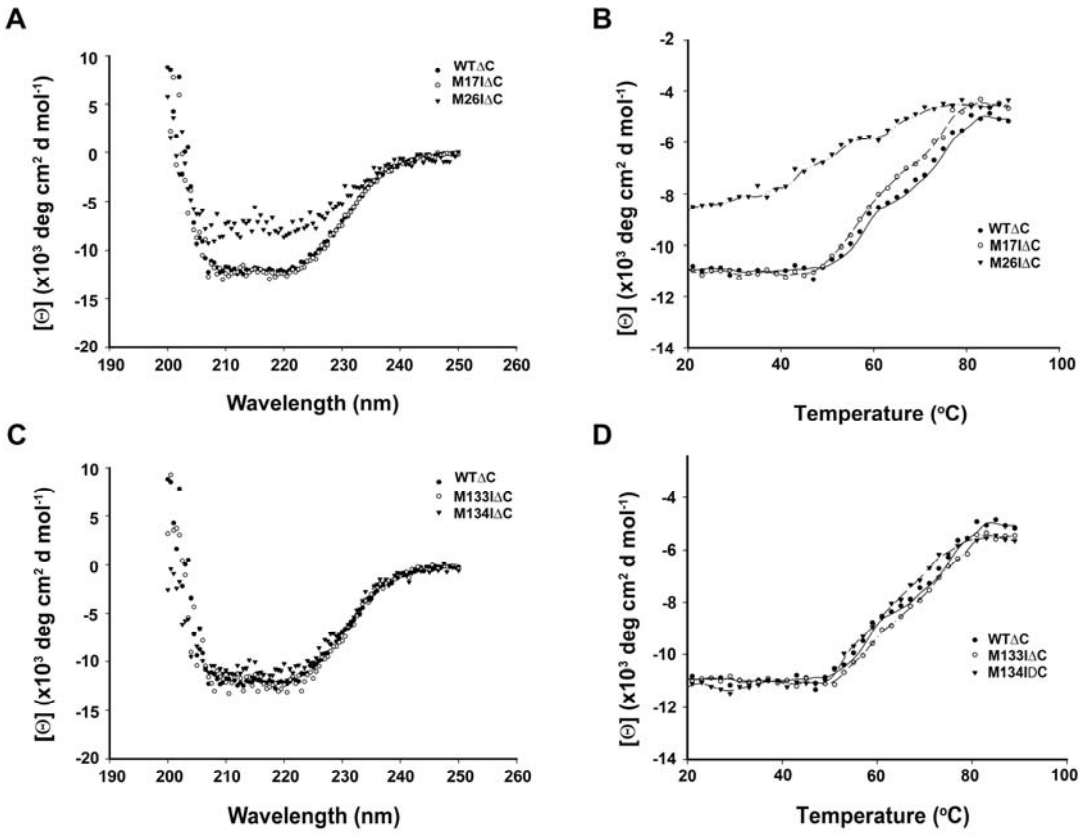

Fig.6. Far UV CD spectroscopic analysis of the secondary structure and thermal unfolding of DJ-1 WT and methionine mutants in active forms. (A and B) Far UV CD spectra of DJ-1 WT and the indicated DJ-1 mutants at 25 °C. **(C and D)** Thermal denaturation of DJ-1 and the indicated DJ-1 mutants. Ellipticity was recorded at 222 nm at temperatures from 20 °C to 90 °C with 2 °C step increases. deg, degrees.

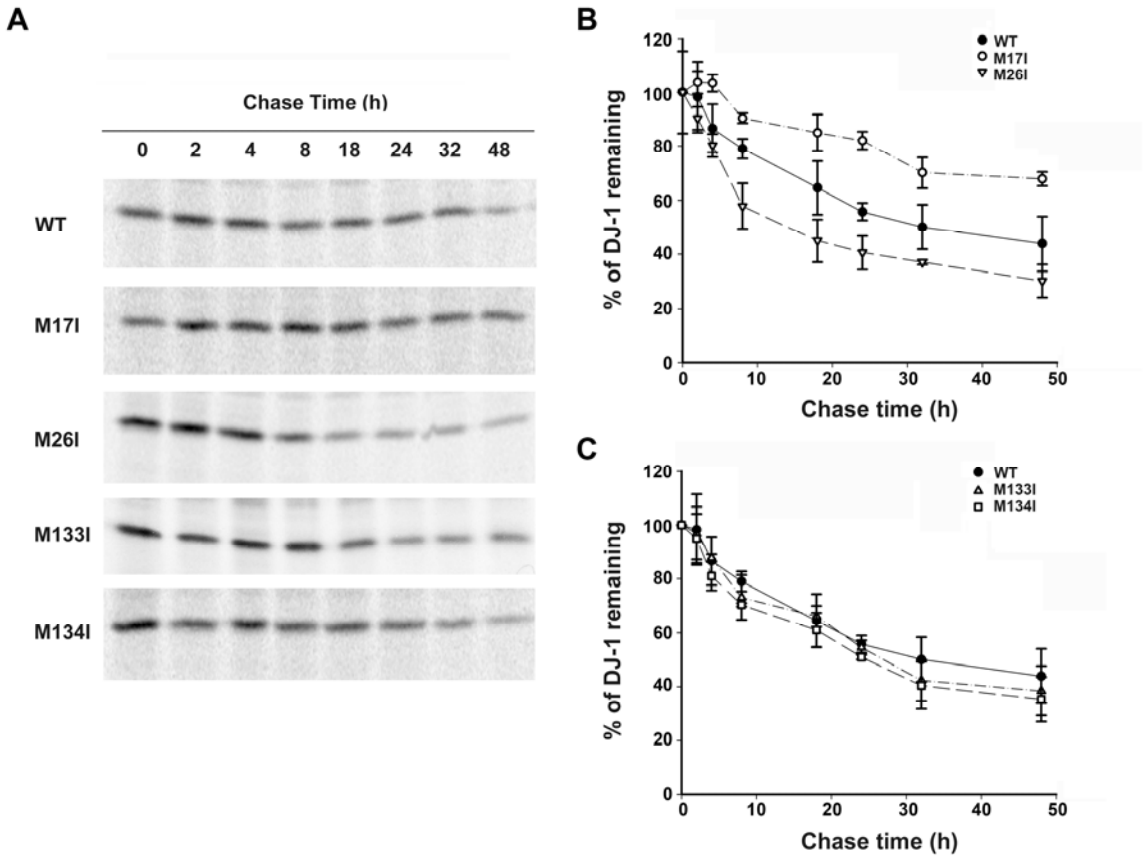

Fig.7. M26I mutation destabilizes DJ-1 protein. (A) SH-SY5Y cells expressing Myc-tagged DJ-1 WT or the indicated DJ-1 mutants were pulse-labeled for 1 hr in [^{35}S]Met/Cys-containing medium and chased with non-radioactive Met/Cys for the indicated time. ^{35}S-labeled WT or mutant DJ-1 proteins were immunoprecipitated from lysates with anti-Myc antibodies and detected by SDS-PAGE and autoradiography. **(B and C)** The levels of wild-type or indicated mutant DJ-1 proteins were quantified and plotted relative to the corresponding DJ-1 levels at 0 hr. Data represent mean ± S.E. of the results from at least three independent experiments.

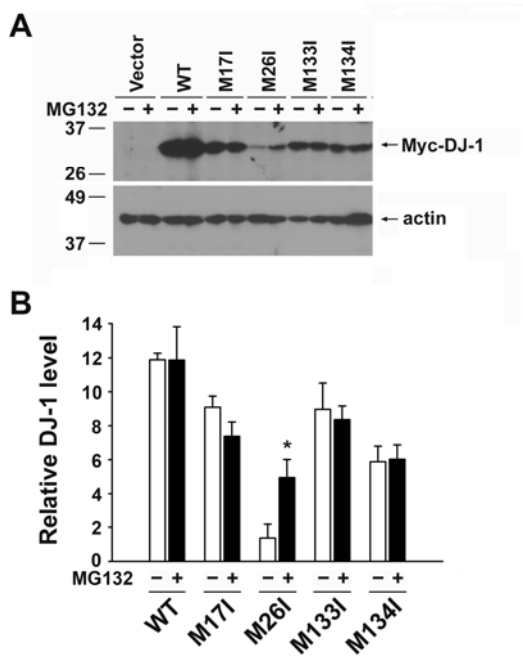

Fig.8. DJ-1 M26I mutant is partly degraded by proteasome (A) SH-SY5Y cells expressing Myc-vector, Myc-tagged DJ-1 WT, or indicated DJ-1 mutants were treated with 20 μM MG132 or DMSO for 16 h. Lysates were analyzed by SDS-PAGE and immunoblotting with anti-Myc and anti-actin antibodies. **(B)** DJ-1 level was measured by quantification of the intensity of the wild-type or mutant DJ-1 band and normalized to the actin level in the corresponding lane. The relative level of DJ-1 in the presence or absence of MG132 was averaged from at least three independent experiments and was shown as mean ± SEM from three independent experiments. *Significantly different from DJ-1 WT expressing cells ($p < 0.05$).

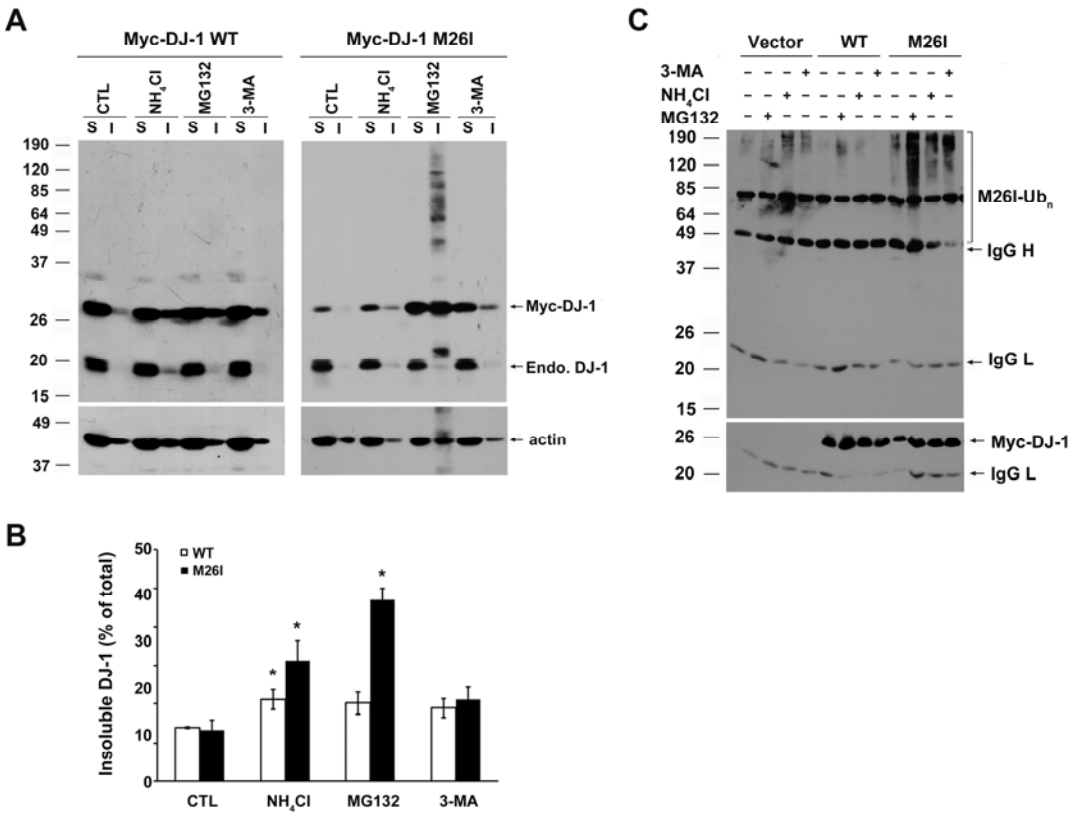

Fig.9. DJ-1 M26I mutant is ubiquitinated and forms aggregates upon inhibition of proteasomal and autophagic degradation. **(A)** SH-SY5Y cells transfected with Myc-DJ-1 WT or Myc-DJ-1 M26I for 24 h were treated with the following for 24 h, 4 μM MG132, 25 mM NH4Cl, 2.5 mM 3-MA, or vehicle control. Cell lysates were separated into triton soluble (S) and insoluble (I) fractions and resolved by SDS-PAGE, immunoblotted for Myc-DJ-1 and actin. **(B)** Quantification of the percentage of insoluble Myc-DJ-1 WT (open bar) and Myc-DJ-1 M26I (solid bar). The intensity of Myc-DJ-1 in the soluble and insoluble fractions was measured using Scion Image. The % of the insoluble DJ-1 was calculated by dividing the insoluble DJ-1 by the total (soluble + insoluble). The smear in the insoluble fraction of DJ-1 M26I transfected cells, treated with MG132 was not counted as the total DJ-1 M26I level. Data was shown as mean ±

SEM from three independent experiments and was analyzed using one way ANOVA analysis. *Significantly different from the corresponding vehicle treated control ($P < 0.05$). **(C)** SH-SY5Y co-transfected with HA-ubiquitin and Myc-DJ-1 WT, Myc-DJ-1 M26I or Myc-vector for 24 h, were treated with the following for 24 h, 4 μM MG132, 25mM NH_4Cl, 2.5 mM 3-MA, or vehicle control. Cell lysates were subjected to denatured immunoprecipitated using an antibody against Myc epitope, and probed for HA-ubiquitin and Myc-DJ-1. IgG H, immunoglobin heavy chain; IgG L, immunoglobin light chain.

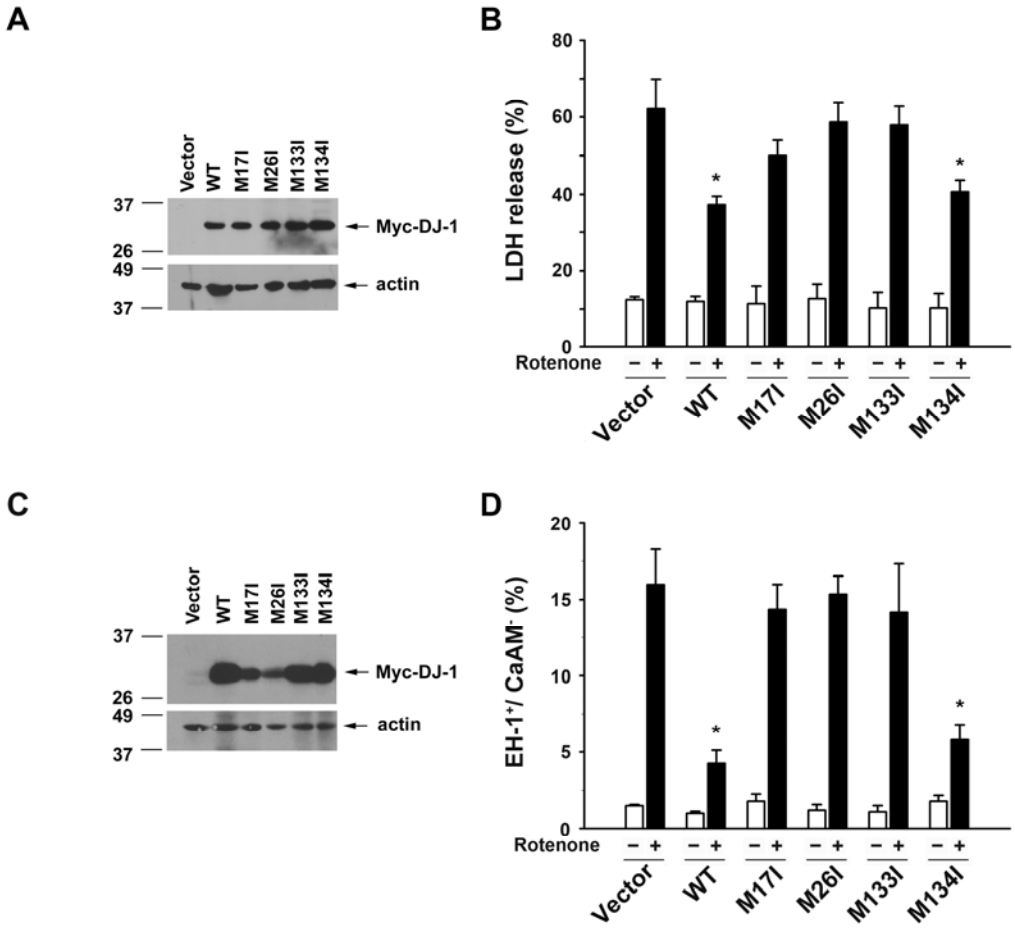

Fig.10. Met-17, Met-26, and Met-133 are important for DJ-1 cytoprotective function. **(A and C)** SH-SY5Y cells transiently (A) or stably (C) transfected with the indicated DJ-1 or empty vector were treated with 100 nM rotenone for 24 h. Cell lysates were separated on SDS-PAGE gel and DJ-1 was detected using immunoblot analysis. **(B)** SH-SY5Y transiently transfected with indicated plasmids were treated with 100 nM rotenone for 24 h. The extent of cell death was assessed by measuring LDH released to the culture medium and normalized to the total level of LDH release upon cell lysis. Data was expressed as mean ± SEM from four independent experiments.* Significantly different from cells expressing Myc-vector ($p < 0.05$). **(D)** SH-SY5Y cells stably expressing indicated plasmids were treated with 100 nM rotenone for 24 h. The extent of cell death

was assessed by staining cells 0.1 μM CaAM and 1 μM EH-1 for 20min. Percentage of cells stained with either marker was measured using flow cytometry analysis. Percentage of cells stained with positive with EH-1 but negative CaM stain ($EH\text{-}1^{+}/CaM^{-}$) was regarded as dead cells and was quantified from three independent experiments. Data was expressed as mean ± SEM. * Significantly different from cells expressing Myc-vector ($p < 0.05$).

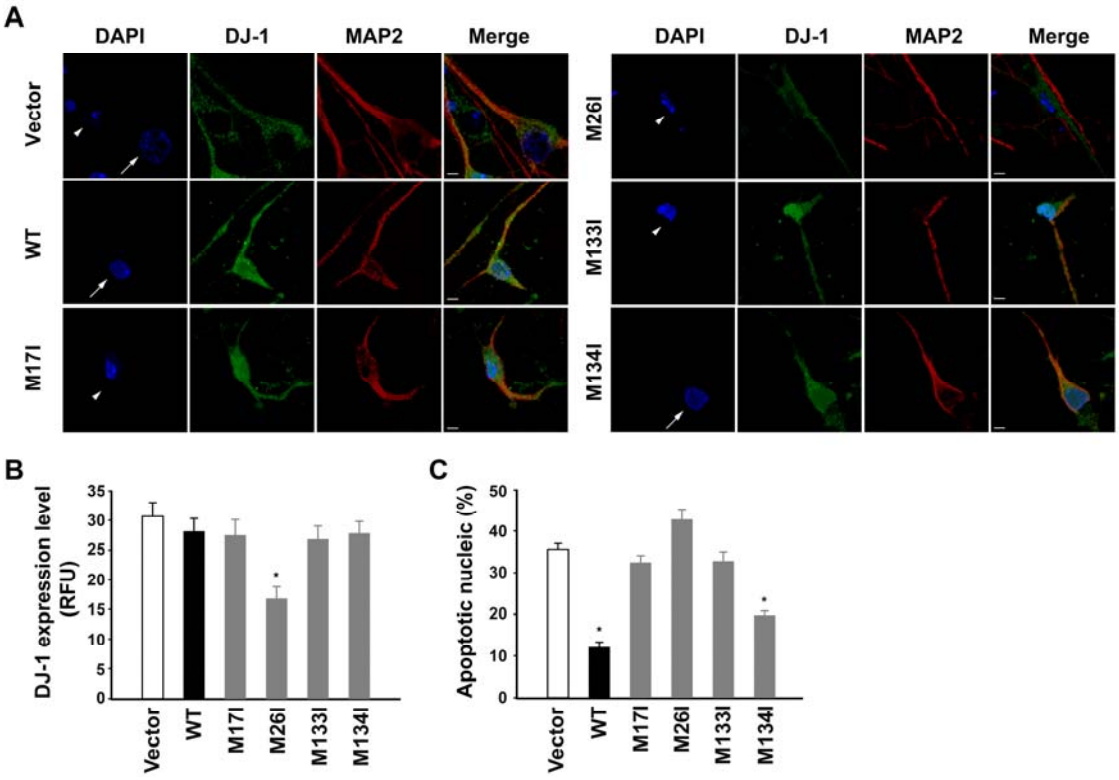

Fig.11. DJ-1 M17I, M26I, and M133I fail to rescue the pro-apoptotic phenotype of *DJ-1*$^{-/-}$ cortical neurons. (A) DJ-1 $^{-/-}$ cortical neurons were infected with lentivirus carrying indicated plasmids for 48 h starting at DIV4. Neurons were then treated with 5 nM rotenone for 24 h before processed for staining. Neurons were stained with anti-MAP antibody (green), transfected neurons were identified by anti-DJ-1 (P7F) immunostaining (red) and nuclear integrity was assessed by DAPI staining (blue). Arrows indicate neurons with normal nuclei, whereas arrowheads indicate neurons with apoptotic nuclei. Scale bar, 10 μm. (**B**) The expression level of wild-type or mutant DJ-1 protein was quantified and is presented as the fluorescence intensity of DJ-1 immunofluorescence in transfected neurons. Data represent mean ± SEM from three independent experiments. RFU, relative fluorescence units. (**C**) Apoptosis is expressed as the percentage of transfected neurons with apoptotic nuclear morphology. Data represent mean ± SEM

from four independent experiments with a total number of 150-200 neurons being scored.

*$P < 0.05$.

Table III-1. T_m and % of α- helix of DJ-1 proteins

Full length			ΔC		
DJ-1	**T_m**	**% α-helix**	**DJ-1**	**T_m**	**% α-helix**
WT	70	35.7	WTΔC	65	33.5
C106A	70	35.0	C106AΔC	63	33.7
M17I	70	32.3	M17IΔC	65	33.3
M26I	63	29.6	M26IΔC	52	16.0
M133I	70	35.8	M133IΔC	66	31.5
M134I	68	36.2	M134IΔC	64	32.0

CHAPTER IV

DISCUSSION AND FUTURE DIRECTIONS

Summary of findings

In this thesis I investigated the activation mechanisms of DJ-1 zymogen, the functional significance of DJ-1 as a protease, and the regulation of DJ-1 zymogen activation by methionine residues. The findings presented in chapters II-III demonstrate that:

1. DJ-1 exists as a zymogen that can be activated via C-terminal cleavage, and the activated DJ-1 functions as a cysteine protease that confers cytoprotective function against oxidative stress induced cell death.
2. DJ-1 zymogen cleavage is likely regulated by oxidation of Met-17 residue, while Met-26 is structurally important because the PD-linked mutation M26I disrupts DJ-1 folding and results in faster degradation of DJ-1 via both proteasome and autophagy pathways.

A discussion of the implications of these findings for understanding the biological functions of DJ-1, the regulation of DJ-1 function by cellular redox status and pathological mechanisms of PD, as well as potential future directions are provided in this chapter.

DJ-1 exists as a zymogen that can be activated via C-terminal cleavage

DJ-1 protease activity can be activated via C-terminal cleavage

Despite the structural similarity of DJ-1 with PfpI protease family members, DJ-1 has an additional α-helix at the c-terminus. This helix is predicted to prevent the formation of a mature catalytic site and inhibit substrate binding (145). In support of this hypothesis, we found that removal of the C-terminal tail remarkably enhances DJ-1 protease activity by a

13.2-fold decreases in K_m and a 1.9-fold increases the $k_{cat,}$, resulting in a 25-fold net-increase of catalytic efficiency (k_{cat} /K_m) than DJ-1 WT, suggesting that the deletion of C-terminal helix facilitates substrate binding and enhances catalytic efficiency. The deletion may open up the substrate binding pocket to allow substrate entering or trigger conformational changes that can allow the formation of a functional catalytic triad or diad. The increase in catalytic efficiency after zymogen activation varies considerably among proteases (table IV-1), ranging from 10 to 10,000 fold increase. For proteases with low zymogenicity such as tissue type plasminogen activator (tPA) and caspase 9, it is believed that allosteric modulation substitutes the requirement of proteolysis of zymogen for significant protease activation (322). For example, the cleaved form of caspase-9 is only marginally more active than casapse-9 zymogen, but association with the cofactor (apoptosome) dramatically increases the catalytic activity of the processed caspase-9 for up to 1000 fold (86,322). The zymogenicity of DJ-1 is comparable to that of caspase 9 and tPA (table IV-1), suggesting that cofactors may be required for DJ-1 exerting its maximum activity. The low zymogenicity of DJ-1 could also be attributed to the fact that casein may not be the optimal substrate for DJ-1 and thus catalytic efficiency for casein is not the best reflection for DJ-1 catalytic efficiency. Notably, other enzymatic activities of DJ-1 have been reported, including peroxidase activity (13), RNA binding activity (347), and chaperone activity (303,379). It would be important to confirm whether DJ-1 zymogen possesses these reported enzymatic activities and how the C-terminal tail of DJ-1 influences these enzymatic activities.

We found that DJ-1 protease activity is abolished by mutating the predicted catalytic cysteine residue, supporting the hypothesis that DJ-1 is a cysteine protease and

the Cys-106 is the catalytic residue. This finding could explain observations that overexpression of DJ-1 C106A mutant has no protection in various models (46,222,303,329) as the reactive cysteine is indispensable for DJ-1 protease activity. We also demonstrated that like most cysteine proteases DJ-1 protease activity is inhibited by oxidation. This raises the possibility that DJ-1 protease activity would be impaired by oxidation, a well recognized contributing factor of PD. In fact, irreversible oxidation of DJ-1 protein has been found specifically in brain tissues from sporadic forms of PD patients not from control patients (60), supporting the hypothesis that DJ-1 function could be inhibited by oxidative modification in sporadic PD patients. It is possible that DJ-1 inactivation would be the common theme underlying both sporadic and familial PD pathogenesis. Our finding that DJ-1 protease activity is sensitive to oxidation could also explain why other investigators failed to detect DJ-1 protease activity using non-reducing condition either during the purification of DJ-1 protein or protease activity measurement (192,303). Oxidation of the catalytic cysteine has been reported during the purification of caspases (322). Not surprisingly, the catalytic cysteine Cys-106 has been shown to be oxidized during purification (360), which may account for its loss of protease activity.

The activation of DJ-1 zymogen is redox-dependent

We demonstrate in this study that DJ-1 could be cleaved at the c-terminus and the cleavage of DJ-1 reaches a peak under mild oxidation when cell death and apoptosis are not apparent (Fig. II-5), suggesting that DJ-1 processing happens before activation of apoptosis or cell death pathways. The fact that level of endo. DJ-1_p is not further increased at higher level of oxidation argues against the possibility that DJ-1 is cleaved

nonspecifically due to oxidation. The oxidation induced C-terminal cleavage of DJ-1 may allow DJ-1 to act as a redox sensor, which will activate anti-oxidative pathways in response to mild oxidation and prevent damage caused by more severe oxidation. It has been shown that depending on the degree of oxidative stress, different pathways will be activated sequentially to initiate appropriate cellular responses, from proliferation, differentiation, apoptosis, to necrosis (345). We showed that 1 mM H_2O_2 is enough to almost completely abolish DJ-1 protease activity *in vitro*, while the cleavage of DJ-1 is most significant when cells were treated with 100 μM H_2O_2, suggesting that DJ-1 may be only active in certain range of the cellular redox state though the exact redox potential required for maximum DJ-1 protease activity remains to be characterized. It has been shown that caspase 3 is only active when cells were treated by 50~200 μM H_2O_2 or 200~500 μM diamide (345), suggesting that the activity of cysteine proteases is largely influenced by the cellular redox status in addition to other regulatory mechanisms. Similar to caspases, DJ-1 protease may also be active within a limited range of redox state to ensure appropriate cellular responses to various degrees of oxidative stress. The concentrations of H_2O_2 needed to activate DJ-1 protease may vary among cell lines since the abundance of the antioxidative enzymes and other small antioxidants varies between cells. More studies need to be conducted to characterize the optimal redox potential that activates DJ-1 protease in other cells.

Molecular mechanisms regulating DJ-1 zymogen activation are unclear

DJ-1 has been reported to autoproteolyzed between residue 156 and 157 in a redox-dependent manner (265). However, we failed to detect self-cleavage of DJ-1 under similar experimental conditions. The cleavage between residue 156 and 157 of DJ-1

essentially removes two α-helixes (H7 and H8) from the C-terminus. The α-helix H7 has been shown to participate in the dimerization of DJ-1 protein (145,149,360) and removal of H7 may disrupt homodimerization of DJ-1 protein. Thus, the redox-dependent DJ-1 self-cleavage reported by Ooe et al (265) is likely to be an inactivation of DJ-1 due to strong oxidation since intensive oxidation is known to break up the backbone of the polypeptide (27), although auto-proteolysis of DJ-1 as an activation mechanism can not be ruled out as the presence of co-factors may be required for auto-proteolysis.

It is also likely that DJ-1 may be cleaved by other proteases, like the activation of executor caspases by the initiator caspases (86,304). Interestingly, matrix metalloprotease-14 (MMP-14) has been demonstrated to cleave recombinant GST-DJ-1 fusion protein at multiple sites (41). DJ-1 has also been shown to be processed by other matrix metalloproteases, including MMP-1, -2, -8, and -9, although neither of the processed forms of DJ-1 resembles DJ-1ΔC (41). Given that MMP proteases family mainly function in extracellular matrix while DJ-1 is mainly a cytosolic protein, how and where MMP cleaves DJ-1 is very intriguing. More recently, DJ-1 was reported to be cleaved at the carboxyl side of D149 by caspase 6 and the C-terminal 40aa fragment of DJ-1 was demonstrated to be more cytoprotective than DJ-1 WT (108). It is uncertain, though, whether binding partners are required for stabilizing the 40aa C-terminal fragment of DJ-1 and how the C-terminal fragment of DJ-1 exerts its cytoprotective function. Since the putative catalytic cysteine residue, Cys-106, is absent from the C-terminal fragment, biological activity of DJ-1 that is independent of Cys-106 remains to be discovered. Using proteases database available (MEROPS and PeptideCutter), we were unable to identify proteases that can hydrolyze DJ-1 protein at C-terminus and

release the C-terminal helix H8 without disrupting the folding of DJ-1 protein. However, most of the proteases databases predict substrates cleavage site based on the consensus and primary sequence, increasing chances of getting false negative search result. Future research to characterize reported DJ-1 interactors may help identify regulators of DJ-1 protease activity.

The activated DJ-1 functions as a cysteine protease that confer cytoprotective function against oxidative stress induced cell death

Limited proteolysis of DJ-1 substrate(s) may confer cytoprotection

DJ-1 has been shown to activate cellular antioxidant responses and prevent apoptosis through stabilizing nuclear factor erythroid 2-related factor (Nrf2)(67); repressing p53 transcriptional activity(95); upregulating glutathione synthesis (377); and inhibiting apoptosis signal-regulating kinase (ASK1) activity (158). While the mechanisms underlying DJ-1 mediated pro-survivial and anti-apoptosis effects are unknown, one possibility is that DJ-1 protease regulates the stability or nuclear transport of transcription factors since proteolysis is known to control the stability and intracellular localization of transcription factors (146). It is also likely that DJ-1 modulate the binding affinity or function of its client proteins by proteolysis-induced conformational changes. It would be interesting to test whether the reported DJ-1 binding proteins are the substrates of DJ-1 protease in order to understand the substrate specificity and cellular roles of DJ-1 protease. So far, two putative substrates of DJ-1 have been proposed, homeodomain interacting protein kinase 1 (HIPK1) (297) and transthyretin (TTR) (174). Although DJ-1

has not been proved to directly cleave these two proteins, it has been shown to negatively regulate the protein level of HIPK1 and TTR proteins and Cys-106 of DJ-1 is required for this negative regulation (174,297), suggesting that the nucleophilic cysteine Cys-106 is essential for the down-regulation of HIPK1 and TTR protein level by DJ-1. However, the relevance of these two proteins as DJ-1 protease substrate to PD pathogenesis is elusive. In order to better understand the functional implication of DJ-1 as a protease, it will be important to identify DJ-1 substrates and the biological consequences of accumulation of DJ-1 substrates resulting from loss-of-function of DJ-1.

DJ-1 may function as a de-SUMO or de-ubiquitin protease

De-SUMO proteases and de-ubiquitin proteases are cysteine proetases that deconjugate SUMO or ubiquitin from the corresponding substrates and hydrolyze SUMO or ubiquitin precursors to the mature forms. Using cDNA from human adult brains as prey library, DJ-1 was found to interact with SUMO-1, SUMO-activating enzyme Uba2, and SUMO-conjugating enzymes Ubc9 (158). In a separate yeast two hybrid study, DJ-1 has been shown to interact with an SUMO E3 ligase PIASxα using cDNA library from human testis as prey (332). It is likely that DJ-1 itself is SUMOylated therefore it interacts with SUMO machinery. This hypothesis is supported by findings that DJ-1 can be SUMOylated at Lys-130 and SUMOylation of DJ-1 is required for its cytoprotective functions (94,306). The E3 that regulates DJ-1 SUMOylation has not been defined but DJ-1 has been shown to interact with two E3 ligases, PIASxα (332) and TOPOR/p53BP3 (307). In addition to being a substrate of SUMOylation, several lines of evidence also suggest that DJ-1 may act as a DeSUMO protease. DJ-1 has also been shown to inhibit SUMOylation of PSF (373,374) and p53 (307), and release the transcriptional

suppression of SUMOylation on these two transcription factors. However, DJ-1 does not share structure homology with the known SENPs (sentrin specific proteases) and the de-SUMO activity of DJ-1 has not been demonstrated, especially de-conjugation of SUMO from substrates requires isopeptidase activity instead of endopeptidase activity.

Interaction of DJ-1 with both ubiquitin E3 ligase and de-ubiquitin protease has also been reported. DJ-1 was found to be present with two other PD linked proteins, Parkin and PINK1, in the same complex and promote the ubiquitination of Parkin on Synphilin-1, a putative Parkin substrate, as well as auto-ubiquitination of Parkin (363). However, how DJ-1 promotes the E3 ligase activity of Parkin warrants further investigations. More recently, DJ-1 has been shown to interact with a de-ubiquitin protease Cezanne/OTUD7B/Za20d1 and inhibits the de-ubiquitin protease activity of Cezanne (229). Although the exact mechanism of how DJ-1 inhibits the protease activity of Cezanne is undefined, DJ-1 is likely to compete with Cezanne for binding to polyubiquitin chain without hydrolyzing the polyubiquitin chain. Combined this with the finding that DJ-1 enhances the E3 ligase activity of Parkin, it is plausible that DJ-1 interacts with poly-ubiquitinated proteins and assists the modification of the polyubiquitin chain by other enzymes. It is also likely that DJ-1 possesses polyubiquitin chain editing function as well but can only de-conjugate specific substrates.

Regulation of DJ-1 zymogen activation, protease activity and cytoprotective function by methionine residues

Met-17 is important for DJ-1 zymogen cleavage

DJ-1 zymogen activation occurs when cells are under mild oxidative stress, possibly due to redox-dependent changes on DJ-1 or on proteases activating DJ-1 (52). Oxidative modifications on DJ-1 have been shown previously, including oxidation of cysteine residues, nitrosylation of non-catatlytic cysteines, oxidation of methionines, and carbonylation of DJ-1 protein (74). As carbonylation is irreversible modification and usually occurs in response to intensive oxidative stress, it is unlikely to be responsible for DJ-1 zymogen activation. We have previously demonstrated that two methioniones are oxidized to a reversible oxidative form in healthy human brain samples, while we failed to detect nitrosylation of the two non-catalytic cysteines (59). This suggests that methionine oxidation is more likely to be physiolocially relevant than nitrosylation of noncatalytic cysteines. Since DJ-1 protease activity relies on the catalytic cysteine residue to be in the reducing condition, if oxidation of the catalytic cysteine itself regulates DJ-1 zymogen activation, it would require reduction of that catalytic cysteine immediately after zymogen activation to carry out proteolytic reaction. Therefore, oxidation of methionine is more suitable to regulate the activation of DJ-1 zymogen efficiently.

Met-17 is the most conserved methionine of the four methionines on DJ-1 protein that locates in the middle of the helix H1, in close proximity to helix H8 (Fig.I-1) (150,338). We found that helix H8 of M17I mutant cannot be cleaved in response to mild oxidation, supporting an important role of Met-17 in regulating DJ-1 zymogen activation. However, zymogen activation can be triggered by either conformational changes induced by oxidation of Met-17 or by oxidation-independent interactions established by Met-17. In support of the first possibility, oxidation of methionine to MetO can increase the

polarity and hydrophilicity of the side chain, therefore alters local conformation (50). In addition, although Met-17 is buried in the core of DJ-1 protein, it is more readily oxidized than Met-133 or Met-134 (59). This suggests that Met-17 is not a general antioxidant to buffer free radicals but rather plays specific roles in regulating redox-dependent events. Similarly regulation of protein function via oxido-reduction of methionine residues has been demonstrated in other proteins, such as IκBα and calcineurin (3). However, detection of oxidized methionine residues remains a major challenge that has limited the study of how methionine oxidation regulates functions of individual proteins.

M26I mutant is slightly unfolded and degraded through proteasome and lysosome

Homozygous mutation of M26I was identified in an early onset PD patient, but the pathological mechanisms of this mutation are still unclear. Reports on how DJ-1 M26I mutation affects on the secondary structure, stability, quandary structure, and cytoprotective function of DJ-1 are inconsistent (29,151,184,198,331,371). Our data suggest that DJ-1 M26I mutant is slightly unfolded compared to DJ-1 WT, but the unfolding effect is not as dramatic as another well-characterized DJ-1 mutant L166P. M26I mutant can still form homodimer or heterodimer with DJ-1 WT, and the half-life of DJ-1 M26I is about 22h, slightly shorter than DJ-1 WT (33h) but much longer than DJ-1 L166P (3h) (Figure III-6). The degradation pathway of this PD linked mutant (DJ-1 M26I) has not been well defined. In the present study, we find that DJ-1 M26I mutant can be poly-ubiquitinated and degraded through both proteasome and autophagy pathways,

characteristic of misfolded proteins(263,335). Additionally, we also demonstrate that DJ-1 M26I forms aggregate when proteasomal or autophagic degradation is inhibited, suggesting that the degradation of M26I follows the same degradation pattern of another misfolded protein DJ-1 L66P mutant (262,264). However, the percentage of the misfolded and aggregated DJ-1 M26I is undetermined and is likely to be less than DJ-1 L166P. It is also plausible that there are two pools of DJ-1 M26I existing (soluble and insoluble) and are in dynamic exchange with each other, depending on the cellular environment (such as the availability of chaperones, ATP level, and the activity of ubiquitin proteasome degradation system).

Despite the relatively mild effects on the structure and stability of DJ-1 protein, M26I mutation almost abolishes the protease activity of DJ-1 (Figure III-4) and shows no cytoprotective function (Figure III-8 and Figure III-9). This suggests that the remaining, non-degraded soluble portion of DJ-1 M26I protein in the cell probably losses its normal function as well. The almost complete loss of protease activity and cytoprotection induced by M26I mutation is possibility due to the structural disturbance but it is also likely to be caused by the non-oxidizable effect of Met-26 residue. Further studies on whether oxidation on Met-26 residue could contribute to DJ-1 zymogen activation, protease function and cytoprotective activity can be carried out using conservative mutation of Met-26 to other residues such as Leu or Val. Both Leu (23,63) and Val (328) have been used by other researchers to prevent methionine from oxidation in order to study the functional implications of methionine oxidation. These mutations can avoid the

steric repulsion between Ile-26 and Ile-31, which is proposed to cause the unpack effect of the M26I mutation (151).

Future directions

Identification of DJ-1 protease substrates

Identification of DJ-1 substrates will yield insight into the downstream effects of DJ-1 protease activity and the cellular pathways that DJ-1 may be involved. The conformation of the active sites of proteases largely determines substrate specificity (Figure I-2). A small peptide library can be used to identify the preferred substrate cleavage sites of DJ-1. This method allows high-throughput enzymatic studies and has been successfully used by several groups to identify the substrate specificity of proteases (85). Based on the substrate specificities determined by comparative analysis of the synthetic peptide library, a search against the published human database can be carried out to find potential substrates. To verify the candidate substrate(s), co-localization and interaction of DJ-1 with the candidate substrate(s) *in vivo* will determined, and the cleavage of the putative substrate(s) by DJ-1 can be further confirmed.

If the optimal cleavage sites obtained from the small peptide screening failed to fish out any substrate from the human protein database, additional libraries containing more cleavage sites can be screened to provide more information on the cleavage specificity of DJ-1. In addition, the cleavage site(s) on casein and the identified DJ-1 substrate transthyretin can be identified by Edman degradation sequencing. The

combined information on the DJ-1 cleavage sites should enhance the chance of substrate identification in the human genome database.

It is possible that DJ-1 may recognize tertiary structures instead of primary amino acid sequence. In this case, the optimal cleavage site will be hard to identified using small peptide library screening. An alternative approach will be to compare protein expression pattern of brain homogenates from DJ-1 WT and KO mice using 2-dimensional gel electrophoresis. Proteins with elevated expression in DJ-1 KO mice can be identified by mass spectrometry and further verified using *in vitro* binding assay and protease assay.

If both the library screening and comparison of protein expression pattern in DJ-1 WT and KO tissues fail to identify DJ-1 substrates, another method to try would be using DJ-1ΔC as the antigen for affinity purification from cell lysates or brain homogenates to identify proteins preferentially bind to DJ-1ΔC. The putative interactors can be further characterized using *in vivo* and *in vitro* binding assay as well as protease assay. The reason to use DJ-1ΔC as bait is because DJ-1ΔC should have higher affinity with substrates than DJ-1WT based on our data (Fig. II-4), and therefore is more likely to detect potential interactors. It is unlikely that the catalytic defective mutant DJ-1C106AΔC has reduced affinity with substrates compared to DJ-1WTΔC, since the substrate affinity is normally determined by the substrate binding pocket instead of the catalytic residue. Therefore DJ-1C106AΔC can still bind to the substrate as strongly as DJ-1 WTΔC does, but unlike DJ-1WTΔC it cannot hydrolyze the substrate once it binds,

so using DJ-1C106AΔC should enable us to identify endogenous substrates more efficiently than DJ-1WTΔC.

Is DJ-1 protease activity required for maintaining mitochondrial homeostasis?

Given the important role of mitochondrial homeostasis in PD pathogenesis (76), localization of DJ-1 to mitochondria has prompted hypothesis that DJ-1 may exert its neuroprotection by maintaining mitochondrial homeostasis (29,46,195,371). Despite controversial reports on the translocation of DJ-1 to mitochondria upon oxidative stress (46) and the submitochondrial localization of DJ-1 in mitochondria (46), DJ-1 has been shown to confer resistances against mitochondrial toxins in cell models (46,329) and rodent models (165,215) . In support of the important roles DJ-1 play in maintaining mitochondrial function, it has been shown that artificially targeting DJ-1 by fusing a mitochondrial targeting signal to DJ-1 increased its cytoprotection against oxidative stress induced cytotoxicity (157). The precise role of DJ-1 in mitochondria remains to be elucidated, but it has been proposed to be involved in anti-oxidative stress. DJ-1 may act as a chaperone or a protease within mitochondria to reduce protein misfolding and restore mitochondrial function or it may simply act as a free radical scavenger to restore the redox balance in mitochondria.

We have demonstrated that DJ-1 functions as a cysteine protease that requires activation in response to mild oxidative stress (52). Understanding the major cellular compartments where DJ-1 protease resides and functions under oxidative stress would an important step towards revealing DJ-1 biological functions. Since mitochondria are the major source of endogenous ROS and localization of DJ-1 WT to mitochondria has been

reported, it would be interesting to test whether DJ-1 protease activity is important for maintining mitochondrial homeostatis in response to mitochondria-derived oxidative stress. By expressing constitutively active DJ-1 mutant (DJ-1 WTΔC), protease-defective form of DJ-1 mutant (DJ-1 WTΔC) and DJ-1WT in DJ-1 KO primary neurons via virus expression, we could examine whether DJ-1 WTΔC can restore mitochondrial dynamics and polarity more efficiently than DJ-1 WT. The subcellular localization of active DJ-1 protease and DJ-1 zymogen should also be investigated via biochemical assays and immunocytochemistry to gain knowledge of where DJ-1 active proteases are mostly needed and where the majority of DJ-1 substrates would be, in response to oxidative stress induced by different reagents.

More recent data shows that DJ-1 may also play a role in maintaining mitochondrial dynamics. Absence of DJ-1 resulted in mitochondrial depolarization and fragmentation (30,153,177). ROS has been proposed to play a role in these mitochondrial abnormalities seen in DJ-1 KO cells, as ROS scavengers can rescue the phenotypes (153). Additionally, Parkin and PINK1 overexpression can also rescue mitochondrial defects caused by loss of DJ-1 (153), and Parkin was able to rescue mitochondrial aberrations due to lack of DJ-1 in a separate study (341). A plausible explanation would be DJ-1 acting upstream of Parkin in the same pathway in maintaining mitochondrial dynamics, but interaction of DJ-1 WT with Parkin has not been convincingly demonstrated. Additionally, DJ-1 could still prevent mitochondrial fission in the absence of PINK1, which has been shown to be upstream of Parkin in terms of maintaining mitochondrial dynamics using genetic models (64), suggesting that DJ-1 can act independent of PINK1 and Parkin. Based on these data, another model that DJ-1 acts in parallel to PINK1 and

Parkin in maintaining mitochondrial dynamics has been proposed (341). In both models whether DJ-1 protease activity is responsible for maintinaing mitochondrial dynamics remains to be examined. A recent study demonstrated that DJ-1WT, but not C106A mutant that lacks DJ-1 protease activity, could rescue mitochondrial fission induced by α-syn (161), suggesting that DJ-1 protease activity is required for regulating mitochondrial fusion and fission. However, how DJ-1 protease regulates mitochondrial fusion and fission remains unknown. One possibility is that DJ-1 could regulate stability and function of mitochondrial fusion and fission proteins via proteolysis of these proteins. To test this, stability and activity of these proteins could be examined in the presence and absence of DJ-1 WT, DJ-1 WTΔC, and DJ-1 C106AΔC in primary neurons as well as using *in vitro* assays. If the effect of DJ-1 is independent of known mitochondrial fusion and fission proteins, it would be important to identify DJ-1 interacting proteins in healthy mitochondria and in mitochondria under stress, using methods as mentioned above. Revealing whether DJ-1 mediated mitochondrial protection is dependent on its protease activity would shed light on the pathogenic role of mitochondrial dysfunction in PD and the molecular mechanisms of neuroprotection offered by DJ-1.

Determine whether oxidation of Met-17 or Met-26 is involved in zymogen activation

More experiments are needed to determine whether oxidation of Met-17 and Met-26 residues is involved in DJ-1 zymogen activation. For example, DJ-1 zymogen cleavage could be tested in cells overexpressing Msr. If zymogen cleavage of the endogenous DJ-1 or overexpressed DJ-1 WT, but not DJ-1 M17I or DJ-1 M26I mutant, could be reduced by Msr overexpression, then it is likely that the zymogen cleavage of DJ-1 is regulated by

methionine oxidation of Met-17 or Met-26 residue. But since general overexpression of Msr in cells could reduce methionine residues on other proteins, it is possible that the activity of the proteases or cofactors involved in DJ-1 zymogen cleavage is also regulated by methionine oxidation. The net effect of methionine oxidation on DJ-1 zymogen cleavage is possibly influenced by methionine oxidation on other proteins relevant to DJ-1 zymogene cleavage. After the identification of upstream proteases that cleave DJ-1 zymogen, it would be easier to show more directly whether methionine oxidation on DJ-1 prevents its zymogen cleavage in an *in vitro* recombinant system.

Another way to test whether oxidation of Met-17 or Met-26 induces DJ-1 zymogen cleavage is to examine whether oxidation-mimic mutant of these two residues activates DJ-1 zymogen cleavage. Glutamine has been used to mimic MetO without disrupting the global structure of the original protein, since it has comparable polarity and hydrophobicity as MetO but possesses similar propensity to form α-helices as Met (19,48). If Met-17 or Met-26 oxidation is responsible for the zymogen activation, M17Q or M26Q mutation should enhance DJ-1 zymogen activation even under basal condition when DJ-1 WT is not activated. However, if Met-17 or Met-26 itself is required for zymogen activation, then M17Q or M26Q mutation should abolish DJ-1 zymogen activation, similar to Ile mutation.

Understand the role of Met-133 in regulating DJ-1 cytoprotective function

Our findings show that although mutation of Met-133 does not affect DJ-1 zymogen activation or protease activity, it still abolishes DJ-1 cytoprotective function. One

possibility is that Met-133 is important for DJ-1 to interact with its substrates or adaptor proteins as Met-133 is at the periphery of DJ-1 protein. To test this possibility, interactions between DJ-1 and putative DJ-1 interactors can be examined to see whether Met-133 residue is required for the interactions. Among the reported DJ-1 interactors, ASK1 has been shown to interact with DJ-1 in a redox-dependent manner (152), thus whether Met-133 regulates the interaction between DJ-1 and ASK1 in response to oxidative stress could be tested first. Another possibility is that Met-133 is involved in the SUMOylation of DJ-1 as it is close to Lys-130, the reported SUMOylation residue on DJ-1 (94,306). To test whether Met-133 is required for DJ-1 SUMOylation, SUMOylation of DJ-1 WT and DJ-1 M133I mutant can be compared both *in vivo* and *in vitro*. If M133I prevents DJ-1 from being SUMOylated, it will be also interesting to see whether SUMOylation of DJ-1 is dependent on oxidation of Met-133 or Met-133 itself. Again oxidation mimic mutations, such as M133Q, can be made to test whether oxidation of Met-133 promotes SUMOylation of DJ-1. Completion of these experiments would allow better understanding of how Met-133 regulates DJ-1 function and elucidate redox-dependent events that regulate DJ-1 mediated cytoprotection.

Detection of methionine oxidation on DJ-1 protein

Establishing simple and reliable assays to detect oxidative status of specific methionine residues on a particular protein will greatly facilitate our understanding of the mechanisms of reversible methionine oxidation, but these assays are still limited. Generating protein-specific antibodies recognizing a single protein with selective Met residues oxidized are technically challenging and general antibodies against oxidized Met residues in all proteins are still lacking. Additionally, method of chemical derivatization

of MetO has not been developed yet for easy detection. However, there are several assays available to detect oxidized or reduced methionine, which are reviewed as follows.

MetO reduction in cells could be detected by using isotope-labeled [^{3}H]MetO as the substrate. Reduced [^{3}H]Met in cells can be identified by thin layer chromatography (TLC) fractionation, visualized by ninhydrin treatment, and extracted for quantification of radioactivity (40). However, this assay is technically complicated and is not always reliable due to incomplete extraction. Another way to detect oxidative status of a particular methionine residue is to use dabsylated Met as substrate. The reduced product can be detected using high performance lipid chromatography (HPLC) by monitoring absorbance of dabsylated Met at 436 nm (233). This method is more sensitive and reliable, but requires more syphysicated equipment and exerptise. An enzyme-coupled method relying on the detection of the absorbance change of NAPDH at 340nm has also been used. This method is based on the reduction of Msr by Trx at the expense of oxidation of NADPH by thioredoxin reductase to regenerate thioredoxin (240). This assay is not as sensitive as HPLC assay but it can be used for free MetO forms of substrate. Another assay based on immunoreactivity has also been developed. Polyclonal antibodies specific for oxidized methionine rich proteins (MRP, higher than 20% methionine content) have been generated (201,255). These antibodies have been demonstrated to react strongly with sulfoxidized MRPs and can be used to monitor Msr activity using SDS-PAGE based or ELISA based assays. However, whether these antibodies can recognize other MetO containing proteins are not clear. Lastly, mass spectrometry can also be used to detect oxidative status of methionine residues. In

addition to the technical difficulty, this method sometimes can result in false positive due to oxidation during sample processing or lack of complete coverage.

The above mentioned assays could be tried to learn 1) which methionine residues on DJ-1 are oxidized, 2) under what conditions these methionine residues are oxidized and to which form, 3) whether the oxidation is reversible, 4) whether oxidation of methionine residues happens prior to DJ-1 zymogen activation. In combination with mutagenesis, these findings will help us to understand how methionine oxidation regulates DJ-1 function.

Final words

Data presented in this thesis demonstrate that C-terminal proteolysis activates DJ-1 zymogen, resulting in higher affinity of substrate binding and increased catalytic efficiency. In addition, we demonstrate that DJ-1 with activated protease activity has enhanced cytoprotectvie function, suggesting that protease activity of DJ-1 accounts for its cytoprotective function. Furthermore, our results reveal that Met-17 and Met-26 residues are critical for DJ-1 zymogen activation. Given the proximity of these two residues to helix H8 and their susceptibility to oxidation, Met-17 and Met-26 are likely to be involved in the regulation of H8 cleavage. Additionally, we find that PD linked M26I mutation unfolds and destabilizes DJ-1 protein, causing faster degradation through proteasome and autophagy pathways. Together, our findings have enriched our understanding of the biological functions of DJ-1, and have significant implications

regarding the pathogenic mechanisms of DJ-1 mutations and the roles of methionine residues in redox-dependent cellular responses.

Table IV-1. Zymogenicity* of proteases

Proteases	Zymogenicity	Type of proteases	Activity of zymogens	Processed by	References
DJ-1	25	Cysteine protease C56	131	Unknown	(262)
Caspase 3	>10,000	Cysteine protease C14	860	Upstream caspases (caspase 8, 10), Granzyme B	(97,342)
Caspase 8	100	Cysteine protease C14	10^4	Autoproteolysis	(245)
Caspase 9	10	Cysteine protease C14	151	Autoproteolysis	(314,381,382)
Trypsin	>10,000	Serine protease S1	10	Enteropeptidase, autoproteolysis	(327)
Urokinase-type plasminogen activator (uPA)	250	Serine protease S14	12.5	Matrix metalloproteinase -3	(202,336,348)
Tissue type plasminogen activator (tPA)	2-10	Serine protease S1	3.7×10^4	Plasmin	(327)

*Zymogenicity is the ratio of the activity of a processed protease to the activity of the zymogen on any given substrate. It is a measure of how effectively the zymogen is constrained, with a large number corresponding to insignificant activity of the zymogen.

References

1. Abdallah J, Kern R, Malki A, Eckey V, Richarme G. Cloning, expression, and purification of the general stress protein YhbO from Escherichia coli. *Protein Expr Purif* 47: 455-460, 2006.
2. Abou-Sleiman PM, Healy DG, Quinn N, Lees AJ, Wood NW. The role of pathogenic DJ-1 mutations in Parkinson's disease. *Annals of Neurology* 54: 283-286, 2003.
3. Agbas A, Moskovitz J. The Role of Methionine Oxidation/Reduction in the Regulation of Immune Response. *Current signal transduction therapy* 4: 46-50, 2009.
4. Ahlemeyer B, Baumgart-Vogt E. Optimized protocols for the simultaneous preparation of primary neuronal cultures of the neocortex, hippocampus and cerebellum from individual newborn (P0.5) C57Bl/6J mice. *J. Neurosci. Methods* 149: 110-120, 2005.
5. Alam ZI, Daniel SE, Lees AJ, Marsden DC, Jenner P, Halliwell B. A Generalised Increase in Protein Carbonyls in the Brain in Parkinson's but Not Incidental Lewy Body Disease. *Journal of Neurochemistry* 69: 1326-1329, 1997.
6. Alam ZI, Jenner A, Daniel SE, Lees AJ, Cairns N, Marsden CD, Jenner P, Halliwell B. Oxidative DNA Damage in the Parkinsonian Brain: An Apparent Selective Increase in 8-Hydroxyguanine Levels in Substantia Nigra. *Journal of Neurochemistry* 69: 1196-1203, 1997.
7. Alves G, Forsaa E, Pedersen K, Dreetz Gjerstad M, Larsen J. Epidemiology of Parkinson's disease. *Journal of Neurology* 255: 18-32, 2008.
8. Ambani LM, Van Woert MH, Murphy S. Brain Peroxidase and Catalase in Parkinson Disease. *Arch. Neurol.* 32: 114-118, 1975.
9. Aminoff MJ. Pharmacologic Management of Parkinsonism & Other Movement Disorders. In: *Basic and Clinical Pharmacology*. edited by Katzung BG, Masters SB, Trevor AJ. McGraw Hill Professional; 2009.
10. Anbanandam A, Bieber Urbauer RJ, Bartlett RK, Smallwood HS, Squier TC, Urbauer JL. Mediating Molecular Recognition by Methionine Oxidation: Conformational Switching by Oxidation of Methionine in the Carboxyl-Terminal Domain of Calmodulin†. *Biochemistry* 44: 9486-9496, 2005.
11. Anbanandam A, BieberUrbauer RJ, Bartlett RK, Smallwood HS, Squier TC, Urbauer JL. Mediating Molecular Recognition by Methionine Oxidation: Conformational Switching by Oxidation of Methionine in the Carboxyl-Terminal Domain of Calmodulin. *Biochemistry* 44: 9486-9496, 2005.
12. Anderson LR, Betarbet R, Gearing M, Gulcher J, Hicks AA, Stefansson K, Lah JJ, Levey AI. PARK10 Candidate RNF11 Is Expressed by Vulnerable Neurons and Localizes to Lewy Bodies in Parkinson Disease Brain. *Journal of Neuropathology & Experimental Neurology* 66: 955-964.
13. Andres-Mateos E, Perier C, Zhang L, Blanchard-Fillion B, Greco TM, Thomas B, Ko HS, Sasaki M, Ischiropoulos H, Przedborski S, Dawson TM, Dawson VL. DJ-1 gene deletion reveals that DJ-1 is an atypical peroxiredoxin-like peroxidase. *Proc Natl Acad Sci USA* 104: 14807-14812, 2007.
14. Anliker B, Abel T, Kneissl S, Hlavaty J, Caputi A, Brynza J, Schneider IC, Munch RC, Petznek H, Kontermann RE, Koehl U, Johnston ICD, Keinanen K, Muller UC, Hohenadl C, Monyer H, Cichutek K, Buchholz CJ. Specific gene transfer to neurons, endothelial cells and hematopoietic progenitors with lentiviral vectors. *Nat. Meth.* 7: 929-935, 2009.
15. Annesi G, Savettieri G, Pugliese P, D'Amelio M, Tarantino P, Ragonese P, La Bella V, Piccoli T, Civitelli D, Annesi F, Fierro B, Piccoli F, Arabia G, Caracciolo M, Cirò Candiano IC, Quattrone A. DJ-1 mutations and parkinsonism-dementia-amyotrophic lateral sclerosis complex. *Annals of Neurology* 58: 803-807, 2005.

16. Ascherio A, Chen H, Weisskopf MG, O'Reilly E, McCullough ML, Calle EE, Schwarzschild MA, Thun MJ. Pesticide exposure and risk for Parkinson's disease. *Annals of Neurology* 60: 197-203, 2006.
17. Baburina I, Jackowski S. Cellular Responses to Excess Phospholipid. *Journal of Biological Chemistry* 274: 9400-9408, 1999.
18. Baldi I, Lebailly P, Mohammed-Brahim B, Letenneur L, Dartigues J-F, Brochard P. Neurodegenerative Diseases and Exposure to Pesticides in the Elderly. *American Journal of Epidemiology* 157: 409-414, 2003.
19. Balog EM, Norton LE, Bloomquist RA, Cornea RL, Black DJ, Louis CF, Thomas DD, Fruen BR. Calmodulin Oxidation and Methionine to Glutamine Substitutions Reveal Methionine Residues Critical for Functional Interaction with Ryanodine Receptor-1. *Journal of Biological Chemistry* 278: 15615-15621, 2003.
20. Balsinde J, Balboa MA. Cellular regulation and proposed biological functions of group VIA calcium-independent phospholipase A2 in activated cells. *Cellular Signalling* 17: 1052-1062, 2005.
21. Bandopadhyay R, Kingsbury AE, Cookson MR, Reid AR, Evans IM, Hope AD, Pittman AM, Lashley T, Canet-Aviles R, Miller DW, McLendon C, Strand C, Leonard AJ, Abou-Sleiman PM, Healy DG, Ariga H, Wood NW, de Silva R, Revesz T, Hardy JA, Lees AJ. The expression of DJ-1 (PARK7) in normal human CNS and idiopathic Parkinson's disease. *BMC Evol Biol* 127: 420-430, 2004.
22. Bandyopadhyay S, Cookson M. Evolutionary and functional relationships within the DJ1 superfamily. 2004. pp. 6.
23. Bartlett RK, Bieber Urbauer RJ, Anbanandam A, Smallwood HS, Urbauer JL, Squier TC. Oxidation of Met144 and Met145 in Calmodulin Blocks Calmodulin Dependent Activation of the Plasma Membrane Ca-ATPase†. *Biochemistry* 42: 3231-3238, 2003.
24. Batra R, Khayat R, Tong L. Molecular mechanism for dimerization to regulate the catalytic activity of human cytomegalovirus protease. *Nat Struct Biol* 8: 810, 2001.
25. Berg EM, Tymoczko JL, Stryer L. Catalytic Strategies. In: *Biochemistry*. edited by Berg EM, Tymoczko JL, Stryer L. W. H. Freeman and Company.; 2002.
26. Berg JM, Tymoczko JL, Stryer L. Catalytic Strategies. In: *Biochemistry*. edited by Berg JM, Tymoczko JL, Stryer L. New York: W H Freeman; 2002.
27. Berlett BS, Stadtman ER. Protein Oxidation in Aging, Disease, and Oxidative Stress. *The Journal of Biological Chemistry* 272: 20313-20316, 1997.
28. Betarbet R, Sherer TB, MacKenzie G, Garcia-Osuna M, Panov AV, Greenamyre1 JT. Chronic systemic pesticide exposure reproduces features of Parkinson's disease. *Nature Neuroscience* 3: 1301 - 1306 2000.
29. Blackinton J, Ahmad R, Miller DW, van der Brug MP, Canet-Avil RM, Hague SM, Kaleem M, Cookson MR. Effects of DJ-1 mutations and polymorphisms on protein stability and subcellular localization. *Molecular Brain Research* 134: 76-83, 2005.
30. Blackinton J, Lakshminarasimhan M, Thomas KJ, Ahmad R, Greggio E, Raza AS, Cookson MR, Wilson MA. Formation of a Stabilized Cysteine Sulfinic Acid Is Critical for the Mitochondrial Function of the Parkinsonism Protein DJ-1. *Journal of Biological Chemistry* 284: 6476-6485, 2009.
31. Boatright KM, Salvesen GS. Mechanisms of caspase activation. *Curr Opin Cell Biol* 15: 725-731, 2003.
32. Bonifati V, Rizzu P, van Baren MJ, Schaap O, Breedveld GJ, Krieger E, Dekker MCJ, Squitieri F, Ibanez P, Joosse M, van Dongen JW, Vanacore N, van Swieten JC, Brice A, Meco G, van Duijn CM, Oostra BA, Heutink P. Mutations in the DJ-1 Gene Associated with Autosomal Recessive Early-Onset Parkinsonism. *Science* 299: 256-259, 2003.
33. Bonifati VM. Is GIGYF2 the defective gene at the PARK11 locus? *Current neurology and neuroscience reports* 9: 185-187, 2009.

34. Botella J, Bayersdorfer F, Gmeiner F, Schneuwly S. Modelling Parkinson's Disease in <i>Drosophila</i&gt. *NeuroMolecular Medicine* 11: 268-280, 2009.
35. Braak H, Bohl JR, Müller CM, Rüb U, de Vos RAI, Del Tredici K. Stanley Fahn Lecture 2005: The staging procedure for the inclusion body pathology associated with sporadic Parkinson's disease reconsidered. *Movement Disorders* 21: 2042-2051, 2006.
36. Braak H, Tredici KD, Rub U, de Vos RAI, Jansen Steur ENH, Braak E. Staging of brain pathology related to sporadic Parkinson's disease. *Neurobiology of Aging* 24: 197-211, 2003.
37. Brandes N, Schmitt S, Jakob U. Thiol-Based Redox Switches in Eukaryotic Proteins. *Antioxid. Redox Signal.* 11: 997-1014, 2009.
38. Bretaud S, Allen C, Ingham PW, Bandmann O. p53-dependent neuronal cell death in a DJ-1-deficient zebrafish model of Parkinson's disease. *Journal of Neurochemistry* 100: 1626-1635, 2007.
39. Breydo L, Bocharova OV, Makarava N, Salnikov VV, Anderson M, Baskakov IV. Methionine Oxidation Interferes with Conversion of the Prion Protein into the Fibrillar Proteinase K-Resistant Conformation. *Biochemistry* 44: 15534-15543, 2005.
40. Brot N, Werth J, Koster D, Weissbach H. Reduction of N-acetyl methionine sulfoxide: a simple assay for peptide methionine sulfoxide reductase. *Anal. Biochem.* 122: 291-294, 1982.
41. Butler GS, Dean RA, Tam EM, Overall CM. Pharmacoproteomics of a metalloproteinase hydroxamate inhibitor in breast cancer cells: Dynamics of matrix metalloproteinase-14 (MT1-MMP) mediated membrane protein shedding. *Molecular Cell Biology.* 122: 4896-4914, 2008.
42. Butler GS, Dean RA, Tam EM, Overall CM. Pharmacoproteomics of a Metalloproteinase Hydroxamate Inhibitor in Breast Cancer Cells: Dynamics of Membrane Type 1 Matrix Metalloproteinase-Mediated Membrane Protein Shedding. *Mol. Cell. Biol.* 28: 4896-4914, 2008.
43. Canello T, Frid K, Gabizon R, Lisa S, Friedler A, Moskovitz J, Gasset M, Gabizon R. Oxidation of Helix-3 Methionines Precedes the Formation of PK Resistant PrP. *PLoS Pathology* 6: e1000977, 2010.
44. Canet-Aviles RM, Wilson MA, Miller DW, Ahmad R, McLendon C, Bandyopadhyay S, Baptista MJ, Ringe D, Petsko GA, Cookson MR. The Parkinson's disease protein DJ-1 is neuroprotective due to cysteine-sulfinic acid-driven mitochondrial localization. *Proc. Natl. Acad. Sci. USA* 101: 9103-9108, 2004.
45. Canet-Aviles RM, Wilson MA, Miller DW, Ahmad R, Mclendon C, Bandyopadhyay S, Baptista MJ, Ringe D, Petsko GA, Cookson MR. The Parkinson's disease protein DJ-1 is neuroprotective due to cysteine-sulfinic acid-driven mitochondrial localization. *Proc. Natl. Acad. Sci. USA* 101: 9103-9108, 2004.
46. Canet-Aviles RM, Wilson MA, Miller DW, Ahmad R, Mclendon C, Bandyopadhyay S, Baptista MJ, Ringe D, Petsko GA, Cookson MR. The Parkinson's disease protein DJ-1 is neuroprotective due to cysteine-sulfinic acid-driven mitochondrial localization. *Proc Natl Acad Sci USA* 101: 9103-9108, 2004.
47. Cannon JR, Tapias VM, Na HM, Honick AS, Drolet RE, Greenamyre JT. A highly reproducible rotenone model of Parkinson's disease. *Neurobiolical disorders* 34: 279–290, 2009.
48. Chakrabartty A, Baldwin R. Stability of alpha-helices. *Advances in protein chemistry* 46: 141-176, 1995.
49. Chang Y-F, Cheng C-M, Chang L-K, Jong Y-J, Yuo C-Y. The F-box protein Fbxo7 interacts with human inhibitor of apoptosis protein cIAP1 and promotes cIAP1 ubiquitination. *Biochemical and Biophysical Research Communications* 342: 1022-1026, 2006.

50. Chao C-C, Ma Y-S, Stadtman ER. Modification of protein surface hydrophobicity and methionine oxidation by oxidative systems. *Proc. Natl. Acad. Sci. USA* 94: 2969-2974, 1997.
51. Chen J, Li L, Chin L-S. Parkinson disease protein DJ-1 converts from a zymogen to a protease by carboxyl-terminal cleavage. *Hum. Mol. Genet.* 19: 2395-2408, 2010.
52. Chen J, Li L, Chin L-S. Parkinson disease protein DJ-1 converts from a zymogen to a protease by carboxyl-terminal cleavage. *Human Molecular Genetics* 19: 2395-2408, 2010.
53. Chen L, Cagniard B, Mathews T, Jones S, Koh HC, Ding Y, Carvey PM, Ling Z, Kang UJ, Zhuang X. Age-dependent Motor Deficits and Dopaminergic Dysfunction in DJ-1 Null Mice. *The Journal of biological chemistry* 280: 21418-21426, 2005.
54. Chen L, Cagniard B, Mathews T, Jones S, Koh HC, Ding Y, Carvey PM, Ling Z, Kang UJ, Zhuang X. Age-dependent Motor Deficits and Dopaminergic Dysfunction in DJ-1 Null Mice. *J. Biol. Chem.* 280: 21418-21426, 2005.
55. Chen Y, Yang J, Chau K. Determination of the helix and beta form of proteins in aqueous solution by circular dichroism. *Biochemistry* 13: 3350-3359, 1974.
56. Chinta SJ, Andersen JK. Redox imbalance in Parkinson's disease. *Biochimica et Biophysica Acta (BBA) - General Subjects* 1780: 1362-1367, 2008.
57. Choi D-H, Hwang O, Lee K-H, Lee J, Beal MF, Kim Y-S. DJ-1 Cleavage by Matrix Metalloproteinase 3 Mediates Oxidative Stress-Induced Dopaminergic Cell Death. *Antioxidants & redox signaling*: Epub, 2011.
58. Choi J, Levey AI, Weintraub ST, Rees HD, Gearing M, Chin L-S, Li L. Oxidative Modifications and Down-regulation of Ubiquitin Carboxyl-terminal Hydrolase L1 Associated with Idiopathic Parkinson's and Alzheimer's Diseases. *Journal of Biological Chemistry* 279: 13256-13264, 2004.
59. Choi J, Sullards MC, Olzmann JA, Rees HD, Weintraub ST, Bostwick DE, Gearing M, Levey AI, Chin L-S, li L. Oxidative damage of DJ-1 is linked to sporadic parkinson's and alzheimer's diseases. *J. Biol. Chem*, 2006.
60. Choi J, Sullards MC, Olzmann JA, Rees HD, Weintraub ST, Bostwick DE, Gearing M, Levey AI, Chin L-S, Li L. Oxidative Damage of DJ-1 Is Linked to Sporadic Parkinson and Alzheimer Diseases. 2006. pp. 10816-10824.
61. Choi W-S, Kruse SE, Palmiter RD, Xia Z. Mitochondrial complex I inhibition is not required for dopaminergic neuron death induced by rotenone, MPP^+, or paraquat. *Proceedings of the National Academy of Sciences* 105: 15136-15141, 2008.
62. Ciechanover A. Proteolysis: from the lysosome to ubiquitin and the proteasome. *Nat Rev Mol Cell Biol* 6: 79-87, 2005.
63. Ciorba MA, Heinemann SH, Weissbach H, Brot N, Hoshi T. Modulation of potassium channel function by methionine oxidation and reduction. *Proceedings of the National Academy of Sciences of the United States of America* 94: 9932-9937, 1997.
64. Clark IE, Dodson MW, Jiang C, Cao JH, Huh JR, Seol JH, Yoo SJ, Hay BA, Guo M. Drosophila pink1 is required for mitochondrial function and interacts genetically with parkin. *Nature* 441: 1162-1166, 2006.
65. Clausen T, Southan C, Ehrmann M. The HtrA Family of Proteases: Implications for Protein Composition and Cell Fate. *Mol cell* 10: 443-455, 2002.
66. Clements CM, McNally RS, Conti BJ, Mak TW, Ting JPY. DJ-1, a cancer- and Parkinson's disease-associated protein, stabilizes the antioxidant transcriptional master regulator Nrf2. *Proc. Natl. Acad. Sci. USA* 103: 15091-15096, 2006.
67. Clements CM, McNally RS, Conti BJ, Mak TW, Ting JPY. DJ-1, a cancer- and Parkinson's disease-associated protein, stabilizes the antioxidant transcriptional master regulator Nrf2. *Proc Natl Acad Sci USA* 103: 15091-15096, 2006.
68. Cole RN, Hart GW. Cytosolic O-glycosylation is abundant in nerve terminals. *Journal of Neurochemistry* 79: 1080-1089, 2001.

69. Colombo G, Meli M, Morra G, Gabizon R, Gasset M. Methionine Sulfoxides on Prion Protein Helix-3 Switch on the α-Fold Destabilization Required for Conversion. *PLoS ONE* 4: e4296, 2009.
70. Conway KA, Lee S-J, Rochet J-C, Ding TT, Williamson RE, Lansbury PT. Acceleration of oligomerization, not fibrillization, is a shared property of both α-synuclein mutations linked to early-onset Parkinson's disease: Implications for pathogenesis and therapy. *Proc Natl Acad Sci U S A* 97: 571-576, 2000.
71. Cook C, Petrucelli L. A critical evaluation of the ubiquitin-proteasome system in Parkinson's disease. *Biochimica et Biophysica Acta (BBA) - Molecular Basis of Disease* 1792: 664-675, 2009.
72. Cookson MR. The biochemistry of Parkinson disease. *Annual Review of Biochemistry* 74: 29-52, 2005.
73. Cookson MR. The role of leucine-rich repeat kinase 2 (LRRK2) in Parkinson's disease. *Nat Rev Neurosci* 11: 791-797, 2010.
74. da Costa CA. DJ-1: A New Comer in Parkinson's Disease Pathology. *Curr Mol Med* 7: 650-657, 2007.
75. Das C, Hoang QQ, Kreinbring CA, Luchansky SJ, Meray RK, Ray SS, Lansbury PT, Ringe D, Petsko GA. Structural basis for conformational plasticity of the Parkinson's disease-associated ubiquitin hydrolase UCH-L1. *Proceedings of the National Academy of Sciences of the United States of America* 103: 4675-4680, 2006.
76. Dauer W, Przedborski S. Parkinson's Disease: Mechanisms and Models. *Neuron* 39: 889-909, 2003.
77. Davidson WS, Jonas A, Clayton DF, George JM. Stabilization of α-Synuclein Secondary Structure upon Binding to Synthetic Membranes. *J. Biol. Chem.* 273: 9443-9449, 1998.
78. Davis AA, Fritz JJ, Wess J, Lah JJ, Levey AI. Deletion of M1 Muscarinic Acetylcholine Receptors Increases Amyloid Pathology In Vitro and In Vivo. *J. Neurosci.* 30: 4190-4196, 2010.
79. Day BJ, Patel M, Calavetta L, Chang L-Y, Stamler JS. A mechanism of paraquat toxicity involving nitric oxide synthase. *Proceedings of the National Academy of Sciences of the United States of America* 96: 12760-12765, 1999.
80. Deas E, Plun-Favreau H, Wood NW. PINK1 function in health and disease. *EMBO Molecular Medicine* 1: 152-165, 2009.
81. Deas E, Wood NW, Plun-Favreau H. Mitophagy and Parkinson's disease: The PINK1-parkin link. *Biochimica et Biophysica Acta (BBA) - Molecular Cell Research* In Press, Corrected Proof, 2010.
82. Deng H, Dodson MW, Huang H, Guo M. The Parkinson's disease genes pink1 and parkin promote mitochondrial fission and/or inhibit fusion in Drosophila. *Proceedings of the National Academy of Sciences* 105: 14503-14508, 2008.
83. Dexter DT, Carter CJ, Wells FR, Javoy-Agid F, Agid Y, Lees A, Jenner P, Marsden CD. Basal Lipid Peroxidation in Substantia Nigra Is Increased in Parkinson's Disease. *Journal of Neurochemistry* 52: 381-389, 1989.
84. Di Fonzo A, Chien HF, Socal M, Giraudo S, Tassorelli C, Iliceto G, Fabbrini G, Marconi R, Fincati E, Abbruzzese G, Marini P, Squitieri F, Horstink MW, Montagna P, Libera AD, Stocchi F, Goldwurm S, Ferreira JJ, Meco G, Martignoni E, Lopiano L, Jardim LB, Oostra BA, Barbosa ER, Bonifati V. ATP13A2 missense mutations in juvenile parkinsonism and young onset Parkinson disease. *Neurology* 68: 1557-62, 2007.
85. Diamond SL. Methods for mapping protease specificity. *Current Opinion in Chemical Biology* 11: 46-51, 2007.
86. Donepudi M, Grutter MG. Structure and zymogen activation of caspases. *Biophys Chem* 101-102: 145-153, 2002.

87. Du X, Choi I-G, Kim R, Wang W, Jancarik J, Yokota H, Kim S-H. Crystal structure of an intracellular protease from Pyrococcus horikoshii at 2-A resolution. *Proc Natl Acad Sci USA* 97: 14079-14084, 2000.
88. Ekstrand MI, Terzioglu M, Galter D, Zhu S, Hofstetter C, Lindqvist E, Thams S, Bergstrand A, Hansson FS, Trifunovic A, Hoffer B, Cullheim S, Mohammed AH, Olson L, Larsson N-G. Progressive parkinsonism in mice with respiratory-chain-deficient dopamine neurons. *Proceedings of the National Academy of Sciences* 104: 1325-1330, 2007.
89. Elbaz A, Levecque C, Clavel J, Vidal J-S, Richard F, Amouyel P, Alpérovitch A, Chartier-Harlin M-C, Tzourio C. CYP2D6 polymorphism, pesticide exposure, and Parkinson's disease. *Annals of Neurology* 55: 430-434, 2004.
90. Erin JF, Jason RC, Kelvin HL. Kinetic characterization of sequencing grade modified trypsin. *Proteomics* 5: 2319-2321, 2005.
91. Evans AH, Lawrence AD, Potts J, MacGregor L, Katzenschlager R, Shaw K, Zijlmans J, Lees AJ. Relationship between impulsive sensation seeking traits, smoking, alcohol and caffeine intake, and Parkinson's disease. *Journal of Neurology, Neurosurgery & Psychiatry* 77: 317-321, 2006.
92. Exner N, Treske B, Paquet D, Holmstrom K, Schiesling C, Gispert S, Carballo-Carbajal I, Berg D, Hoepken H-H, Gasser T, Kruger R, Winklhofer KF, Vogel F, Reichert AS, Auburger G, Kahle PJ, Schmid B, Haass C. Loss-of-Function of Human PINK1 Results in Mitochondrial Pathology and Can Be Rescued by Parkin. *J. Neurosci.* 27: 12413-12418, 2007.
93. Fahn S. Parkinson's Disease and Related Disorders. In: *Hazzard's Geriatric Medicine and Gerontology* edited by Halter eB, Ouslander JG, Tinetti ME, Studenski S, High KP, Asthana S. Hazzard's Geriatric Medicine and Gerontology, 6e; 2009.
94. Fan J, Ren H, Fei E, Jia N, Ying Z, Jiang P, Wu M, Wang G. Sumoylation is critical for DJ-1 to repress p53 transcriptional activity. *FEBS letters* 582: 1151-1156, 2008.
95. Fan J, Ren H, Jia N, Fei E, Zhou T, Jiang P, Wu M, Wang G. DJ-1 Decreases Bax Expression through Repressing p53 Transcriptional Activity. *The Journal of biological chemistry* 283: 4022-4030, 2008.
96. Farmer WH, Yuan Z. A continuous fluorescent assay for measuring protease activity using natural protein substrate. *Anal Biochem* 197: 347-352, 1991.
97. Feeney B, Tripathy A, Clark AC. Mutations in the Procaspase-3 Dimer Interface Affect the Activity of the Zymogen. *Biochemistry* 42: 12311-12320, 2003.
98. Finkel T, Holbrook NJ. Oxidants, oxidative stress and the biology of ageing. *Nature* 408: 239-247, 2000.
99. Firestone JA, Smith-Weller T, Franklin G, Swanson P, Longstreth WT, Jr, Checkoway H. Pesticides and Risk of Parkinson Disease: A Population-Based Case-Control Study. *Arch Neurol* 62: 91-95, 2005.
100. Floor E, Wetzel MG. Increased Protein Oxidation in Human Substantia Nigra Pars Compacta in Comparison with Basal Ganglia and Prefrontal Cortex Measured with an Improved Dinitrophenylhydrazine Assay. *Journal of Neurochemistry* 70: 268-275, 1998.
101. Fonzo ADMD, Dekker MCJM, Montagna PM, Baruzzi AM, Yonova EHB, Guedes LCMD, Szczerbinska AB, Zhao TB, Dubbel-Hulsman LOM, Wouters CHP, de Graaff EP, Oyen WJGM, Simons EJ, Breedveld GJ, Oostra BAP, Horstink MWM, Bonifati VM. FBXO7 mutations cause autosomal recessive, early-onset parkinsonian-pyramidal syndrome SYMBOL. *Neurology* 72: 240-245, 2009.
102. Forno L, DeLanney L, Irwin I, Langston J. Similarities and differences between MPTP-induced parkinsonsim and Parkinson's disease. Neuropathologic considerations. *Advances in neurology* 60: 600-8, 1993.

103. Freed CR, Greene PE, Breeze RE, Tsai W-Y, DuMouchel W, Kao R, Dillon S, Winfield H, Culver S, Trojanowski JQ, Eidelberg D, Fahn S. Transplantation of Embryonic Dopamine Neurons for Severe Parkinson's Disease. *The New England Journal of Medicine* 344: 710-719, 2001.
104. Gabbita SP, Aksenov MY, Lovell MA, Markesbery WR. Decrease in Peptide Methionine Sulfoxide Reductase in Alzheimer's Disease Brain. *Journal of Neurochemistry* 73: 1660-1666, 1999.
105. Gautier CA, Kitada T, Shen J. Loss of PINK1 causes mitochondrial functional defects and increased sensitivity to oxidative stress. *Proceedings of the National Academy of Sciences* 105: 11364-11369, 2008.
106. Gerstner B, DeSilva TM, Genz K, Armstrong A, Brehmer F, Neve RL, Felderhoff-Mueser U, Volpe JJ, Rosenberg PA. Hyperoxia Causes Maturation-Dependent Cell Death in the Developing White Matter. *J Neurosci* 28: 1236-1245, 2008.
107. Ghazavi F, Fazlali Z, Banihosseini SS, Hosseini S-R, Kazemi MH, Shojaee S, Parsa K, Sadeghi H, Sina F, Rohani M, Shahidi G-A, Ghaemi N, Ronaghi M, Elahi E. PRKN, DJ-1, and PINK1 screening identifies novel splice site mutation in PRKN and two novel DJ-1 mutations. *Movement Disorders*: Epub, 2010.
108. Giaime E, Sunyach C, Druon C, Scarzello S, Robert G, Grosso S, Auberger P, Goldberg MS, Shen J, Heutink P, Pouyssegur J, Pages G, Checler F, Alves da Costa C. Loss of function of DJ-1 triggered by Parkinson's disease-associated mutation is due to proteolytic resistance to caspase-6. *Cell Death Differ*, 2009.
109. Giaime E, Sunyach C, Druon C, Scarzello S, Robert G, Grosso S, Auberger P, Goldberg MS, Shen J, Heutink P, Pouyssegur J, Pages G, Checler F, Alves da Costa C. Loss of function of DJ-1 triggered by Parkinson's disease-associated mutation is due to proteolytic resistance to caspase-6. *Cell Death Differ* 17: 158-169, 2009.
110. Giles LM, Chen J, Li L, Chin L-S. Dystonia-associated mutations cause premature degradation of torsinA protein and cell-type-specific mislocalization to the nuclear envelope. *Hum. Mol. Genet.* 17: 2712-2722, 2008.
111. Giles LM, Chen J, Li L, Chin L-S. Dystonia-associated mutations cause premature degradation of torsinA protein and cell-type-specific mislocalization to the nuclear envelope. *Hum Mol Genet* 17: 2712-2722, 2008.
112. Gill SS, Patel NK, Hotton GR, O'Sullivan K, McCarter R, Bunnage M, Brooks DJ, Svendsen CN, Heywood P. Direct brain infusion of glial cell line-derived neurotrophic factor in Parkinson disease. *Nat Med* 9: 589-595, 2003.
113. Gitler AD, Chesi A, Geddie ML, Strathearn KE, Hamamichi S, Hill KJ, Caldwell KA, Caldwell GA, Cooper AA, Rochet J-C, Lindquist S. α-Synuclein is part of a diverse and highly conserved interaction network that includes PARK9 and manganese toxicity. *Nat Genet* 41: 308-315, 2009.
114. Goldberg MS, Pisani A, Haburcak M, Vortherms TA, Kitada T, Costa C, Tong Y, Martella G, Tscherter A, Martins A, Bernardi G, Roth BL, Pothos EN, Calabresi P, Shen J. Nigrostriatal Dopaminergic Deficits and Hypokinesia Caused by Inactivation of the Familial Parkinsonism-Linked Gene DJ-1. *Neuron* 45: 489-496, 2005.
115. Goll DE, Thompson VF, Li H, Wei WEI, Cong J. The Calpain System. *Physiol Rev* 83: 731-801, 2003.
116. Gorner K, Holtorf E, Odoy S, Nuscher B, Yamamoto A, Regula JT, Beyer K, Haass C, Kahle PJ. Differential Effects of Parkinson's Disease-associated Mutations on Stability and Folding of DJ-1. *J. Biol. Chem.* 279: 6943-6951, 2004.
117. Gorner K, Holtorf E, Waak J, Pham T-T, Vogt-Weisenhorn DM, Wurst W, Haass C, Kahle PJ. Structural Determinants of the C-terminal Helix-Kink-Helix Motif Essential for Protein Stability and Survival Promoting Activity of DJ-1. *J. Biol. Chem.* 282: 13680-13691, 2007.

118. Gottesman S, Wickner S, Maurizi MR. Protein quality control: triage by chaperones and proteases. *Genes & Development* 11: 815-823, 1997.
119. Grazia A, Giovanni S, Pierfrancesco P, Marco DA, Patrizia T, Paolo R, Vincenzo La B, Tommaso P, Donatella C, Ferdinanda A, Brigida F, Federico P, Gennarina A, Manuela C, Innocenza Claudia CC, Aldo Q. DJ-1 mutations and parkinsonism-dementia-amyotrophic lateral sclerosis complex. *Ann Neurol* 58: 803-807, 2005.
120. Gregory AM, Westaway SKP, Holm IEMDD, Kotzbauer PTMDP, Hogarth PM, Sonek SB, Coryell JCM, Nguyen TMB, Nardocci NM, Zorzi GM, Rodriguez DM, Desguerre IM, Bertini EM, Simonati AM, Levinson BM, Dias CM, Barbot CM, Carrilho IM, Santos MM, Malik IP, Gitschier JP, Hayflick SJM. Neurodegeneration associated with genetic defects in phospholipase A2 SYMBOL. *Neurology* 71: 1402-1409, 2008.
121. Grunewald A, Gegg ME, Taanman JW, King RH, Kock N, Klein C, Schapira AHV. Differential effects of PINK1 nonsense and missense mutations on mitochondrial function and morphology. *Experimental Neurology* 219: 266-273, 2009.
122. Guo JF, Xiao B, Liao B, Zhang XW, Nie LL, Zhang YH, Shen L, Jiang H, Xia K, Pan Q, Yan XX, Tang BS. Mutation analysis of Parkin, PINK1, DJ-1 and ATP13A2 genes in Chinese patients with autosomal recessive early-onset Parkinsonism. *Movement Disorders* 23: 2074-2079, 2008.
123. Guttmann RP, Johnson GVW. Oxidative Stress Inhibits Calpain Activity in Situ. *Journal of Biological Chemistry* 273: 13331-13338, 1998.
124. Haas R, Nasirian F, Nakano K, Ward D, Pay M, Hill R, Shults C. Low platelet mitochondrial complex I and complex II/III activity in early untreated Parkinson's disease. *Annals of neurology* 37: 714-22, 1995.
125. Hague S, Rogaeva E, Hernandez D, Gulick C, Singleton A, Hanson M, Johnson J, Weiser R, Gallardo M, Ravina B, Gwinn-Hardy K, Crawley A, George-Hyslop PHS, Lang AE, Heutink P, Bonifati V, Hardy J, Singleton A. Early-onset Parkinson's disease caused by a compound heterozygous DJ-1 mutation. *Annals of Neurology* 54: 271-274, 2003.
126. Halio SB, Bauer MW, Mukund S, Adams MWW, Kelly RM. Purification and Characterization of Two Functional Forms of Intracellular Protease PfpI from the Hyperthermophilic Archaeon Pyrococcus furiosus. *Appl Environ Microbiol* 63: 289-295, 1997.
127. Halio SB, Blumentals, II, Short SA, Merrill BM, Kelly RM. Sequence, expression in Escherichia coli, and analysis of the gene encoding a novel intracellular protease (PfpI) from the hyperthermophilic archaeon Pyrococcus furiosus. *J Bacteriol* 178: 2605-2612, 1996.
128. Halliday GM, McCann H. The progression of pathology in Parkinson's disease. *Annals of the New York Academy of Sciences* 1184: 188-195, 2010.
129. Halliwell B. Oxidative stress and neurodegeneration: where are we now? *J Neurochem* 97: 1634-1658, 2006.
130. Hampton MB, Fadeel B, Orrenius S. Redox Regulation of the Caspases during Apoptosisa. *Annals of the New York Academy of Sciences* 854: 328-335, 1998.
131. Hancock DB, Martin ER, Stajich JM, Jewett R, Stacy MA, Scott BL, Vance JM, Scott WK. Smoking, Caffeine, and Nonsteroidal Anti-inflammatory Drugs in Families With Parkinson Disease. *Arch Neurol* 64: 576-580, 2007.
132. Hatcher JM, Pennell KD, Miller GW. Parkinson's disease and pesticides: a toxicological perspective. *Trends in Pharmacological Sciences* 29: 322-329, 2008.
133. Hattori N, Mizuno Y. Pathogenetic mechanisms of parkin in Parkinson's disease. *The Lancet* 364: 722-724, 2004.
134. Haugarvoll K, Toft M, Skipper L, Heckman MG, Crook JE, Soto A, Ross OA, Hulihan MM, Kachergus JM, Sando SB, White LR, Lynch T, Gibson JM, Uitti RJ, Wszolek ZK,

Aasly JO, Farrer MJ. Fine-mapping and candidate gene investigation within the PARK10 locus. *Eur J Hum Genet* 17: 336-343, 2008.

135. Hedrich K, Schafer N, Hering R, Hagenah J, Lanthaler AJ, Schwinger E, Kramer PL, Ozelius LJ, Bressman SB, Abbruzzese G, Martinelli P, Kostic V, Pramstaller PP, Vieregge P, Riess O, Klein C. The R98Q variation in DJ-1represents a rare polymorphism. *Ann. Neurol.* 55: 145-150, 2004.
136. Hedrich K, Schäfer N, Hering R, Hagenah J, Lanthaler AJ, Schwinger E, Kramer PL, Ozelius LJ, Bressman SB, Abbruzzese G, Martinelli P, Kostic V, Pramstaller PP, Vieregge P, Riess O, Klein C. The R98Q variation in DJ-1 represents a rare polymorphism. *Annals of Neurology* 55: 145-145, 2004.
137. Hegde R, Srinivasula SM, Zhang Z, Wassell R, Mukattash R, Cilenti L, DuBois G, Lazebnik Y, Zervos AS, Fernandes-Alnemri T, Alnemri ES. Identification of Omi/HtrA2 as a Mitochondrial Apoptotic Serine Protease That Disrupts Inhibitor of Apoptosis Protein-Caspase Interaction. *J. Biol. Chem.* 277: 432-438, 2002.
138. Hering R, Strauss KM, Tao X, Bauer A, Woitalla D, Mietz E-M, Petrovic S, Bauer P, Schaible W, Muller T, Schols L, Klein C, Berg D, Meyer PT, Schulz JB, Wollnik B, Tong L, Kruger R, Riess O. Novel homozygous p.E64D mutation in DJ1 in early onset Parkinson disease (PARK7). *Human Mutation* 24: 321-329, 2004.
139. Hering R, Strauss KM, Tao X, Bauer A, Woitalla D, Mietz EM, Petrovic S, Bauer P, Schaible W, Müller T, Schöls L, Klein C, Berg D, Meyer PT, Schulz JB, Wollnik B, Tong L, Krüger R, Riess O. Novel homozygous p.E64D mutation in DJ1 in early onset Parkinson disease (PARK7). *Human Mutation* 24: 321-329, 2004.
140. Hicks AA, Pétursson H, Jónsson T, Stefánsson H, Jóhannsdóttir HS, Sainz J, Frigge ML, Kong A, Gulcher JR, Stefánsson K, Sveinbjörnsdóttir S. A susceptibility gene for late-onset idiopathic Parkinson's disease. *Annals of Neurology* 52: 549-555, 2002.
141. Ho M, Ou C, Chan Yr, Chien CT, Pi H. The utility F-box for protein destruction. *Cellular and Molecular Life Sciences* 65: 1977-2000, 2008.
142. Hod Y, Pentyala SN, Whyard TC, El-Maghrabi MR. Identification and characterization of a novel protein that regulates RNA-protein interaction. *J. Cell. Biochem.* 72: 435-444, 1999.
143. Höglinger GU, Féger J, Prigent A, Michel PP, Parain K, Champy P, Ruberg M, Oertel WH, Hirsch EC. Chronic systemic complex I inhibition induces a hypokinetic multisystem degeneration in rats. *Journal of Neurochemistry* 84: 491-502, 2003.
144. Hokenson MJ, Uversky VN, Goers J, Yamin G, Munishkina LA, Fink AL. Role of Individual Methionines in the Fibrillation of Methionine-Oxidized α-Synuclein†. *Biochemistry* 43: 4621-4633, 2004.
145. Honbou K, Suzuki NN, Horiuchi M, Niki T, Taira T, Ariga H, Inagaki F. The Crystal Structure of DJ-1, a Protein Related to Male Fertility and Parkinson's Disease. *J. Biol. Chem.* 278: 31380-31384, 2003.
146. Hoppe T, Rape M, Jentsch S. Membrane-bound transcription factors: regulated release by RIP or RUP. *Current Opinion in Cell Biology* 13: 344-348, 2001.
147. Hoshi T, Heinemann SH. Regulation of cell function by methionine oxidation and reduction. *Journal of Physiology* 531: 1-11, 2001.
148. Hsu J-M, Lee Y-CG, Yu C-TR, Huang C-YF. Fbx7 Functions in the SCF Complex Regulating Cdk1-Cyclin B-phosphorylated Hepatoma Up-regulated Protein (HURP) Proteolysis by a Proline-rich Region. *Journal of Biological Chemistry* 279: 32592-32602, 2004.
149. Huai Q, Sun Y, Wang H, Chin L-S, Li L, Robinson H, Ke H. Crystal structure of DJ-1/RS and implication on familial Parkinson's disease. *FEBS Lett* 549: 171-175, 2003.
150. Huai Q, Sun Y, Wang H, Chin L-S, Li L, Robinson H, Ke H. Crystal structure of DJ-1/RS and implication on familial Parkinson's disease. *FEBS Lett.* 549: 171-175, 2003.

151. Hulleman JD, Mirzaei H, Guigard E, Taylor KL, Ray SS, Kay CM, Regnier FE, Rochet JC. Destabilization of DJ-1 by Familial Substitution and Oxidative Modifications: Implications for Parkinson's Disease. *Biochemistry* 46: 5776-5789, 2007.
152. Im J-Y, Lee K-W, Junn E, Mouradian MM. DJ-1 protects against oxidative damage by regulating the thioredoxin/ASK1 complex. *Neuroscience Research* 67: 203-208, 2010.
153. Irrcher I, Aleyasin H, Seifert EL, Hewitt SJ, Chhabra S, Phillips M, Lutz AK, Rousseaux MWC, Bevilacqua L, Jahani-Asl A, Callaghan S, MacLaurin JG, Winklhofer KF, Rizzu P, Rippstein P, Kim RH, Chen CX, Fon EA, Slack RS, Harper ME, McBride HM, Mak TW, Park DS. Loss of the Parkinson's disease-linked gene DJ-1 perturbs mitochondrial dynamics. *Human Molecular Genetics* 19: 3734-3746, 2010.
154. Jensen PH, Nielsen MS, Jakes R, Dotti CG, Goedert M. Binding of α-Synuclein to Brain Vesicles Is Abolished by Familial Parkinson Disease Mutation. 1998. pp. 26292-26294.
155. Jones JM, Datta P, Srinivasula SM, Ji W, Gupta S, Zhang Z, Davies E, Hajnoczky G, Saunders TL, Van Keuren ML, Fernandes-Alnemri T, Meisler MH, Alnemri ES. Loss of Omi mitochondrial protease activity causes the neuromuscular disorder of mnd2 mutant mice. *Nature* 425: 721-727, 2003.
156. Jones LJ, Upson RH, Haugland RP, Panchuk-Voloshina N, Zhou M, Haugland RP. Quenched BODIPY Dye-Labeled Casein Substrates for the Assay of Protease Activity by Direct Fluorescence Measurement. *Analytical Biochemistry* 251: 144-152, 1997.
157. Junn E, Jang WH, Zhao X, Jeong BS, Mouradian MM. Mitochondrial localization of DJ-1 leads to enhanced neuroprotection. *Journal of Neuroscience Research* 87: 123-129, 2009.
158. Junn E, Taniguchi H, Jeong BS, Zhao X, Ichijo H, Mouradian MM. Interaction of DJ-1 with Daxx inhibits apoptosis signal-regulating kinase 1 activity and cell death. *Proc Natl Acad Sci USA* 102: 9691-9696, 2005.
159. Junn E, Taniguchi H, Jeong BS, Zhao X, Ichijo H, Mouradian MM. Interaction of DJ-1 with Daxx inhibits apoptosis signal-regulating kinase 1 activity and cell death. *Proc. Natl. Acad. Sci. USA* 102: 9691-9696, 2005.
160. Kahle PJ, Haass C. How does parkin ligate ubiquitin to Parkinson's disease? . *EMBO reports* 5: 681-685, 2004.
161. Kamp F, Exner N, Lutz AK, Wender N, Hegermann J, Brunner B, Nuscher B, Bartels T, Giese A, Beyer K, Eimer S, Winklhofer KF, Haass C. Inhibition of mitochondrial fusion by [alpha]-synuclein is rescued by PINK1, Parkin and DJ-1. *EMBO J* 29: 3571-3589, 2010.
162. Keeney PM, Xie J, Capaldi RA, Bennett JP, Jr. Parkinson's Disease Brain Mitochondrial Complex I Has Oxidatively Damaged Subunits and Is Functionally Impaired and Misassembled. *J. Neurosci.* 26: 5256-5264, 2006.
163. Kim RH, Mak TW. Tumours and tremors: how PTEN regulation underlies both. *Br. J. Cancer* 94: 620-624, 2006.
164. Kim RH, Peters M, Jang Y, Shi W, Pintilie M, Fletcher GC, DeLuca C, Liepa J, Zhou L, Snow B, Binari RC, Manoukian AS, Bray MR, Liu F-F, Tsao M-S, Mak TW. DJ-1, a novel regulator of the tumor suppressor PTEN. *Cancer Cell* 7: 263-273, 2005.
165. Kim RH, Smith PD, Aleyasin H, Hayley S, Mount MP, Pownall S, Wakeham A, You-Ten AJ, Kalia SK, Horne P, Westaway D, Lozano AM, Anisman H, Park DS, Mak TW. Hypersensitivity of DJ-1-deficient mice to 1-methyl-4-phenyl-1,2,3,6-tetrahydropyrindine (MPTP) and oxidative stress. *Proc Natl Acad Sci USA* 102: 5215-5220, 2005.
166. Kim RH, Smith PD, Aleyasin H, Hayley S, Mount MP, Pownall S, Wakeham A, You-Ten AJ, Kalia SK, Horne P, Westaway D, Lozano AM, Anisman H, Park DS, Mak TW. Hypersensitivity of DJ-1-deficient mice to 1-methyl-4-phenyl-1,2,3,6-

tetrahydropyrindine (MPTP) and oxidative stress. *Proc. Natl. Acad. Sci. USA* 102: 5215-5220, 2005.

167. Kim Y-C, Kitaura H, Taira T, M.M S, Iguchi-Ariga, Ariga H. Oxidation of DJ-1-dependent cell transformation through direct binding of DJ-1 to PTEN. *International Journal of Cancer* 35 1331-1341, 2009.
168. Kinumi T, Kimata J, Taira T, Ariga H, Niki E. Cysteine-106 of DJ-1 is the most sensitive cysteine residue to hydrogen peroxide-mediated oxidation in vivo in human umbilical vein endothelial cells. *Biochem Biophys Res Commun* 317: 722-728, 2004.
169. Kirk E, Chin L-S, Li L. GRIF1 binds Hrs and is a new regulator of endosomal trafficking. *J. Cell. Sci.* 119: 4689-4701, 2006.
170. Kirk R, Laman H, Knowles PP, Murray-Rust J, Lomonosov M, Meziane EK, McDonald NQ. Structure of a Conserved Dimerization Domain within the F-box Protein Fbxo7 and the PI31 Proteasome Inhibitor. *Journal of Biological Chemistry* 283: 22325-22335, 2008.
171. Kish SJ, Morito C, Hornykiewicz O. Glutathione peroxidase activity in Parkinson's disease brain. *Neuroscience Letters* 58: 343-346, 1985.
172. Klinefelter GR, Laskey JW, Ferrell J, Suarez JD, Roberts NL. Discriminant analysis indicates a single sperm protein (SP22) is predictive of fertility following exposure to epididymal toxicants. 1997. pp. 139-150.
173. Klinefelter GR, Welch JE, Perreault SD, Moore HD, Zucker RM, Suarez JD, Roberts NL, Bobseine K, Jeffay S. Localization of the sperm protein SP22 and inhibition of fertility in vivo and in vitro. *J Androl* 23: 48-63., 2002.
174. Koide-Yoshida S, Niki T, Ueda M, Himeno S, Taira T, Iguchi-Ariga SMM, Ando Y, Ariga H. DJ-1 degrades transthyretin and an inactive form of DJ-1 is secreted in familial amyloidotic polyneuropathy. *International journal of molecular medicine* E-publish, 2007.
175. Kostrzewa RM, Jacobowitz DM. Pharmacological Actions of 6-Hydroxydopamine. *Pharmacological Reviews* 26: 199-288, 1974.
176. Kraytsberg Y, Kudryavtseva E, McKee AC, Geula C, Kowall NW, Khrapko K. Mitochondrial DNA deletions are abundant and cause functional impairment in aged human substantia nigra neurons. *Nat. Genet.* 38: 518-520, 2006.
177. Krebiehl G, Ruckerbauer S, Burbulla LF, Kieper N, Maurer B, Waak J, Wolburg H, Gizatullina Z, Gellerich FN, Woitalla D, Riess O, Kahle PJ, Proikas-Cezanne T, Krüger R. Reduced Basal Autophagy and Impaired Mitochondrial Dynamics Due to Loss of Parkinson's Disease-Associated Protein DJ-1. *PLoS ONE* 5: e9367, 2010.
178. Krojer T, Garrido-Franco M, Huber R, Ehrmann M, Clausen T. Crystal structure of DegP (HtrA) reveals a new protease-chaperone machine. *Nature* 416: 455-459, 2002.
179. Krojer T, Sawa J, Schafer E, Saibil HR, Ehrmann M, Clausen T. Structural basis for the regulated protease and chaperone function of DegP. *Nature* 453: 885-890, 2008.
180. Krüger R, Kuhn W, Müller T, Woitalla D, Graeber M, Kösel S, Przuntek H, Epplen JT, Schols L, Riess O. Ala30Pro mutation in the gene encoding alpha-synuclein in Parkinson's disease. *Nature Genetics* 18: 106-108, 1998.
181. Kubo S-I, Hattori N, Mizuno Y. Recessive Parkinson's disease. *Movement Disorders* 21: 885-893, 2006.
182. Kubota H. Quality Control Against Misfolded Proteins in the Cytosol: A Network for Cell Survival. 2009. pp. 609-616.
183. Laguna Goya R, Tyers P, Barker RA. The search for a curative cell therapy in Parkinson's disease. *Journal of the Neurological Sciences* 265: 32-42, 2008.
184. Lakshminarasimhan M, Maldonado MT, Zhou W, Fink AL, Wilson MA. Structural Impact of Three Parkinsonism-Associated Missense Mutations on Human DJ-1. *Biochemistry* 47: 1381-1392, 2008.

185. Lang AE, Gill S, Patel NK, Lozano A, Nutt JG, Penn R, Brooks DJ, Hotton G, Moro E, Heywood P, Brodsky MA, Burchiel K, Kelly P, Dalvi A, Scott B, Stacy M, Turner D, Wooten VGF, Elias WJ, Laws ER, Dhawan V, Stoessl AJ, Matcham J, Coffey RJ, Traub M. Randomized controlled trial of intraputamenal glial cell line–derived neurotrophic factor infusion in Parkinson disease. *Annals of Neurology* 59: 459-466, 2006.
186. Lang AE, Lozano AM. Parkinson's Disease- First of Two Parts. *N Engl J Med* 339: 1044-1053, 1998.
187. Langston J, Ballard PJ. Parkinson's disease in a chemist working with 1-methyl-4-phenyl-1,2,5,6-tetrahydropyridine. *New England Journal of Medicine* 309: 310, 1983.
188. Lapointe N, St-Hilaire M, Martinoli M-G, Blanchet J, Gould P, Rouillard C, Cicchetti F. Rotenone induces non-specific central nervous system and systemic toxicity. *FASEB J.*: 03-0677fje, 2004.
189. Larsson PKA, Claesson H-E, Kennedy BP. Multiple Splice Variants of the Human Calcium-independent Phospholipase A2 and Their Effect on Enzyme Activity. *Journal of Biological Chemistry* 273: 207-214, 1998.
190. Le Naour F, Misek DE, Krause MC, Deneux L, Giordano TJ, Scholl S, Hanash SM. Proteomics-based Identification of RS/DJ-1 as a Novel Circulating Tumor Antigen in Breast Cancer. *Clinical Cancer Research* 7: 3328-3335, 2001.
191. Lee JT, Wheeler TC, Li L, Chin L-S. Ubiquitination of α-synuclein by Siah-1 promotes α -synuclein aggregation and apoptotic cell death. *Hum. Mol. Genet.* 17: 906-917, 2008.
192. Lee S-J, Kim SJ, Kim I-K, Ko J, Jeong C-S, Kim G-H, Park C, Kang S-O, Suh P-G, Lee H-S, Cha S-S. Crystal Structures of Human DJ-1 and Escherichia coli Hsp31, Which Share an Evolutionarily Conserved Domain. *J. Biol. Chem.* 278: 44552-44559, 2003.
193. Lees AJ, Hardy J, Revesz T. Parkinson's disease. *The Lancet* 373: 2055-2066, 2009.
194. Leroy E, Boyer R, Auburger G, Leube B, Ulm G, Mezey E, Harta G, Brownstein MJ, Jonnalagada S, Chernova T, Dehejia A, Lavedan C, Gasser T, Steinbach PJ, Wilkinson KD, Polymeropoulos MH. The ubiquitin pathway in Parkinson's disease. *Nature* 395: 451-452, 1998.
195. Lev N, Ickowicz D, Melamed E, Offen D. Oxidative insults induce DJ-1 upregulation and redistribution: Implications for neuroprotection. *NeuroToxicology* 29: 397-405, 2008.
196. Levine R, Mosoni L, Berlett B, Stadtman ER. Methionine residues as endogenous antioxidants in proteins. *Proc. Natl. Acad. Sci. USA* 93: 15036-15040, 1996.
197. Levine RL, Moskovitz J, Stadtman ER. Oxidation of Methionine in Proteins: Roles in Antioxidant Defense and Cellular Regulation. *IUBMB Life* 50: 301-307, 2000.
198. Li HM, Niki T, Taira T, Iguchi-Ariga SMM, Ariga H. Association of DJ-1 with chaperones and enhanced association and colocalization with mitochondrial Hsp70 by oxidative stress. *Free Radical Research* 39: 1091 - 1099, 2005.
199. Li HM, Niki T, Taira T, Iguchi-Ariga SMM, Ariga H. Association of DJ-1 with chaperones and enhanced association and colocalization with mitochondrial Hsp70 by oxidative stress. *Free Radic. Res.* 39: 1091 - 1099, 2005.
200. Li YJ, Deng J, Mayhew GM, Grimsley JW, Huo X, Vance JM. Investigation of the PARK10 Gene in Parkinson Disease. *Annals of Human Genetics* 71: 639-647, 2007.
201. Liang X, Fomenko DE, Raza AS, Chong C-K, Carlson BA, Hatfield DL, Gladyshev VN. Analysis of Methionine/Selenomethionine Oxidation and Methionine Sulfoxide Reductase Function Using Methionine-Rich Proteins and Antibodies against Their Oxidized Forms *Biochemistry* 47: 6685-6694, 2008.
202. Lijnen HR, Van Hoef B, Nelles L, Collen D. Plasminogen activation with single-chain urokinase-type plasminogen activator (scu-PA). Studies with active site mutagenized plasminogen (Ser740----Ala) and plasmin-resistant scu-PA (Lys158----Glu). *The Journal of biological chemistry* 265: 5232-5236, 1990.

203. Lin CH, Tan EK, Chen ML, Tan LC, Lim HQ, Chen GS, Wu RM. Novel ATP13A2 variant associated with Parkinson disease in Taiwan and Singapore. *Neurology* 71: 1727-32, 2008.
204. Lin MT, Beal MF. Mitochondrial dysfunction and oxidative stress in neurodegenerative diseases. *Nature* 443: 787-795, 2006.
205. Liu Y, Fallon L, Lashuel HA, Liu Z, Lansbury Jr PT. The UCH-L1 Gene Encodes Two Opposing Enzymatic Activities that Affect α-Synuclein Degradation and Parkinson's Disease Susceptibility. *Cell* 111: 209-218, 2002.
206. Liu Y, Fallon L, Lashuel HA, Liu Z, Lansbury PT. The UCH-L1 Gene Encodes Two Opposing Enzymatic Activities that Affect αSynuclein Degradation and Parkinson's Disease Susceptibility. *Cell* 111: 209-218, 2002.
207. Lockwood TD. Cys-His proteases are among the wired proteins of the cell. *Archives of Biochemistry and Biophysics* 432: 12-24, 2004.
208. Lopez-Otin C, Bond JS. Proteases: Multifunctional Enzymes in Life and Disease. *J Biol Chem* 283: 30433-30437, 2008.
209. Lucas JI, Marin I. A New Evolutionary Paradigm for the Parkinson Disease Gene DJ-1. *Mol Biol Evol* 24: 551-561, 2007.
210. Luoma P, Melberg A, Rinne JO, Kaukonen JA, Nupponen NN, Chalmers RM, Oldfors A, Rautakorpi I, Peltonen L, Majamaa K, Somer H, Suomalainen A. Parkinsonism, premature menopause, and mitochondrial DNA polymerase [gamma] mutations: clinical and molecular genetic study. *The Lancet* 364: 875-882, 2004.
211. Macedo MG, Verbaan D, Fang Y, van Rooden SM, Visser M, Anar B, Uras A, Groen JL, Rizzu P, van Hilten JJ, Heutink P. Genotypic and phenotypic characteristics of Dutch patients with early onset Parkinson's disease. *Movement Disorders* 24: 196-203, 2009.
212. MacKeigan JP, Clements CM, Lich JD, Pope RM, Hod Y, Ting JPY. Proteomic Profiling Drug-Induced Apoptosis in Non-Small Cell Lung Carcinoma: Identification of RS/DJ-1 and RhoGDI {alpha}. *Cancer Res.* 63: 6928-6934, 2003.
213. Malgieri G, Eliezer D. Structural effects of Parkinson's disease linked DJ-1 mutations. *Protein Science* 17: 855-868, 2008.
214. Malki A, Caldas T, Abdallah J, Kern R, Eckey V, Kim SJ, Cha S-S, Mori H, Richarme G. Peptidase Activity of the Escherichia coli Hsp31 Chaperone. *J Biol Chem* 280: 14420-14426, 2005.
215. Manning-Bog AB, Caudle WM, Perez XA, Reaney SH, Paletzki R, Isla MZ, Chou VP, McCormack AL, Miller GW, Langston JW, Gerfen CR, DiMonte DA. Increased vulnerability of nigrostriatal terminals in DJ-1-deficient mice is mediated by the dopamine transporter. *Neurobiology of Disease* 27: 141-150, 2007.
216. Manning-Bog AB, McCormack AL, Li J, Uversky VN, Fink AL, Di Monte DA. The Herbicide Paraquat Causes Up-regulation and Aggregation of α-Synuclein in Mice. *Journal of Biological Chemistry* 277: 1641-1644, 2002.
217. Maraganore DM, de Andrade M, Lesnick TG, Strain KJ, Farrer MJ, Rocca WA, Pant PVK, Frazer KA, Cox DR, Ballinger DG. High-Resolution Whole-Genome Association Study of Parkinson Disease. *American journal of human genetics* 77: 685-693, 2005.
218. Maraganore DMM, Farrer MJP, Hardy JAP, Lincoln SJB, McDonnell SKM, Rocca WAMM. Case-control study of the ubiquitin carboxy-terminal hydrolase L1 gene in Parkinson's disease. *Neurology* 53: 1858-1860, 1999.
219. Marcum JL, Mathenia JK, Chan R, Guttmann RP. Oxidation of thiol-proteases in the hippocampus of Alzheimer's disease. *Biochemical and Biophysical Research Communications* 334: 342-348, 2005.
220. Marella M, Seo BB, Nakamaru-Ogiso E, Greenamyre JT, Matsuno-Yagi A, Yagi T. Protection by the *NDI1* Gene against Neurodegeneration in a Rotenone Rat Model of Parkinson's Disease. *PLoS One* 3: e1433, 2008.

221. Maroteaux L, Campanelli JT, Scheller RH. Synuclein: a neuron-specific protein localized to the nucleus and presynaptic nerve terminal. 1988. pp. 2804-2815.
222. Martinat C, Shendelman S, Jonason A, Leete T, Beal F, Yang L, Floss T, Abeliovich A. Sensitivity to Oxidative Stress in DJ-1-Deficient Dopamine Neurons: An ES- Derived Cell Model of Primary Parkinsonism. *PLoS Biology* 2: 1754-1764, 2004.
223. Martinelli P, Rugarli EI. Emerging roles of mitochondrial proteases in neurodegeneration. *Biochimica et Biophysica Acta (BBA) - Bioenergetics* 1797: 1-10, 2010.
224. Martins LM, Morrison A, Klupsch K, Fedele V, Moisoi N, Teismann P, Abuin A, Grau E, Geppert M, Livi GP, Creasy CL, Martin A, Hargreaves I, Heales SJ, Okada H, Brandner S, Schulz JB, Mak T, Downward J. Neuroprotective Role of the Reaper-Related Serine Protease HtrA2/Omi Revealed by Targeted Deletion in Mice. *Mol. Cell. Biol.* 24: 9848-9862, 2004.
225. Marttila RJ, Lorentz H, Rinne UK. Oxygen toxicity protecting enzymes in Parkinson's disease: Increase of superoxide dismutase-like activity in the substantia nigra and basal nucleus. *Journal of the Neurological Sciences* 86: 321-331, 1988.
226. Mattson MP, Kroemer G. Mitochondria in cell death: novel targets for neuroprotection and cardioprotection. *Trends in Molecular Medicine* 9: 196-205, 2003.
227. McFarlane S. Metalloproteases: Carving Out a Role in Axon Guidance. *Neuron* 37: 559-562, 2003.
228. McLean PJ, Kawamata H, Shariff S, Hewett J, Sharma N, Ueda K, Breakefield XO, Hyman BT. TorsinA and heat shock proteins act as molecular chaperones: suppression of α-synuclein aggregation. *Journal of Neurochemistry* 83: 846-854, 2002.
229. McNally R, Davis B, Clements C, Accavitti-Loper M, Mak T, Ting J. DJ-1 enhances cell survival through the binding of cezanne, a negative regulator of NF-κB. *J Biol. Chem.* Epub, 2010.
230. Meray RK, Lansbury PT. Reversible Monoubiquitination Regulates the Parkinson Disease-associated Ubiquitin Hydrolase UCH-L1. *Journal of Biological Chemistry* 282: 10567-10575, 2007.
231. Meulener M, Whitworth AJ, Armstrong-Gold CE, Rizzu P, Heutink P, Wes PD, Pallanck LJ, Bonini NM. Drosophila DJ-1 Mutants Are Selectively Sensitive to Environmental Toxins Associated with Parkinson's Disease. *Curr Biol* 15: 1572-1577, 2005.
232. Midwinter RG, Cheah F-C, Moskovitz J, Vissers MC, Winterbourn CC. IκB is a sensitive target for oxidation by cell-permeable chloramines: inhibition of NF-κB activity by glycine chloramine through methionine oxidation. *Biochemical Journal* 396: 71-78, 2006.
233. Minetti G, Balduini C, Brovelli A. Reduction of DABS-L-methionine-dl-sulfoxide by protein methionine sulfoxide reductase from polymorphonuclear leukocytes: stereospecificity towards the l-sulfoxide. *Ital. J. Biochem.* 1994: 6, 1994.
234. Mitsumoto A, Nakagawa Y. DJ-1 is an indicator for endogenous reactive oxygen species elicited by endotoxin. *Free Radical Research* 35: 885-893, 2001.
235. Mitsumoto A, Nakagawa Y, Takeuchi A, Okawa K, Iwamatsu A, Takanezawa Y. Oxidized forms of peroxiredoxins and DJ-1 on two-dimensional gels increased in response to sublethal levels of paraquat. *Free Radical Research* 35: 301-310, 2001.
236. Mitsumoto A, Takanezawa Y, Okawa K, Iwamatsu A, Nakagawa Y. Variants of peroxiredoxins expression in response to hydroperoxide stress. *Free Radical Biology and Medicine* 30: 625-635, 2001.
237. Mo J-S, Jung J, Yoon J-H, Hong J-A, Kim M-Y, Ann E-J, Seo M-S, Choi Y-H, Park H-S. DJ-1 modulates the p38 mitogen-activated protein kinase pathway through physical interaction with apoptosis signal-regulating kinase 1. *J. Cell. Biochem.* 110: 229-237, 2010.

238. Moore DJ, Zhang L, Dawson TM, Dawson VL. A missense mutation (L166P) in DJ-1, linked to familial Parkinson's disease, confers reduced protein stability and impairs homo-oligomerization. *Journal of Neurochemistry* 87: 1558-1567, 2003.
239. Morgan NV, Westaway SK, Morton JEV, Gregory A, Gissen P, Sonek S, Cangul H, Coryell J, Canham N, Nardocci N, Zorzi G, Pasha S, Rodriguez D, Desguerre I, Mubaidin A, Bertini E, Trembath RC, Simonati A, Schanen C, Johnson CA, Levinson B, Woods CG, Wilmot B, Kramer P, Gitschier J, Maher ER, Hayflick SJ. PLA2G6, encoding a phospholipase A2, is mutated in neurodegenerative disorders with high brain iron. *Nat Genet* 38: 752-754, 2006.
240. Moskovitz J, Weissbach H, Brot N. Cloning the expression of a mammalian gene involved in the reduction of methionine sulfoxide residues in proteins. *Proc. Natl. Acad. Sci. U.S.A.* 93: 2095-2099, 1996.
241. Muchowski PJ. Protein Misfolding, Amyloid Formation, and Neurodegeneration: A Critical Role for Molecular Chaperones? *Neuron* 35: 9-12, 2002.
242. Muchowski PJ, Wacker JL. Modulation of neurodegeneration by molecular chaperones. *Nat Rev Neurosci* 6: 11-22, 2005.
243. Murphy DD, Rueter SM, Trojanowski JQ, Lee VMY. Synucleins Are Developmentally Expressed, and alpha -Synuclein Regulates the Size of the Presynaptic Vesicular Pool in Primary Hippocampal Neurons. *J. Neurosci.* 20: 3214-3220, 2000.
244. Muthane U, Ramsay KA, Jiang H, Jackson-Lewis V, Donaldson D, Fernando S, Ferreira M, Przedborski S. Differences in Nigral Neuron Number and Sensitivity to 1-Methyl-4-phenyl-1,2,3,6-tetrahydropyridine in C57/bl and CD-1 Mice. *Experimental Neurology* 126: 195-204, 1994.
245. Muzio M, Stockwell BR, Stennicke HR, Salvesen GS, Dixit VM. An Induced Proximity Model for Caspase-8 Activation. *The Journal of biological chemistry* 273: 2926-2930, 1998.
246. Nagakubo D, Taira T, Kitaura H, Ikeda M, Tamai K, Iguchi-Ariga SMM, Ariga H. DJ-1, a Novel Oncogene Which Transforms Mouse NIH3T3 Cells in Cooperation withras. *Biochemical and Biophysical Research Communications* 231: 509-513, 1997.
247. Naiki H, Nagai Y. Molecular Pathogenesis of Protein Misfolding Diseases: Pathological Molecular Environments Versus Quality Control Systems Against Misfolded Proteins. 2009. pp. 751-756.
248. Naito S, Mochizuki H, Yasuda T, Mizuno Y, Furusaka M, Ikeda S, Adachi T, Shimizu HM, Suzuki J, Fujiwara S, Okada T, Nishikawa K, Aoki S, Wada K. Characterization of multimetric variants of ubiquitin carboxyl-terminal hydrolase L1 in water by small-angle neutron scattering. *Biochemical and Biophysical Research Communications* 339: 717-725, 2006.
249. Najim al-Din A, Wriekat A, Mubaidin A, Dasouki M, Hiari M. Pallido-pyramidal degeneration, supranuclear upgaze paresis and dementia: Kufor-Rakeb syndrome. *Acta. Neurol. Scand.* 89: 347-352, 1994.
250. Nakabeppu Y, Tsuchimoto D, Yamaguchi H, Sakumi K. Oxidative damage in nucleic acids and Parkinson's disease. *Journal of Neuroscience Research* 85: 919-934, 2007.
251. Neumann M, Müller V, Görner K, Kretzschmar H, Haass C, Kahle P. Pathological properties of the Parkinson's disease-associated protein DJ-1 in a-synucleinopathies and tauopathies: relevance for multiple system atrophy and Pick's disease. *Acta Neuropathol.* 107: 489-496, 2004.
252. Neurath H. The versatility of proteolytic enzymes. *J Cell Biochem* 32: 35-49., 1986.
253. Nishikawa K, Li H, Kawamura R, Osaka H, Wang Y-L, Hara Y, Hirokawa T, Manago Y, Amano T, Noda M, Aoki S, Wada K. Alterations of structure and hydrolase activity of parkinsonism-associated human ubiquitin carboxyl-terminal hydrolase L1 variants. *Biochemical and Biophysical Research Communications* 304: 176-183, 2003.

254. Ohmura T, Ueda T, Hashimoto Y, Imoto T. Tolerance of point substitution of methionine for isoleucine in hen egg white lysozyme. *Protein Engineering* 14: 421-425, 2001.
255. Oien DB, Canello T, Gabizon R, Gasset M, Lundquist BL, Burns JM, Moskovitz J. Detection of oxidized methionine in selected proteins, cellular extracts, and blood serums by novel anti-methionine sulfoxide antibodies. *Arch. Biochem. Biophys.* 485: 35-40, 2009.
256. Oien DB, Moskovitz J. Substrates of the Methionine Sulfoxide Reductase System and Their Physiological Relevance. In: *Current Topics in Developmental Biology*. edited by Gerald PS. Academic Press; 2007. pp. 93-133.
257. Oien DB, Osterhaus GL, Latif SA, Pinkston JW, Fulks J, Johnson M, Fowler SC, Moskovitz J. MsrA knockout mouse exhibits abnormal behavior and brain dopamine levels. *Free Radical Biology and Medicine* 45: 193-200, 2008.
258. Olanow CW, Goetz CG, Kordower JH, Stoessl AJ, Sossi V, Brin MF, Shannon KM, Nauert GM, Perl DP, Godbold J, Freeman TB. A double-blind controlled trial of bilateral fetal nigral transplantation in Parkinson's disease. *Annals of Neurology* 54: 403-414, 2003.
259. Olzmann JA, Bordelon JR, Muly EC, Rees HD, Levey AI, Li L, Chin L-S. Selective enrichment of DJ-1 protein in primate striatal neuronal processes: Implications for Parkinson's disease. *J. Comp. Neurol.* 500: 585-599, 2007.
260. Olzmann JA, Bordelon JR, Muly EC, Rees HD, Levey AI, Li L, Chin L-S. Selective enrichment of DJ-1 protein in primate striatal neuronal processes: Implications for Parkinson's disease. *J. Comp. Neurol.* 500: 585-599, 2007.
261. Olzmann JA, Brown K, Wilkinson KD, Rees HD, Huai Q, Ke H, Levey AI, Li L, Chin L-S. Familial Parkinson's Disease-associated L166P Mutation Disrupts DJ-1 Protein Folding and Function. *The Journal of Biological Chemistry* 279: 8506-8515, 2004.
262. Olzmann JA, Brown K, Wilkinson KD, Rees HD, Huai Q, Ke H, Levey AI, Li L, Chin L-S. Familial Parkinson's Disease-associated L166P Mutation Disrupts DJ-1 Protein Folding and Function. *J. Biol. Chem.* 279: 8506-8515, 2004.
263. Olzmann JA, Chin L-S. Parkin-mediated K63-linked polyubiquitination: A signal for targeting misfolded proteins to the aggresome-autophagy pathway. *Autophagy* 4: 85-87, 2008.
264. Olzmann JA, Li L, Chudaev MV, Chen J, Perez FA, Palmiter RD, Chin L-S. Parkin-mediated K63-linked polyubiquitination targets misfolded DJ-1 to aggresomes via binding to HDAC6. *J Cell Biol* 178: 1025-1038, 2007.
265. Ooe H, Maita C, Maita H, Iguchi-Ariga SMM, Ariga H. Specific cleavage of DJ-1 under an oxidative condition. *Neuroscience Letters* 406: 165-168, 2006.
266. Osaka H, Wang Y-L, Takada K, Takizawa S, Setsuie R, Li H, Sato Y, Nishikawa K, Sun Y-J, Sakurai M, Harada T, Hara Y, Kimura I, Chiba S, Namikawa K, Kiyama H, Noda M, Aoki S, Wada K. Ubiquitin carboxy-terminal hydrolase L1 binds to and stabilizes monoubiquitin in neuron. *Human Molecular Genetics* 12: 1945-1958, 2003.
267. Outeiro TF, Klucken J, Strathearn KE, Liu F, Nguyen P, Rochet J-C, Hyman BT, McLean PJ. Small heat shock proteins protect against [alpha]-synuclein-induced toxicity and aggregation. *Biochemical and Biophysical Research Communications* 351: 631-638, 2006.
268. Oyama G, Yoshimi K, Natori S, Chikaoka Y, Ren Y-R, Funayama M, Shimo Y, Takahashi R, Nakazato T, Kitazawa S, Hattori N. Impaired in vivo dopamine release in parkin knockout mice. *Brain Research* 1352: 214-222, 2010.
269. Palmblad M, Westlind-Danielsson A, Bergquist J. Oxidation of Methionine 35 Attenuates Formation of Amyloid beta -Peptide 1-40 Oligomers. *The Journal of Biological Chemistry* 277: 19506-19510, 2002.
270. Pankratz N, Nichols WC, Uniacke SK, Halter C, Murrell J, Rudolph A, Shults CW, Conneally PM, Foroud T, Group tPS. Genome-wide linkage analysis and evidence of

gene-by-gene interactions in a sample of 362 multiplex Parkinson disease families. *Human Molecular Genetics* 12: 2599-2608, 2003.

271. Pankratz N, Nichols WC, Uniacke SK, Halter C, Rudolph A, Shults C, Conneally PM, Foroud T. Significant Linkage of Parkinson Disease to Chromosome 2q36-37. *American journal of human genetics* 72: 1053-1057, 2003.
272. Pardo M, García Á, Thomas B, Piñeiro A, Akoulitchev A, Dwek RA, Zitzmann N. The characterization of the invasion phenotype of uveal melanoma tumour cells shows the presence of MUC18 and HMG-1 metastasis markers and leads to the identification of DJ-1 as a potential serum biomarker. *International Journal of Cancer* 119: 1014-1022, 2006.
273. Park J, Lee G, Chung J. The PINK1-Parkin pathway is involved in the regulation of mitochondrial remodeling process. *Biochemical and Biophysical Research Communications* 378: 518-523, 2009.
274. Parker Jr WD, Parks JK, Swerdlow RH. Complex I deficiency in Parkinson's disease frontal cortex. *Brain Research* 1189: 215-218, 2008.
275. Paul G, Ahn Y, Li J, Brundin P. Transplantation in Parkinson's disease: The future looks bright. *Adv. Exp. Med. Biol.* 557: 221-248, 2006.
276. Pennathur S, Jackson-Lewis V, Przedborski S, Heinecke JW. Mass Spectrometric Quantification of 3-Nitrotyrosine, ortho-Tyrosine, and Dityrosine in Brain Tissue of 1-Methyl-4-phenyl-1,2,3,6-tetrahydropyridine-treated Mice, a Model of Oxidative Stress in Parkinson's Disease. *J. Biol. Chem* 274: 34621-34628, 1999.
277. Petrovitch H, Ross GW, Abbott RD, Sanderson WT, Sharp DS, Tanner CM, Masaki KH, Blanchette PL, Popper JS, Foley D, Launer L, White LR. Plantation Work and Risk of Parkinson Disease in a Population-Based Longitudinal Study. *Arch Neurol* 59: 1787-1792, 2002.
278. Piccini P, Pavese N, Hagell P, Reimer J, Bjorklund A, Oertel WH, Quinn NP, Brooks DJ, Lindvall O. Factors affecting the clinical outcome after neural transplantation in Parkinson's disease. *Brain* 128: 2977-2986, 2005.
279. Polymeropoulos MH, Lavedan C, Leroy E, Ide SE, Dehejia A, Dutra A, Pike B, Root H, Rubenstein J, Boyer R, Stenroos ES, Chandrasekharappa S, Athanassiadou A, Papapetropoulos T, Johnson WG, Lazzarini AM, Duvoisin RC, Di Iorio G, Golbe LI, Nussbaum RL. Mutation in the α-Synuclein Gene Identified in Families with Parkinson's Disease. 1997. pp. 2045-2047.
280. Poole AC, Thomas RE, Andrews LA, McBride HM, Whitworth AJ, Pallanck LJ. The PINK1/Parkin pathway regulates mitochondrial morphology. *Proc Natl Acad Sci USA* 105: 1638-1643, 2008.
281. Powers KM, Kay DM, Factor SA, Zabetian CP, Higgins DS, Samii A, Nutt JG, Griffith A, Leis B, Roberts JW, Martinez ED, Montimurro JS, Checkoway H, Payami H. Combined effects of smoking, coffee, and NSAIDs on Parkinson's disease risk. *Movement Disorders* 23: 88-95, 2008.
282. Pridgeon JW, Olzmann JA, Chin L-S, Li L. PINK1 Protects against Oxidative Stress by Phosphorylating Mitochondrial Chaperone TRAP1. *PLoS Biol* 5: e172, 2007.
283. Priyadarshi A, Khuder S, Schaub E, Shrivastava S. A meta-analysis of Parkinson's disease and exposure to pesticides. *Neurotoxicology* 21: 435-440, 2000.
284. Ramachandiran S, Hansen JM, Jones DP, Richardson JR, Miller GW. Divergent Mechanisms of Paraquat, MPP+, and Rotenone Toxicity: Oxidation of Thioredoxin and Caspase-3 Activation. *Toxicological sciences* 95: 163-171, 2007.
285. Ramirez A, Heimbach A, Grundemann J, Stiller B, Hampshire D, Cid LP, Goebel I, Mubaidin AF, Wriekat A-L, Roeper J, Al-Din A, Hillmer AM, Karsak M, Liss B, Woods CG, Behrens MI, Kubisch C. Hereditary parkinsonism with dementia is caused by

mutations in ATP13A2, encoding a lysosomal type 5 P-type ATPase. *Nat Genet* 38: 1184-1191, 2006.

286. Ramsey CP, Giasson BI. L10p and P158DEL DJ-1 mutations cause protein instability, aggregation, and dimerization impairments. *Journal of Neuroscience Research* 88: 3111-3124, 2010.
287. Reddy VY, Desorchers PE, Pizzo SV, Gonias SL, Sahakian JA, Levine RL, Weiss SJ. Oxidative dissociation of human alpha 2-macroglobulin tetramers into dysfunctional dimers. *Journal of Biological Chemistry* 269: 4683-4691, 1994.
288. Rekas A, Adda CG, Andrew Aquilina J, Barnham KJ, Sunde M, Galatis D, Williamson NA, Masters CL, Anders RF, Robinson CV, Cappai R, Carver JA. Interaction of the Molecular Chaperone αB-Crystallin with α-Synuclein: Effects on Amyloid Fibril Formation and Chaperone Activity. *Journal of Molecular Biology* 340: 1167-1183, 2004.
289. Rizzu P, Hinkle DA, Zhukareva V, Bonifati V, Severijnen L-A, Martinez D, Ravid R, Kamphorst W, Eberwine JH, Lee VMY, Trojanowski JQ, Heutink P. DJ-1 colocalizes with tau inclusions: A link between parkinsonism and dementia. *Ann. Neurol.* 55: 113-118, 2004.
290. Ross GW, Petrovitch H. Current Evidence for Neuroprotective Effects of Nicotine and Caffeine Against Parkinson's Disease. *Drugs & Aging* 18: 797-806, 2001.
291. Saaksjarvi K, Knekt P, Rissanen H, Laaksonen MA, Reunanen A, Mannisto S. Prospective study of coffee consumption and risk of Parkinson's disease. *Eur J Clin Nutr* 62: 908-915, 2007.
292. Saggu H, Cooksey J, Dexter D, Wells FR, Lees A, Jenner P, Marsden CD. A Selective Increase in Particulate Superoxide Dismutase Activity in Parkinsonian Substantia Nigra. *Journal of Neurochemistry* 53: 692-697, 1989.
293. Saigoh K, Wang Y-L, Suh J-G, Yamanishi T, Sakai Y, Kiyosawa H, Harada T, Ichihara N, Wakana S, Kikuchi T, Wada K. Intragenic deletion in the gene encoding ubiquitin carboxy-terminal hydrolase in gad mice. *Nat Genet* 23: 47-51, 1999.
294. Schapira A, Mann V, Cooper J, Dexter D, Daniel S, Jenner P, Clark J, Marsden C. Anatomic and disease specificity of NADH CoQ1 reductase (complex I) deficiency in Parkinson's disease. *J. Neurochem.* 55: 2142-5, 1990.
295. Schulz JB, Matthews RT, Muqit MMK, Browne SE, Beal MF. Inhibition of Neuronal Nitric Oxide Synthase by 7-Nitroindazole Protects Against MPTP-Induced Neurotoxicity in Mice. *Journal of Neurochemistry* 64: 936-939, 1995.
296. Scott WK, Nance MA, Watts RL, Hubble JP, Koller WC, Lyons K, Pahwa R, Stern MB, Colcher A, Hiner BC, Jankovic J, Ondo WG, Allen FH, Goetz CG, Small GW, Masterman D, Mastaglia F, Laing NG, Stajich JM, Slotterbeck B, Booze MW, Ribble RC, Rampersaud E, West SG, Gibson RA, Middleton LT, Roses AD, Haines JL, Scott BL, Vance JM, Pericak-Vance MA. Complete Genomic Screen in Parkinson Disease. *JAMA: The Journal of the American Medical Association* 286: 2239-2244, 2001.
297. Sekito A, Koide-Yoshida S, Niki T, Taira T, Iguchi-Ariga SMM, Ariga H. DJ-1 interacts with HIPK1 and affects H_2O_2-induced cell death. *Free radical Research* 40: 155 - 165, 2006.
298. Seniuk NA, Tatton WG, Greenwood CE. Dose-dependent destruction of the coeruleus-cortical and nigral-striatal projections by MPTP. *Brain Research* 527: 7-20, 1990.
299. Setsuie R, Wada K. The functions of UCH-L1 and its relation to neurodegenerative diseases. *Neurochemistry International* 51: 105-111, 2007.
300. Setsuie R, Wang Y-L, Mochizuki H, Osaka H, Hayakawa H, Ichihara N, Li H, Furuta A, Sano Y, Sun Y-J, Kwon J, Kabuta T, Yoshimi K, Aoki S, Mizuno Y, Noda M, Wada K. Dopaminergic neuronal loss in transgenic mice expressing the Parkinson's disease-associated UCH-L1 I93M mutant. *Neurochemistry International* 50: 119-129, 2007.

301. Shacka JJ, Klocke BJ, Young C, Shibata M, Olney JW, Uchiyama Y, Saftig P, Roth KA. Cathepsin D Deficiency Induces Persistent Neurodegeneration in the Absence of Bax-Dependent Apoptosis. 2007. pp. 2081-2090.
302. Shao B, Cavigiolio G, Brot N, Oda MN, Heinecke JW. Methionine oxidation impairs reverse cholesterol transport by apolipoprotein A-I. *Proc. Natl. Acad. Sci. USA* 105: 12224-12229, 2008.
303. Shendelman S, Jonason A, Martinat C, Leete T, Abeliovich A. DJ-1 Is a Redox-Dependent Molecular Chaperone That Inhibits alpha-Synuclein Aggregate Formation. *PLoS Biology* 2: e362, 2004.
304. Shi Y. Caspase Activation: Revisiting the Induced Proximity Model. *Cell* 117: 855-858, 2004.
305. Shimizu K, Ohtaki K, Matsubara K, Aoyama K, Uezono T, Saito O, Suno M, Ogawa K, Hayase N, Kimura K, Shiono H. Carrier-mediated processes in blood-brain barrier penetration and neural uptake of paraquat. *Brain Research* 906: 135-142, 2001.
306. Shinbo Y, Niki T, Taira T, Ooe H, Takahashi-Niki K, Maita C, Seino C, Iguchi-Ariga SMM, Ariga H. Proper SUMO-1 conjugation is essential to DJ-1 to exert its full activities. *Cell Death Differ* 13: 96-108, 2005.
307. Shinbo Y, Taha T, Niki T, Iquchi-Ariga SMM, Ariga H. DJ-1 restores p53 transcription activity inhibited by Topors/p53BP3. *International Journal of Oncology* 26: 641-648, 2005.
308. Shojaee S, Sina F, Banihosseini SS, Kazemi MH, Kalhor R, Shahidi G-A, Fakhrai-Rad H, Ronaghi M, Elahi E. Genome-wide Linkage Analysis of a Parkinsonian-Pyramidal Syndrome Pedigree by 500 K SNP Arrays. *American journal of human genetics* 82: 1375-1384, 2008.
309. Shults CW, Haas RH, Passov D, Beal MF. Coenzyme Q10 levels correlate with the activities of complexes I and II/III in mitochondria from parkinsonian and nonparkinsonian subjects. *Annals of Neurology* 42: 261-264, 1997.
310. Sian J, Dexter DT, Lees AJ, Daniel S, Agid Y, Javoy-Agid F, Jenner P, Marsden CD. Alterations in glutathione levels in Parkinson's disease and other neurodegenerative disorders affecting basal ganglia. *Annals of Neurology* 36: 348-355, 1994.
311. Singleton AB, Farrer M, Johnson J, Singleton A, Hague S, Kachergus J, Hulihan M, Peuralinna T, Dutra A, Nussbaum R, Lincoln S, Crawley A, Hanson M, Maraganore D, Adler C, Cookson MR, Muenter M, Baptista M, Miller D, Blancato J, Hardy J, Gwinn-Hardy K. α-Synuclein Locus Triplication Causes Parkinson's Disease. *Science* 302: 841, 2003.
312. Sirinathsinghji D, Kupsch A, Mayer E, Zivin M, Pufal D, WH O. Cellular localization of tyrosine hydroxylase mRNA and cholecystokinin mRNA-containing cells in the ventral mesencephalon of the common marmoset: effects of 1-methyl-4-phenyl-1,2,3,6-tetrahydropyridine. *Brain research. Molecular brain research* 12: 267-74, 1992.
313. Spiess C, Beil A, Ehrmann M. A Temperature-Dependent Switch from Chaperone to Protease in a Widely Conserved Heat Shock Protein. *Cell* 97: 339-347, 1999.
314. Srinivasula SM, Ahmad M, Fernandes-Alnemri T, Alnemri ES. Autoactivation of Procaspase-9 by Apaf-1-Mediated Oligomerization. 1: 949-957, 1998.
315. Stadtman ER, Berlett BS. Reactive Oxygen-Mediated Protein Oxidation in Aging and Disease. *Drug Metabolism Reviews* 30: 225-243, 1998.
316. Stadtman ER, Levine RL. Free radical-mediated oxidation of free amino acids and amino acid residues in proteins. *Amino Acids* 25: 207-218, 2003.
317. Stadtman ER, Moskovitz J, Berlett BS, Levine RL. Cyclic oxidation and reduction of protein methionine residues is an important antioxidant mechanism. *Molecular and Cellular Biochemistry* 234-235: 3-9, 2002.

318. Stadtman ER, Moskovitz J, Levine RL. Oxidation of Methionine Residues of Proteins: Biological Consequences. *Antioxidant and Redox Signaling* 5: 577-582, 2003.
319. Stadtman ER, Moskovitz J, Levine RL. Oxidation of Methionine Residues of Proteins: Biological Consequences. *Antioxid. Redox Signal.* 5: 577-582, 2003.
320. Stadtman ER, Van Remmen H, Richardson A, Wehr NB, Levine RL. Methionine oxidation and aging. *Biochimica et Biophysica Acta (BBA) - Proteins & Proteomics* 1703: 135-140, 2005.
321. Stadtman ER, Van Remmen H, Richardson A, Wehr NB, Levine RL. Methionine oxidation and aging. *Biochim. Biophys. Acta.* 1703: 135-140, 2005.
322. Stennicke H, Salvesen GS. Catalytic properties of the caspases. *Cell Death Differ* 6: 1054-1059, 1999.
323. Strauss KM, Martins LM, Plun-Favreau H, Marx FP, Kautzmann S, Berg D, Gasser T, Wszolek Z, Muller T, Bornemann A, Wolburg H, Downward J, Riess O, Schulz JB, Kruger R. Loss of function mutations in the gene encoding Omi/HtrA2 in Parkinson's disease. *Hum. Mol. Genet.* 14: 2099-2111, 2005.
324. Subrini O, Betton J-M. Assemblies of DegP underlie its dual chaperone and protease function. *FEMS Microbiology Letters* 296: 143-148, 2009.
325. Suzuki Y, Imai Y, Nakayama H, Takahashi K, Takio K, Takahashi R. A Serine Protease, HtrA2, Is Released from the Mitochondria and Interacts with XIAP, Inducing Cell Death. *Molecular Cell* 8: 613-621, 2001.
326. Swerdlow R, Parks J, Davis Jn, Cassarino D, Trimmer P, Currie L, Dougherty J, Bridges W, Bennett JJ, Wooten G, WD P. Matrilineal inheritance of complex I dysfunction in a multigenerational Parkinson's disease family. *Ann Neurol* 44: 873-81, 1998.
327. Tachias K, Madison EL. Converting Tissue-type Plasminogen Activator into a Zymogen. *J Biol Chem* 271: 28749-28752, 1996.
328. Taggart C, Cervantes-Laurean D, Kim G, McElvaney NG, Wehr N, Moss J, Levine RL. Oxidation of either Methionine 351 or Methionine 358 in α1-Antitrypsin Causes Loss of Anti-neutrophil Elastase Activity. *Journal of Biological Chemistry* 275: 27258-27265, 2000.
329. Taira T, Saito Y, Niki T, Iguchi-Ariga S, Takahashi K, Ariga H. DJ-1 has a role in antioxidative stress to prevent cell death. *EMBO Rep* 5: 213-218, 2004.
330. Taira T, Saito Y, Niki T, Iguchi-Ariga S, Takahashi K, Ariga H. DJ-1 has a role in antioxidative stress to prevent cell death. *EMBO Rep.* 5: 213-218, 2004.
331. Takahashi-Niki K, Niki T, Taira T, Iguchi-Ariga SMM, Ariga H. Reduced anti-oxidative stress activities of DJ-1 mutants found in Parkinson's disease patients. *Biochemical and Biophysical Research Communications* 320: 389-397, 2004.
332. Takahashi K, Taira T, Niki T, Seino C, Iguchi-Ariga SMM, Ariga H. DJ-1 Positively Regulates the Androgen Receptor by Impairing the Binding of PIASxalpha to the Receptor. 2001. pp. 37556-37563.
333. Takao Nomura RKIIYCYSKS. Oxidation of methionine residue at hydrophobic core destabilizes p53 tetrameric structure. *Biopolymers* 91: 78-84, 2009.
334. Tan E-K, Kwok H-K, Tan LC, Zhao W-T, Prakash KM, Au W-L, Pavanni R, Ng Y-Y, Satake W, Zhao Y, Toda T, Liu J-J. Analysis of GWAS-linked loci in Parkinson disease reaffirms PARK16 as a susceptibility locus. *Neurology* 75: 508-512, 2010.
335. Tan JMM, Wong ESP, Lim K-L. Protein Misfolding and Aggregation in Parkinson's Disease. *Antioxidants & redox signaling* 11: 2119-2134, 2009.
336. Tang W, Sun Z-Y, Kung W, Pannell R, Sarmientos P, Gurewich V. A Site-Directed Mutagenesis of Pro-urokinase Which Substantially Reduces Its Intrinsic Activity 鈥?AU - Liu, Jian-Ning. *Biochemistry* 35: 14070-14076, 1996.
337. Tanner CM, Ottman R, Goldman SM, Ellenberg J, Chan P, Mayeux R, Langston JW. Parkinson Disease in Twins: An Etiologic Study. *JAMA* 281: 341-346, 1999.

338. Tao X, Tong L. Crystal Structure of Human DJ-1, a Protein Associated with Early Onset Parkinson's Disease. *J. Biol. Chem.* 278: 31372-31379, 2003.
339. Terzioglu M, Galter D. Parkinson's disease: genetic versus toxin-induced rodent models. *FEBS Journal* 275: 1384-1391, 2008.
340. Thoenen H, Tranzer JP. The Pharmacology of 6-Hydroxydopamine. *Annual Review of Pharmacology* 13: 169-180, 1973.
341. Thomas KJ, McCoy M, Blackinton J, Beilina A, van der Brug M, Sandebring A, Miller D, Maric D, Cedazo-Minguez A, Cookson MR. DJ-1 acts in parallel to the PINK1/parkin pathway to control mitochondrial function and autophagy. *Human Molecular Genetics*, 2010.
342. Thornberry NA, Lazebnik Y. Caspases: Enemies Within. *Science* 281: 1312-1316, 1998.
343. Tomimatsu Y, Idemoto S, Moriguchi S, Watanabe S, Nakanishi H. Proteases involved in long-term potentiation. *Life Sci.* 72: 355-361, 2002.
344. Twelves D, Perkins KSM, Counsell C. Systematic review of incidence studies of Parkinson's disease. *Movement Disorders* 18: 19-31, 2003.
345. Ueda S, Masutani H, Nakamura H, Tanaka T, Ueno M, Yodoi J. Redox Control of Cell Death. *Antioxidants & redox signaling* 4: 405-414, 2002.
346. Uversky VN, Yamin G, Souillac PO, Goers J, Glaser CB, Fink AL. Methionine oxidation inhibits fibrillation of human [alpha]-synuclein in vitro. *FEBS Letters* 517: 239-244, 2002.
347. van der Brug MP, Blackinton J, Chandran J, Hao L-Y, Lal A, Mazan-Mamczarz K, Martindale J, Xie C, Ahmad R, Thomas KJ, Beilina A, Gibbs JR, Ding J, Myers AJ, Zhan M, Cai H, Bonini NM, Gorospe M, Cookson MR. RNA binding activity of the recessive parkinsonism protein DJ-1 supports involvement in multiple cellular pathways. *Proc Natl Acad Sci USA* 105: 10244-10249, 2008.
348. Van Hoef B, Bini A, Collen D, Lijnen HR. Proteolytic Cleavage of Urokinase-Type Plasminogen Activator by Stromelysin-1 (MMP-3). *Biochemistry* 37: 7231-7236, 1998.
349. Varastet M, Riche D, Maziere M, Hantraye P. Chronic MPTP treatment reproduces in baboons the differential vulnerability of mesencephalic dopaminergic neurons observed in parkinson's disease. *Neuroscience* 63: 47-56, 1994.
350. Vasseur S, Afzal S, Tardivel-Lacombe J, Park DS, Iovanna JL, Mak TW. DJ-1/PARK7 is an important mediator of hypoxia-induced cellular responses. *Proc. Natl. Acad. Sci. USA* 106: 1111-1116, 2009.
351. Volles MJ, Lee S-J, Rochet J-C, Shtilerman MD, Ding TT, Kessler JC, Lansbury PT. Vesicle Permeabilization by Protofibrillar α-Synuclein: Implications for the Pathogenesis and Treatment of Parkinson's Disease *Biochemistry* 40: 7812-7819, 2001.
352. Waak J, Weber SS, Gorner K, Schall C, Ichijo H, Stehle T, Kahle PJ. Oxidizable Residues Mediating Protein Stability and Cytoprotective Interaction of DJ-1 with Apoptosis Signal-regulating Kinase 1. *J. Biol. Chem.* 284: 14245-14257, 2009.
353. Walker RK, Krishnaswamy S. The activation of prothrombin by the prothrombinase complex. The contribution of the substrate-membrane interaction to catalysis. *J. Biol. Chem.* 269: 27441-27450, 1994.
354. West AB, Dawson VL, Dawson TM. To die or grow: Parkinson's disease and cancer. *Trends Neurosci.* 28: 348-352, 2005.
355. West AB, Zimprich A, Lockhart PJ, Farrer M, Singleton A, Holtom B, Lincoln S, Hofer A, Hill L, Müller-Myhsok B, Wszolek ZK, Hardy J, Gasser T. Refinement of the PARK3 locus on chromosome 2p13 and the analysis of 14 candidate genes. *European Journal of Human Genetics* 9: 659-666, 2001.
356. Wickner S, Maurizi MR, Gottesman S. Posttranslational Quality Control: Folding, Refolding, and Degrading Proteins. *Science* 286: 1888-1893, 1999.
357. Wilkinson K. DUBs at a glance. *J Cell Sci* 122: 2325-9, 2009.

358. Wilkinson K, Lee K, Deshpande S, Duerksen-Hughes P, Boss J, Pohl J. The neuron-specific protein PGP 9.5 is a ubiquitin carboxyl-terminal hydrolase. *Science* 246: 670-673, 1989.
359. Wilson KP, Black J-AF, Thomson JA, Kim EE, Griffith JP, Navia MA, Murcko MA, Chambers SP, Aldape RA, Raybuck SA, Livingston DJ. Structure and mechanism of interleukin-1 beta converting enzyme. *Nature* 370: 270-275, 1994.
360. Wilson MA, Collins JL, Hod Y, Ringe D, Petsko GA. The 1.1-A resolution crystal structure of DJ-1, the protein mutated in autosomal recessive early onset Parkinson's disease. *Proc Natl Acad Sci U S A* 100: 9256-9261, 2003.
361. Wilson MA, Collins JL, Hod Y, Ringe D, Petsko GA. The 1.1-A resolution crystal structure of DJ-1, the protein mutated in autosomal recessive early onset Parkinson's disease. *Proc. Natl. Acad. Sci. USA* 100: 9256-9261, 2003.
362. Wilson P, Barber P, Hamid Q, Power B, Dhillon A, Rode J, Day I, Thompson R, Polak J. The immunolocalization of protein gene product 9.5 using rabbit polyclonal and mouse monoclonal antibodies. *British journal of experimental pathology* 69: 91-104, 1988.
363. Xiong H, Wang D, Chen L, Choo YS, Ma H, Tang C, Xia K, Jiang W, Ronai Z, Zhuang X, Zhang Z. Parkin, PINK1, and DJ-1 form a ubiquitin E3 ligase complex promoting unfolded protein degradation. *The Journal of Clinical Investigation* 119: 650-660, 2009.
364. Xu J. The parkinson's disease-associated DJ-1 protein is a transcriptional co-activator that protects against neuronal apoptosis. *Hum. Mol. Genet.* 14: 1231-1241, 2005.
365. Yaacov H. Differential control of apoptosis by DJ-1 in prostate benign and cancer cells. *Journal of Cellular Biochemistry* 92: 1221-1233, 2004.
366. Yamaguchi H, Shen J. Absence of dopaminergic neuronal degeneration and oxidative damage in aged DJ-1-deficient mice. *Molecular Neurodegeneration* 2: 1-8, 2007.
367. Yang Y, Gehrke S, Haque ME, Imai Y, Kosek J, Yang L, Beal MF, Nishimura I, Wakamatsu K, Ito S, Takahashi R, Lu B. Inactivation of Drosophila DJ-1 leads to impairments of oxidative stress response and phosphatidylinositol 3-kinase/Akt signaling. *Proc Natl Acad Sci USA* 102: 13670-13675, 2005.
368. Yoritaka A, Hattori N, Uchida K, Tanaka M, Stadtman ER, Mizuno Y. Immunohistochemical detection of 4-hydroxynonenal protein adducts in Parkinson disease. *Proc Natl Acad Sci U S A* 93: 2696-2701, 1996.
369. Young JE, Garden GA, Martinez RA, Tanaka F, Miguel Sandoval C, Smith AC, Sopher BL, Lin A, Fischbeck KH, Ellerby LM, Morrison RS, Taylor JP, La Spada AR. Polyglutamine-Expanded Androgen Receptor Truncation Fragments Activate a Bax-Dependent Apoptotic Cascade Mediated by DP5/Hrk. *J. Neurosci.* 29: 1987-1997, 2009.
370. Yuen H-F, Chan Y-P, Law S, Srivastava G, El-tanani M, Mak T-W, Chan K-W. DJ-1 Could Predict Worse Prognosis in Esophageal Squamous Cell Carcinoma. *Cancer Epidemiol Biomarkers and Prevention* 17: 3593-3602, 2008.
371. Zhang L, Shimoji M, Thomas B, Moore DJ, Yu S-W, Marupudi NI, Torp R, Torgner IA, Ottersen OP, Dawson TM, Dawson VL. Mitochondrial localization of the Parkinson's disease related protein DJ-1: implications for pathogenesis. *Human Molecular Genetics* 14: 2063-2073, 2005.
372. Zhang Y, Gao J, Chung KKK, Huang H, Dawson VL, Dawson TM. Parkin functions as an E2-dependent ubiquitin-protein ligase and promotes the degradation of the synaptic vesicle-associated protein, CDCrel-1. *Proc Natl Acad Sci USA* 97: 13354-13359, 2000.
373. Zhong N, Kim CY, Rizzu P, Geula C, Porter DR, Pothos EN, Squitieri F, Heutink P, Xu J. DJ-1 Transcriptionally Up-regulates the Human Tyrosine Hydroxylase by Inhibiting the Sumoylation of Pyrimidine Tract-binding Protein-associated Splicing Factor. 2006. pp. 20940-20948.

374. Zhong N, Xu J. Synergistic activation of the human MnSOD promoter by DJ-1 and PGC-1{alpha}: regulation by SUMOylation and oxidation. *Hum. Mol. Genet.* 17: 3357-3367, 2008.
375. Zhong N, Xu J. Synergistic activation of the human MnSOD promoter by DJ-1 and PGC-1: regulation by SUMOylation and oxidation. 2008. pp. 3357-3367.
376. Zhou C, Huang Y, Przedborski S. Oxidative Stress in Parkinson's Disease. *Annals of the New York Academy of Sciences* 1147: 93-104, 2008.
377. Zhou W, Freed CR. DJ-1 Up-regulates Glutathione Synthesis during Oxidative Stress and Inhibits A53T α-Synuclein Toxicity. *J. Biol. Chem.* 280: 43150-43158, 2005.
378. Zhou W, Freed CR. DJ-1 up-regulates glutathione synthesis during oxidative stress and inhibits A53T α-synuclein toxicity. *J. Biol. Chem.* 280: 43150-43158, 2005.
379. Zhou W, Zhu M, Wilson MA, Petsko GA, Fink AL. The Oxidation State of DJ-1 Regulates its Chaperone Activity Toward α-Synuclein. *Journal of Molecular Biology* 356: 1036-1048, 2006.
380. Zhou W, Zhu M, Wilson MA, Petsko GA, Fink AL. The Oxidation State of DJ-1 Regulates its Chaperone Activity Toward α-Synuclein. *J. Mol. Biol.* 356: 1036-1048, 2006.
381. Zou H, Li Y, Liu X, Wang X. An APAF-1 Cytochrome c Multimeric Complex Is a Functional Apoptosome That Activates Procaspase-9. *The Journal of biological chemistry* 274: 11549-11556, 1999.
382. Zou H, Yang R, Hao J, Wang J, Sun C, Fesik SW, Wu JC, Tomaselli KJ, Armstrong RC. Regulation of the Apaf-1/Caspase-9 Apoptosome by Caspase-3 and XIAP. *The Journal of biological chemistry* 278: 8091-8098, 2003.
383. Zourlidou A, Payne Smith MD, Latchman DS. HSP27 but not HSP70 has a potent protective effect against α-synuclein-induced cell death in mammalian neuronal cells. *Journal of Neurochemistry* 88: 1439-1448, 2004.